

Self-repair and Sleep in Jellyfish

Thesis by
Michael Abrams

In Partial Fulfillment of the Requirements for the
Degree of
Doctor of Philosophy

The logo for the California Institute of Technology (Caltech), featuring the word "Caltech" in a bold, orange, sans-serif font.

CALIFORNIA INSTITUTE OF TECHNOLOGY
Pasadena, California

2018
Defended May 17, 2018

© 2018

Michael Abrams

ORCID: 0000-0003-1864-1706

All rights reserved

ACKNOWLEDGEMENTS

My parents and brother are my foundations, without their love and advice I would be nowhere. I have been lucky to find true friends throughout my life who are there when I need them. Marta has been my brilliant ally in all things. The Goentoro Lab as a whole, and Ty and Lea in particular, have encouraged and guided my creativity and been integral to my life and work these last six years. Finally, Caltech, and the Division of Biology, have given me the opportunity and support to follow my own path. Words do not suffice, but thank you all.

ABSTRACT

Studying the cnidarian jellyfish, we have pursued basic biological questions related to self-repair mechanisms and sleep behavior. Working in *Aurelia* we have discovered a novel strategy of self-repair; we determined that they can undergo body reorganization after amputations that culminates in the recovery of essential radial symmetry without rebuilding lost parts [1]. Working with *Cassiopea*, we have, for the first time, identified a behavioral sleep-like state in an animal without a centralized nervous system [2], supporting the hypothesis that sleep is ancestral in animals.

PUBLISHED CONTENT AND CONTRIBUTIONS

- [1] Aki H Ohdera, Michael J Abrams, Cheryl L Ames, David M Baker, Luis P Suescun-Bolivar, Allen G Collins, Christopher J Freeman, Edgar Gamero-Mora, Tamar L Goulet, Dietrich K Hofmann, et al. “Upside-Down but Headed in the Right Direction: Review of the Highly Versatile *Cassiopea xamachana* System”. In: *Frontiers in Ecology and Evolution* 6 (2018), p. 35. DOI: 10.3389/fevo.2018.00035.
M.J.A provided a figure and text for one section within the manuscript.
- [2] Ravi D Nath, Claire N Bedbrook, Michael J Abrams, Ty Basinger, Justin S Bois, David A Prober, Paul W Sternberg, Viviana Gradinaru, and Lea Goentoro. “The jellyfish *Cassiopea* exhibits a sleep-like state”. In: *Current Biology* 27.19 (2017), pp. 2984–2990. DOI: 10.1016/j.cub.2017.08.014.
M.J.A. participated in the conception of the project, design and execution of experiments, and the writing of the paper.
- [3] Michael J Abrams and Lea Goentoro. “Symmetrization in jellyfish: reorganization to regain function, and not lost parts”. In: *Zoology* 119.1 (2016), pp. 1–3. DOI: 10.1016/j.zool.2015.10.001.
M.J.A participated in the writing of this invited perspective.
- [4] Michael J Abrams, Ty Basinger, William Yuan, Chin-Lin Guo, and Lea Goentoro. “Self-repairing symmetry in jellyfish through mechanically driven reorganization”. In: *Proceedings of the National Academy of Sciences* 112.26 (2015), E3365–E3373. DOI: 10.1073/pnas.1502497112.
M.J.A. participated in the planning and execution of experiments, design of the mathematical modeling, analyzation of data and writing of the paper.

TABLE OF CONTENTS

Acknowledgements	iii
Abstract	iv
Published Content and Contributions	v
Table of Contents	vi
Chapter I: Introduction	1
1.1 Cnidaria: a sister group to Bilateria	1
1.2 The life cycle of cnidarians can involve two adult forms	3
1.3 Regeneration in cnidarians	6
1.4 The cnidarian neuromuscular system	8
1.5 Behavioral rhythms and conservation with the bilaterian biological clock	12
1.6 Jellyfish provide new insights into self-repair and sleep behavior . . .	14
Chapter II: Self-Repairing Essential Symmetry in Jellyfish	26
2.1 Abstract	26
2.2 Introduction	27
2.3 <i>Aurelia</i> rapidly reorganize their remaining arms and recover radial symmetry after amputation	29
2.4 Symmetrization phenocopies developmental variation	33
2.5 Symmetrization is not driven by cell proliferation, cell death, or muscle reconnection	34
2.6 Symmetrization is driven by muscle contractions in the propulsion machinery	38
2.7 Discussion	44
2.8 Materials and Methods	48
2.9 Supporting Information	53
2.10 Supplemental Movies	57
Chapter III: Sleep in Jellyfish	66
3.1 Abstract	66
3.2 Introduction	66
3.3 Continuous tracking of <i>Cassiopea</i> reveals pulsing quiescence at night	71
3.4 <i>Cassiopea</i> show reduced responsiveness to a sensory stimulus at night	74
3.5 <i>Cassiopea</i> quiescence displays homeostatic rebound	77
3.6 Nighttime quiescence in <i>Cassiopea</i> may be under circadian regulation	80
3.7 <i>Cassiopea</i> activity is depressed in the presence of deeply conserved sleep promoting molecules	82
3.8 Discussion	83
3.9 Materials and Methods	84
3.10 Supplemental Movies	91
Chapter IV: Discussion	97

4.1 Self-repair strategies in *Aurelia* 97
4.2 A sleep-like state in *Cassiopea* 100

Chapter 1

INTRODUCTION

In my thesis, I focus on two main areas of inquiry: how animals respond to injuries and animal sleep behavior. These involve basic biology questions that have been pursued across animal models, and yet many of their underlying mechanisms remain only partially understood [1, 2]. We chose to investigate the scyphomedusae *Aurelia aurita* and *Cassiopea spp.* because each has essential traits that allow us to gain new insights into sleep behavior and self-repair.

1.1 Cnidaria: a sister group to Bilateria

Due to their strange shapes and propensity to regenerate, cnidarians were initially considered plants. This changed in the mid-1700s [3] as naturalists began to classify organisms based on more specific traits. This effort has continued, and with ever expanding databases of published genomes from animals in ancient phyla, it has become clear that among the non-bilaterian metazoans (ctenophores, sponges, placozoans and cnidarians), Cnidaria is the closest lineage to Bilateria (Figure 1.1A) [4].

Though aspects of the tree of life are frequently revised, the number of sequenced species is increasing, and we are gaining confidence in the phylogenetic relationships between organisms (Figure 1.1A). The crown-group Metazoa likely originated in the early-mid Neoproterozoic (1000-720Ma), before the onset the "Snowball Earths" of the Cryogenian (720-635Ma) [5–8]. Molecular evidence suggests that Cnidaria, and the total-group Bilateria, also emerged in the small window before the first global freeze (819 - 686Ma) [9–11].

Cnidaria is composed of a diverse set of animals that form five monophyletic

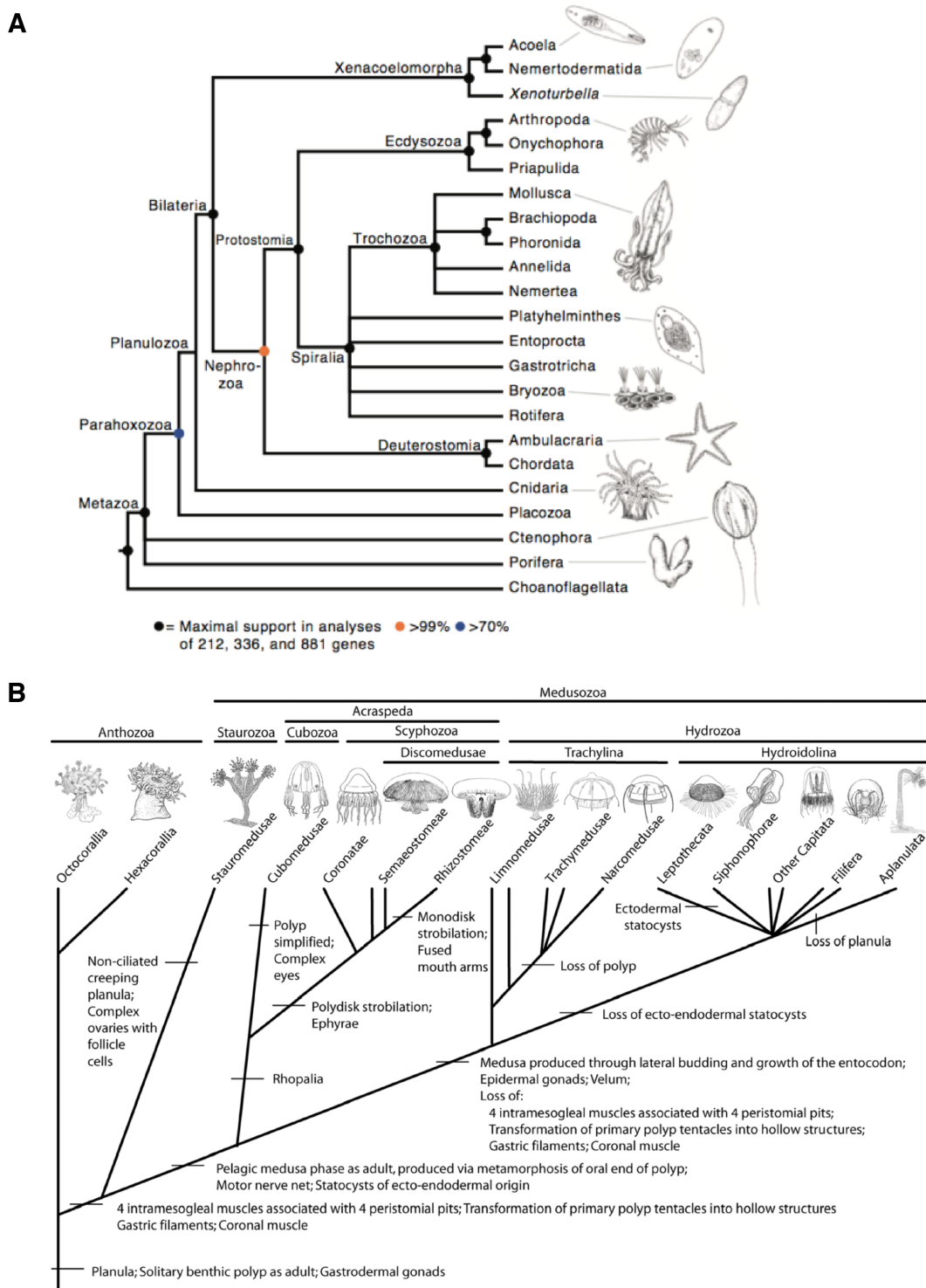


Figure 1.1: Phylogenetic relationships between cnidarians and other metazoans. A) This is a consensus tree of the phylogenetic relations between metazoa. Choanoflagellates are sister group of metazoa and inside metazoa, cnidarians are the sister group to Bilateria; taken from ref. [12]. B) Working hypothesis for cnidarian relationships with selected hypothesized ancestral characters mapped at nodes; taken from ref. [13], and the diagrams representing taxa, from ref. [14, 15].

classes (Figure 1.1B): Anthozoa, sister group to Medusozoa, which tend to be sessile and polypoid (*e.g.*, corals and sea anemones), and the medusozoans: Staurozoa, Cubozoa, Scyphozoa and Hydrozoa, which can have an additional medusa life stage (*e.g.*, jellyfish) [13, 16–19].

1.2 The life cycle of cnidarians can involve two adult forms

Cnidarians evolved life stages that have radially symmetrical body architectures [20]. Interestingly, recent morphological, genomic and fossil evidence points towards the ancestral cnidarian being a polyp-like organism, and that medusae evolved in the branch leading to Medusozoa [4, 21–26].

As in all other animals studied to date, the asymmetrical deposition of maternal transcripts establishes a primary body axis during embryogenesis in cnidarians (Figure 1.2A) [28, 29]. Cnidarian embryo cleavage patterns are highly variable but generally result in two common forms of blastulae: a hollow coeloblastula or a solid stereoblastula [30]. Following gastrulation that produces two cell layers, the endoderm and ectoderm, differentiation begins, and a cylindrical ciliated larva emerges, called a planula (Figure 1.2B) [28, 31, 32].

Most planula larvae, upon settling on a substrate, metamorphose into polyps (Figure 1.2C) by transforming the blastopore site into an oral opening, around which tentacles develop through the evagination of body wall ectoderm and endoderm [33]. Polyps are sac-like animals with supportive gelatinous mesoglea between their two cell layers. The mesoglea is comprised of collagen, an insoluble fibrous protein that composes the extracellular matrix and connective tissue of all animals [34]. Polyps attach to the substrate with their aboral side, and have a circle of tentacles surrounding their oral side. The polyps can be solitary or colonial, and reproduce asexually through budding.

The larva-to-polyp transition can involve many factors. The level of dissolved oxygen may influence settling behavior in *Aurelia aurita* larvae [35]. For *Hydractinia echinata*, the neuropeptide LWamide (Leu-Trp-NH₂) induces the transition

Medusozoan Life Cycle (*Aurelia*)

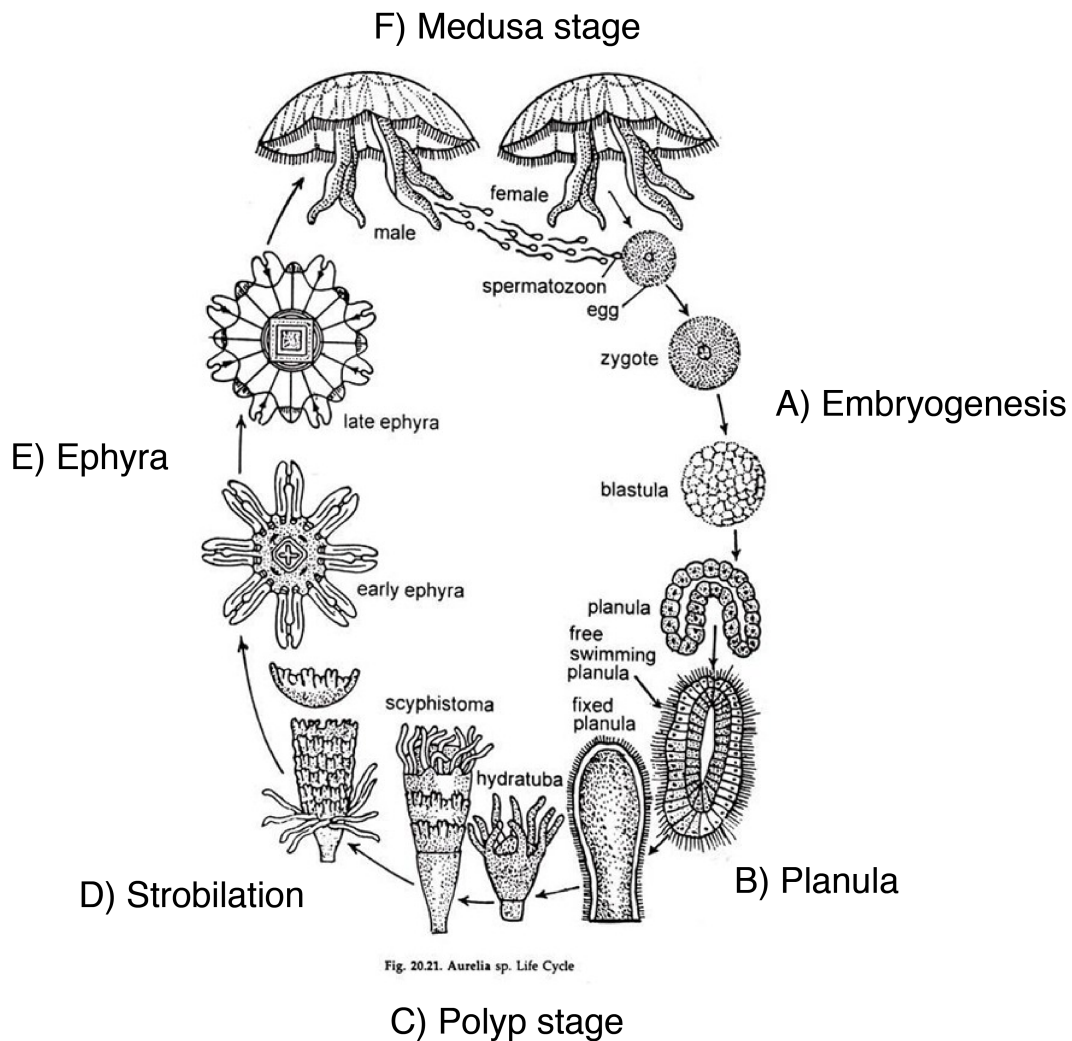


Figure 1.2: **Life cycle of the medusozoan *Aurelia*** (A) Embryogenesis forms a two cell layered blastula, and continues develops into a planula (B). The planula metamorphoses into a sac-like polyp (C), which is an adult stage. In a process called strobilation (D), the polyp undergoes fission, and each segment forms an ephyrae (E). Ephyrae develop into the adult medusa stage (F) over several weeks. (ref. [27])

from larva to polyp [36]. Notably, although anthozoans are sessile as adults, they produce free-swimming larvae that use light as a cue for settlement behavior [37]. The attachment of *Cassiopea* larva to substrate is initiated by a *Vibrio sp.* bacteria [38]. Hence, there does not appear to be a broadly conserved settling cue.

There are two main types of cnidarian life cycle. In anthozoans, the polyp is the gamete-producing form and the cycle is embryo>larva>polyp. However,

Medusozoans generally have an additional life cycle stage, the medusa (Figure 1.2D-F), which is typically the sexual form [39]. The polyp-to-medusa transition involves three successive phases: induction, strobilation and jellyfish morphogenesis. The initiation of the transverse segmentation, or fission, of the polyp body is called strobilation (Figure 1.2D). Each disk-shaped segment develops to form a young jellyfish called an ephyra (Figure 1.2E), which then detaches from the polyp and begins a planktonic life.

Ephyra are generally 3-5mm in diameter, with eight arms in discrete radial symmetry, with a manubrium (an orifice that opens for food and waste) in the center of their bodies. They develop quickly over several weeks, growing in size as they form bell tissue in the space between their arms. This continues, and they develop specialized gamete pouches that connect to their gastric cavity, at which point they are sexually mature jellyfish (Figure 1.2F) [40].

The induction of strobilation is also mechanistically diverse, though it is tightly regulated by environmental stimuli and depends on seasonal rhythms [35, 41–44]. Some jellyfish have been studied for their seasonal synchronous production of millions of jellyfish, which can have major impacts on the marine ecosystem [45]. *Cassiopea* have long been known to strobilate upon infection by their mutualistic symbiont, *symbiodinium* [46]; however, recent screening for pharmacological stimulation of strobilation led to the discovery that indole-containing compounds trigger metamorphosis in many scyphomedusae, including *Aurelia* and *Cassiopea* [47]. We take advantage of this capability, so that we can frequently produce thousands of ephyrae for experimentation. However, these inducers do not effect metamorphosis in two hydromedusae species; suggesting that strobilation and the medusa stage is apomorphic in Medusozoa.

Medusae, or jellyfish, vary widely in size and morphology (Figure 1.1B and Figure 1.2F). Generally, they have bell-shaped bodies with a manubrium, a stalk-like structure that opens into the gastrovascular cavity and hangs from the center of their subumbrella. Often oral arms surround this structure and connect to the

manubrium where it meets the base of the bell. As with the polyps, mesoglea buttresses the two cell layers and acts as a hydrostatic skeleton [48]. Spaced around the bell rim are rhopalia, ganglion-like nerve clusters that integrate information collected by a diffuse nerve net and also organize muscular activity and behavior (described in Section 1.4) [49, 50]. In the next sections, I discuss what is known about the capacity for self-repair in cnidarians and how their neuromuscular systems can exhibit complex behaviors.

1.3 Regeneration in cnidarians

Traditionally self-repair is divided into two general classes: wound healing and regeneration. Both processes across Metazoa involve cellular proliferation, dedifferentiation, migration and redifferentiation [53–56]. Though wound healing [57, 58] and regeneration of bell, manubrium [59] and the complex eye of some medusozoans [60, 61] has been reported, here we focus on the regenerative abilities of cnidarian polyps [62–65], in which there is a richer understanding. Comparative -omics play a critical role in resolving the mechanisms of self-repair, and the genomes of one hydrozoan (*Hydra vulgaris*) and three anthozoans (*Nematostella vectensis*, *Aiptasia pallida* and *Acropora digitifera*) have recently been reported [66–69]. Analysis indicates that cnidarian wound healing and regeneration rely on many genes shared with Bilateria. Though metabolic and stress response pathways have been implicated in regeneration, [35, 70–77], considerably more focus has been spent on the role of deeply conserved signaling pathways [11, 78–81].

How cnidarians, and other animals, regulate their regenerative state is thought to involve the redeployment of signaling pathways also used in development [2, 52, 70] (Figure 1.3A-C). Many of the main signaling pathways, including Wnt, TGF- β , RTK, Notch, Hedgehog and Jak–Stat are present in sponges [82, 83], indicating that many components of the genetic toolkit existed before cnidarian-bilaterian divergence. Molecular analysis in *Hydra vulgaris*, for example, has shown that the Wnt signaling system is involved in axial patterning during head regeneration

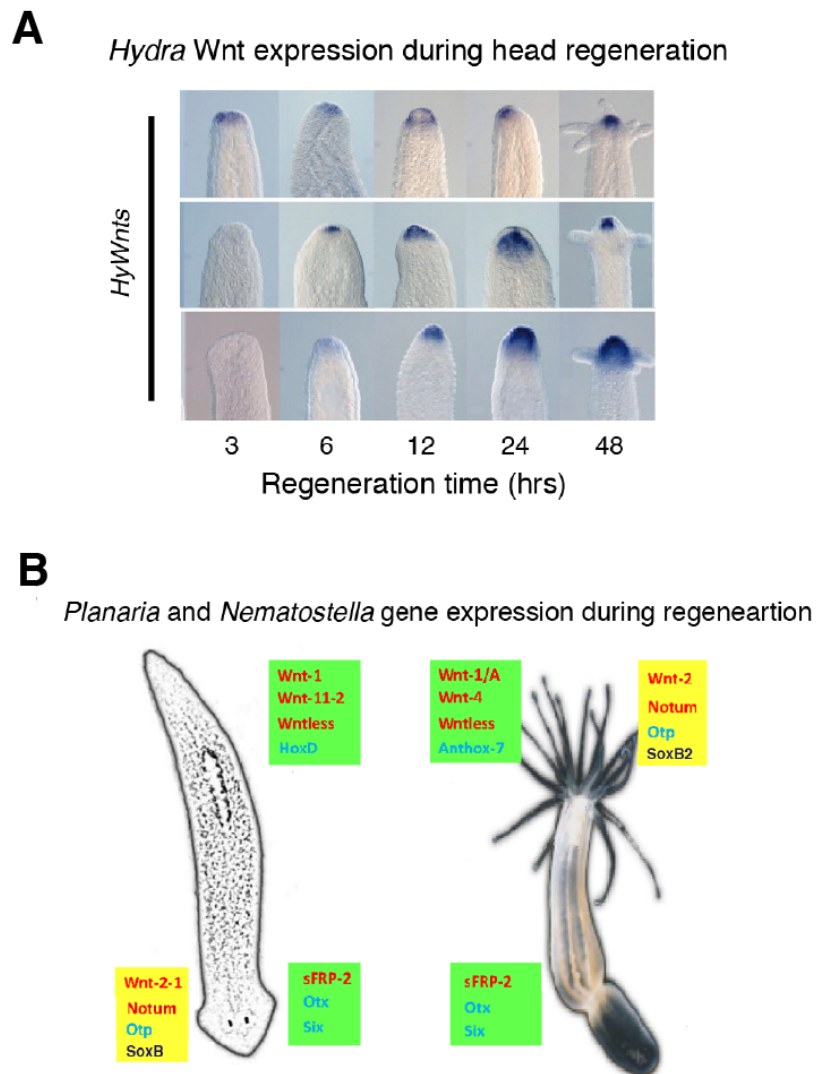


Figure 1.3: **Bilateria signaling pathways involved in self-repair** (A) Expression patterns of Wnt genes during *Hydra* head regeneration; modified from ref. [51] (B) Comparison of “head” vs. “tail” gene expression in the regeneration of *Nematostella vectensis* and *Planaria*. Highlighted in light green are bona fide orthologs that are expressed as expected according to this comparison, while yellow marks polarized genes that are expressed in an ‘inverted’ position, which can indicate evolutionary change in the regeneration program. Wnts and Wnt pathway genes in red and orange, homeobox factors in light blue and transcription factors in dark blue; modified from ref. [52].

and development [51, 52, 84–86] (Figure 1.3A). There also appears to be similar Wnt signaling, homeodomain and other transcription factor involvement between the bilateria flatworm *Planaria* and *Nematostella vectensis* during “head” and “tail”

regeneration (Figure 1.3B) [52, 72]. In bilaterian and cnidarian development, these same components also play key roles in neurogenesis. WNT- β -catenin signaling in these systems activates basic helix-loop-helix (bHLH) proneural genes, including the transcription factor SOXB2 (also involved in regeneration as seen in Figure 1.3B) [87]. Functional perturbation in *Nematostella vectensis* recently revealed that Wnt signaling mediates the oral-aboral axis patterning of two *hox* homeodomain genes [88]; in bilaterians, neural regions are also established by the restricted expression of *hox* genes [89–91]. Though we are still limited in our knowledge of how neurogenesis is functionally regulated in Cnidaria, from histological and physiological assessments we know they have a well organized nervous system.

1.4 The cnidarian neuromuscular system

The ability of an organism to detect and respond to their environment through neurologically controlled movements is a shared trait across nearly all animals and led to the incredible diversification of animal behavior. To understand what structures cnidarians are capable of self-repairing, and how they elicit behaviors like sleep, we must have an understanding of their neuromuscular system.

Action potentials in cnidarians are transmitted throughout the neuromuscular system using voltage-gated ion channels [93, 94]. Characterization of hyperpolarization-activated channels in *Nematostella vectensis* indicates that they are functionally similar to their bilaterian counterparts, and are critical for their neuronal rhythmicity. Cnidaria organize their sensory neurons in a diffuse nerve net (*FMRF* positive cells in Figure 1.4B, D, F and G), and their processes are interspersed among the epithelial cells of both layers [83, 95]. The cnidarian nervous systems rely on many of the same neurotransmitters and neurohormones as bilaterians [96]. Cnidarian neuropeptides are located in neuronal dense-core vesicles and are synthesized as preprohormones. Several *Hydra* neuropeptide genes have been cloned and shown to express in specific subpopulation of neurons [97–103]. Signals transmitted through the nervous system control animal actions, but for more complex behaviors nervous

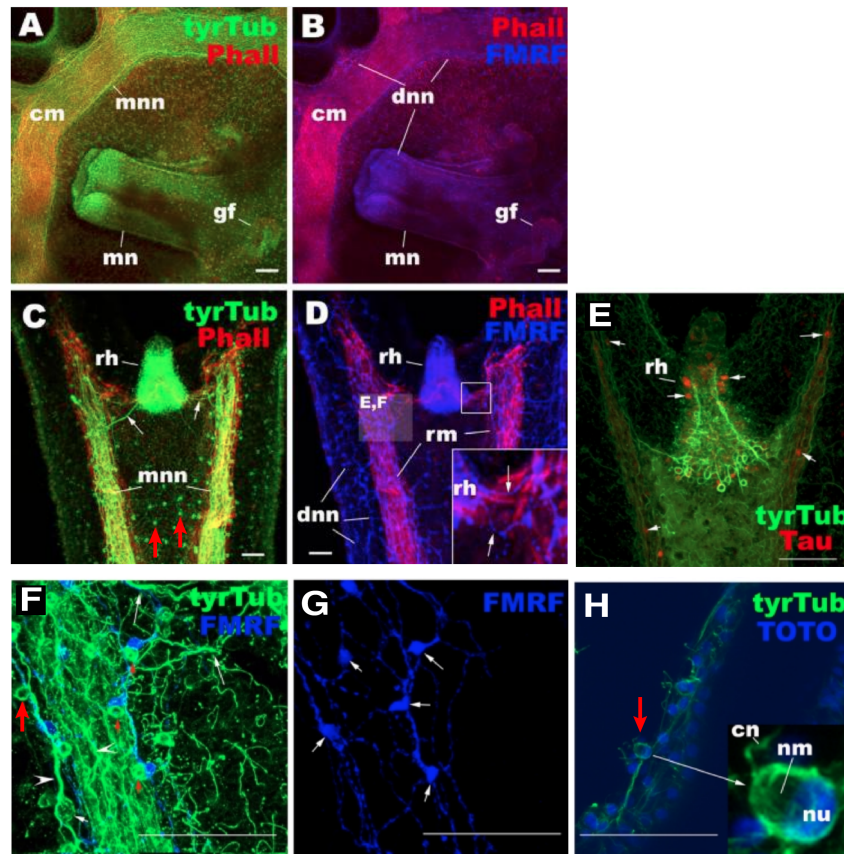
Neuromuscular network of an *Aurelia* ephyra

Figure 1.4: **The neuromuscular network of an *Aurelia* ephyra** Confocal sections of *Aurelia* sp. 1 ephyrae labeled with antibodies against tyrosinated tubulin (*tyrTub*), taurine (*Tau*), and/or FMRFamide (*FMRF*). (A–D) radial (*rm*) and circular (*cm*) muscle fibers are labeled with phalloidin (*Pha*). (H) nuclei (*nu*) are labeled with the fluorescent dye TOTO. In all subpanels, ephyrae are viewed from the oral side: (A and B) manubrium and surrounding subumbrellar epithelium of the bell, (C–H) rhopalar arm. The *tyrTub* antibody strongly labeled the motor nerve net (MNN) (A, C, F), which contains large bipolar neurons (*white arrow* in F) with longitudinally oriented thick neuronal processes (*arrowheads* in F). *tyrTub*-IR cnidocytes with apically located region devoid of staining, presumably occupied by nematocysts (*nm*), are also seen in the ectoderm (*red arrow* in C, F, H; *inset* in H). The taurine antibody labeled a subset of MNN neurons and sensory cells in the rhopalium (*rh*) (*arrows* in E). The FMRFamide antibody labeled the diffuse nerve net (DNN) (B, D, F, G), which contains multipolar neurons with thin neuronal processes (*arrows* in F). The *tyrTub*-IR cnidocytes lie alongside FMRFamide-IR DNN neuronal cell bodies and neurites (see *red arrows* in F), potentially indicating the presence of nervous communication. *cm* circular muscle, *mn* manubrium, *gf* gastric filaments, *mnn* motor nerve net, *dnn* diffused nerve net, *rh* rhopalium, *cn* cnidocil, *nm* nematocyst, *nu* nucleus; modified from ref. [92].

system subfunctionalization is required.

Significant nerve net specialization exists in cnidarians, and is evident in their complex feeding and swimming behaviors. These movements are coordinated by neuron dense sensory-motor integrative units, and cnidarians have varying levels of

nervous system subfunctionalization. For example, in addition to their diffuse nerve net, cnidarian medusae and polyps possess a circular neural network, called a nerve ring (motor nerve net in medusae) (*tyrTub* positive cells in Figure 1.4A, C, E and F), which can be highly specialized allowing for complex swimming contractions [96, 98, 101, 104]. The medusozoans tend to have more elaborate sensory systems and behavioral repertoire enabling more sophisticated behavioral patterns [105, 106]. Sensory information in medusae is integrated at rhopalia (*rh* in Figure 1.4C-E), which is also the location of the pacemaker, allowing it to send regular electrical impulses to cause swimming contractions [92, 96]. Well-developed nerve nets correlate with the presence of basiepithelial muscle fibers directly innervated by nerve net neurons (*Pha* labeled in Figure 1.4A-D) [96, 107–110], indicating a possible evolutionary connection between musculature, and a system of sensory-effector circuits.

Signals from the cnidarian nervous system control muscle contractions. There is striking ultrastructural similarity in the striated muscles of animals, and it was thought to reflect a common evolutionary origin [111]. Many of the proteins involved in striated muscle existed prior to Metazoa, for example, Myosin type II forms a contractile ring in yeast [112, 113]. However, muscle in cnidarians and ctenophores lacks proteins (Troponin and Titin) critical for the functionality of bilaterian muscle. This is consistent with the theory that striated muscle evolved independently in non-bilaterian metazoa, perhaps building on pre-existing, ancestral contractile systems [114, 115]. No matter the extent of the mechanistic conservation, cnidarian muscle is fully capable of being neurologically controlled to elicit behaviors.

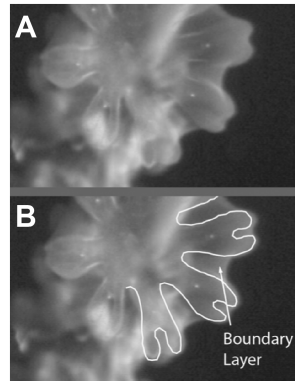
Feeding behaviors exist in every animal and depend on their morphological capabilities. Cnidarians, being gelatinous, are rather delicate animals, but they have evolved a unique stinging cell, nematocysts, for defense and prey capture. Nematocysts vary in morphology and are highly specialized cells (many contain a harpoon-like structure) [116]. The cnidocil, the trigger of a nematocyst (*red arrows* pointed at *nm* and *cn* in Figure 1.4 in C, F and inset H), can be stimulated in

nanoseconds [117] by a variety of chemicals, amino acids and prey [83, 118–123]. In medusae, the tentacles on the umbrella margin sting and stick to the prey on contact, then contract to bring the prey to the bell margin. From there, the oral arms perform a licking motion and bring the prey, using ciliary currents, from the margin to the the mouth, where it selects what to eat and what to reject [124]. It is interesting to consider the evolutionary feedback loop between body shape and prey capture capabilities.

This interplay between form and function is perhaps clearest in the functional symmetry of jellyfish, where perturbations that affect this symmetry impair their ability to generate propulsion. Propulsion systems consists of a source of mechanical power and a propulsor, the means of converting the power into propulsive force. In medusae, the mechanical power comes from the muscle contractions, while the propulsor is their visco-elastic body. Swimming is achieved by the calcium-dependent phasic activation of the neuromuscular system, and the elastic recoil of the medusae body [58, 125]. The full body pulse of medusae allows them to efficiently pull themselves through the water, primarily via suction [126, 127]. Interestingly, water is relatively viscous for ephyrae, so the space between their arms forms a hydrodynamically continuous surface (called a boundary layer in Figure 1.5A and B), important for generating a balanced propulsive force. In both ephyrae and medusae the propulsion system is require to generate the fluid flows that facilitate prey capture, reproduction and the removal of waste [128–131]. Therefore jellyfish depend on their radial symmetry for their overall function.

However, not all jellyfish use their propulsion system for swimming. The scyphomedusae *Cassiopea* (Figure 1.5C) have adopted a unique life style to enhance their symbiots access to light: they lie with their umbrella pulsing on the ground and their oral arms protruding upwards, hence their colloquial name, upside-down jellyfish [132, 133]. This stationary pulsing behavior lends itself to quantification, particularly for those interested in studying jellyfish activity decoupled from swimming [134].

Hydrodynamically continuous surface
(boundary layer) of an *Aurelia* ephyra



Cassiopea (upside-down jellyfish)



Temporal gene expression
of *Nematostella* CRY1a

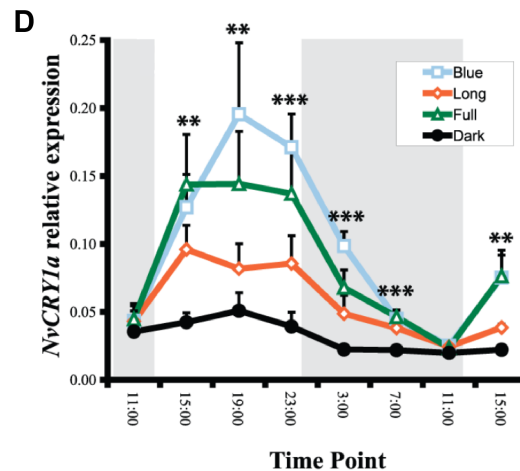


Figure 1.5: Neuromuscular control of behavior and circadian rhythms Dye visualization of boundary layer maintenance between lappets of a swimming ephyra when the bell is near full relaxation. The ephyra (0.28 cm diameter) has passed through fluorescein dye. Dye remains along entire exumbrellar surface of ephyra (A), including both the lappets (outlined in panel B) and the inter-lappet spaces; from ref. [127]. (C) *Cassiopea*, in its natural upside-down orientation; photocredit Jane Easter Photograph. (D) Temporal gene expression of *NvCry1a*, *1b*, and *2* from three light treatments and constant dark show a diverse degree of transcriptional regulation. *NvCry1a* was significantly upregulated in subjective day in all light treatments with higher mean expression in adults in the full-spectrum and blue-light treatments. When light was removed, expression decreased in all treatments but remained significant throughout more than half of subjective night. Asterisks indicate significant difference among treatments (* <0.05, ** <0.001, *** <0.0001) and error bars are + s.d; modified from [135]

1.5 Behavioral rhythms and conservation with the bilaterian biological clock

Circadian rhythms are present in plants, bacteria, fungi and animals [136], and they allow these organisms to anticipate and prepare for daily environment

changes (*e.g.*, light, temperature, food availability). Sleep in many animals is tied to the circadian cycle, and the mechanisms that connect these separate processes are an area of active study [137]. The presence of circadian rhythms in cnidarians makes them an attractive model for characterizing a possible sleep-like state in a non-bilaterian.

Many cnidarians display daily cycles in activity, including vertical migration in direct response to light intensity, larval phototaxis, settlement behavior, expansion and retraction of the body column, and feeding behaviors [138–140]. Gametogenesis and spawning can also be cued to seasonal, lunar and daily changes in light intensity and wavelength [141, 142]. *Acropora millepora* and *Nematostella vectensis* have many diurnally-oscillating genes, some unique, but many in common with each other [143]. Their rhythmicity also continued in the absence of the entraining cue (*e.g.*, light), considered a requirement for a behavior to be circadian, though this did not persist for long [144–146].

Cnidarians detect and respond to light [105, 147, 148], and share at least two classes of photosensitive molecule with Bilateria: opsins and cryptochromes, and both can be involved in the entrainment of circadian rhythms (Figure 1.5D) [135, 145, 149–151]. However, the ability to detect light does not define circadian rhythms, it is the intrinsic underlying molecular clock that organizes and maintains the rhythm.

Some components of the bilaterian transcription–translation feedback loop that regulates the circadian clock exist in Cnidaria; however, with hundreds of millions of years of evolution, cnidarian molecular clocks could be built with both conserved and novel parts [135, 144, 150]. For example, some cnidarians have cryptochromes that are expressed in in a diel cycle (Figure 1.5D), a common component of the bilaterian feedback loop [135, 150]. Other genes, including melatonin, are known to be involved in circadian rhythms and sleep, and in *Nematostella vectensis*, melatonin synthesis genes cycle their expression under diel conditions and melatonin can initiate expression of circadian clock genes [146]. However, how melatonin interacts

with the circadian clock in this system, or regulates sleep in other systems, remains largely unknown [137, 152, 153].

1.6 Jellyfish provide new insights into self-repair and sleep behavior

We leveraged the characteristics of jellyfish - their phylogenetic position, morphology, and behavior - to gain insight into two fundamental questions in biology. In Chapter 2, I describe how we discovered a new mechanism of self-repair in *Aurelia* that does not involve the regeneration of lost parts but instead relies on the propulsion system to power the reorganization of existing parts to regain essential body symmetry. In Chapter 3, I describe how we characterized a behavioral sleep-like state in *Cassiopea*, extending the presence of sleep to an animal without a centralized nervous system.

References

- [1] Ravi Allada and Jerome M Siegel. “Unearthing the phylogenetic roots of sleep”. In: *Current biology* 18.15 (2008), R670–R679.
- [2] Thomas CG Bosch et al. “The Hydra polyp: nothing but an active stem cell community”. In: *Development, growth & differentiation* 52.1 (2010), pp. 15–25.
- [3] TH Morgan. *Regeneration New York*. 1901.
- [4] Felipe Zapata et al. “Phylogenomic analyses support traditional relationships within Cnidaria”. In: *PLoS One* 10.10 (2015), e0139068.
- [5] Douglas H Erwin et al. “The Cambrian conundrum: early divergence and later ecological success in the early history of animals”. In: *science* 334.6059 (2011), pp. 1091–1097.
- [6] J William Schopf and Cornelis Klein. *The Proterozoic biosphere: a multidisciplinary study*. Cambridge University Press, 1992.
- [7] Paul F Hoffman et al. “A Neoproterozoic snowball earth”. In: *science* 281.5381 (1998), pp. 1342–1346.
- [8] Alan D Rooney et al. “A Cryogenian chronology: Two long-lasting synchronous Neoproterozoic glaciations”. In: *Geology* 43.5 (2015), pp. 459–462.

- [9] Eunji Park et al. “Estimation of divergence times in cnidarian evolution based on mitochondrial protein-coding genes and the fossil record”. In: *Molecular phylogenetics and evolution* 62.1 (2012), pp. 329–345.
- [10] A Bekker and HD Holland. “Oxygen overshoot and recovery during the early Paleoproterozoic”. In: *Earth and Planetary Science Letters* 317 (2012), pp. 295–304.
- [11] Nicole King. “The unicellular ancestry of animal development”. In: *Developmental cell* 7.3 (2004), pp. 313–325.
- [12] Johanna Taylor Cannon et al. “Xenacoelomorpha is the sister group to Nephrozoa”. In: *Nature* 530.7588 (2016), p. 89.
- [13] Allen G Collins et al. “Medusozoan phylogeny and character evolution clarified by new large and small subunit rDNA data and an assessment of the utility of phylogenetic mixture models”. In: *Systematic biology* 55.1 (2006), pp. 97–115.
- [14] Alfred Goldsborough Mayer. *Medusae of the world: The Hydromedusae*. Vol. 1. Carnegie institution of Washington, 1910.
- [15] HJ Van Cleave. *The Invertebrates: Protozoa Through Ctenophora*. 1940.
- [16] RC Brusca and GJ Brusca. *Invertebrates Sinauer Associates Sunderland*. 1990.
- [17] Mary N Arai. *A functional biology of Scyphozoa*. Springer Science & Business Media, 2012.
- [18] A Hartigan et al. “New cell motility model observed in parasitic cnidarian *Sphaerospora molnari* (Myxozoa: Myxosporea) blood stages in fish”. In: *Scientific reports* 6 (2016), p. 39093.
- [19] E Sally Chang et al. “Genomic insights into the evolutionary origin of Myxozoa within Cnidaria”. In: *Proceedings of the National Academy of Sciences* 112.48 (2015), pp. 14912–14917.
- [20] Casey W Dunn, Sally P Leys, and Steven HD Haddock. “The hidden biology of sponges and ctenophores”. In: *Trends in ecology & evolution* 30.5 (2015), pp. 282–291.
- [21] John R Finnerty et al. “Origins of bilateral symmetry: Hox and dpp expression in a sea anemone”. In: *Science* 304.5675 (2004), pp. 1335–1337.
- [22] Ehsan Kayal et al. “Cnidarian phylogenetic relationships as revealed by mitogenomics”. In: *BMC Evolutionary Biology* 13.1 (2013), p. 5.
- [23] Mark Q Martindale and Jonathan Q Henry. “The development of radial and biradial symmetry: the evolution of bilaterality”. In: *American Zoologist* 38.4 (1998), pp. 672–684.

- [24] Stefan Berking. “Generation of bilateral symmetry in Anthozoa: a model”. In: *Journal of theoretical biology* 246.3 (2007), pp. 477–490.
- [25] Qiang Ou et al. “Three Cambrian fossils assembled into an extinct body plan of cnidarian affinity”. In: *Proceedings of the National Academy of Sciences* (2017), p. 201701650.
- [26] Heyo Van Iten et al. “Reassessment of the phylogenetic position of conulariids (? Ediacaran-Triassic) within the subphylum medusozoa (phylum cnidaria)”. In: *Journal of Systematic Palaeontology* 4.2 (2006), pp. 109–118.
- [27] Shirya S. *Life Cycle of Aurelia (With Diagram) in Phylum Cnidaria*. 2018. URL: <http://www.notesonzoology.com/phylum-cnidaria/life-cycle-of-aurelia-with-diagram-phylum-cnidaria/5763> (visited on 05/01/2018).
- [28] Yulia Kraus et al. “The embryonic development of the cnidarian *Hydractinia echinata*”. In: *Evolution & development* 16.6 (2014), pp. 323–338.
- [29] Katsuyoshi Takaoka, Masamichi Yamamoto, and Hiroshi Hamada. “Origin and role of distal visceral endoderm, a group of cells that determines anterior–posterior polarity of the mouse embryo”. In: *Nature cell biology* 13.7 (2011), p. 743.
- [30] Vicki J Martin et al. “Embryogenesis in hydra”. In: *The Biological Bulletin* 192.3 (1997), pp. 345–363.
- [31] Eldon E Ball et al. “Implications of cnidarian gene expression patterns for the origins of bilaterality—is the glass half full or half empty?” In: *Integrative and comparative biology* 47.5 (2007), pp. 701–711.
- [32] Jens H Fritzenwanker et al. “Early development and axis specification in the sea anemone *Nematostella vectensis*”. In: *Developmental biology* 310.2 (2007), pp. 264–279.
- [33] David Yuan et al. “Embryonic development and metamorphosis of the scyphozoan *Aurelia*”. In: *Development genes and evolution* 218.10 (2008), pp. 525–539.
- [34] Jean-Yves Exposito et al. “Evolution of collagens”. In: *The Anatomical Record* 268.3 (2002), pp. 302–316.
- [35] Haruto Ishii, Toshifumi Ohba, and Takeshi Kobayashi. “Effects of low dissolved oxygen on planula settlement, polyp growth and asexual reproduction of *Aurelia aurita*”. In: *Plankton and Benthos Research* 3. Supplement (2008), pp. 107–113.
- [36] Jürgen Schmich, Stefan Trepel, and T Leitz. “The role of GLWamide in metamorphosis of *Hydractinia echinata*”. In: *Development genes and evolution* 208.5 (1998), pp. 267–273.

- [37] Craig Mundy and Russ Babcock. “Are vertical distribution patterns of scleractinian corals maintained by pre-or post-settlement processes? A case study of three contrasting species”. In: *Marine Ecology Progress Series* (2000), pp. 109–119.
- [38] R Neumann. “Bacterial induction of settlement and metamorphosis in the planula larvae of *Cassiopea andromeda* (Cnidaria: Scyphozoa, Rhizostomeae)”. In: *Marine Ecology Progress Series* (1979), pp. 21–28.
- [39] Ulrich Technau and Robert E Steele. “Evolutionary crossroads in developmental biology: Cnidaria”. In: *Development* 138.8 (2011), pp. 1447–1458.
- [40] Björn Fuchs et al. “Regulation of polyp-to-jellyfish transition in *Aurelia aurita*”. In: *Current Biology* 24.3 (2014), pp. 263–273.
- [41] DK Hofmann, Ro Neumann, and K Henne. “Strobilation, budding and initiation of scyphistoma morphogenesis in the rhizostome *Cassiopea andromeda* (Cnidaria: Scyphozoa)”. In: *Marine Biology* 47.2 (1978), pp. 161–176.
- [42] T Leitz and T Wagner. “The marine bacterium *Alteromonas espejiana* induces metamorphosis of the hydroid *Hydractinia echinata*”. In: *Marine Biology* 115.2 (1993), pp. 173–178.
- [43] MICHAEL Kroiher, BARBARA Siefker, and STEFAN Berking. “Induction of segmentation in polyps of *Aurelia aurita* (Scyphozoa, Cnidaria) into medusae and formation of mirror-image medusa anlagen.” In: *International Journal of Developmental Biology* 44.5 (2003), pp. 485–490.
- [44] Hiroshi Miyake, Makoto Terazaki, and Yoshiko Kakinuma. “On the polyps of the common jellyfish *Aurelia aurita* in Kagoshima Bay”. In: *Journal of Oceanography* 58.3 (2002), pp. 451–459.
- [45] Anthony J Richardson et al. “The jellyfish joyride: causes, consequences and management responses to a more gelatinous future”. In: *Trends in ecology & evolution* 24.6 (2009), pp. 312–322.
- [46] Nansi J Colley and RK Trench. “Selectivity in phagocytosis and persistence of symbiotic algae by the scyphistoma stage of the jellyfish *Cassiopeia xamachana*”. In: *Proc. R. Soc. Lond. B* 219.1214 (1983), pp. 61–82.
- [47] Patricia Cabrales-Arellano et al. “Indomethacin reproducibly induces metamorphosis in *Cassiopea xamachana* scyphistomae”. In: *PeerJ* 5 (2017), e2979.
- [48] William M Kier. “The diversity of hydrostatic skeletons”. In: *Journal of Experimental Biology* 215.8 (2012), pp. 1247–1257.
- [49] Richard A Satterlie. “Do jellyfish have central nervous systems?” In: *Journal of Experimental Biology* 214.8 (2011), pp. 1215–1223.

- [50] Cheryl Lewis and Tristan AF Long. “Courtship and reproduction in *Carybdea sivickisi* (Cnidaria: Cubozoa)”. In: *Marine Biology* 147.2 (2005), pp. 477–483.
- [51] Tobias Lengfeld et al. “Multiple Wnts are involved in Hydra organizer formation and regeneration”. In: *Developmental biology* 330.1 (2009), pp. 186–199.
- [52] Amos A Schaffer et al. “A transcriptional time-course analysis of oral vs. aboral whole-body regeneration in the Sea anemone *Nematostella vectensis*”. In: *BMC genomics* 17.1 (2016), p. 718.
- [53] Jamie I Morrison et al. “Salamander limb regeneration involves the activation of a multipotent skeletal muscle satellite cell population”. In: *The Journal of cell biology* 172.3 (2006), pp. 433–440.
- [54] Jeremy P Brockes and Phillip B Gates. *Mechanisms underlying vertebrate limb regeneration: lessons from the salamander*. 2014.
- [55] Yaoyao Chen, Nick R Love, and Enrique Amaya. *Tadpole tail regeneration in Xenopus*. 2014.
- [56] Peter W Reddien and Alejandro Sánchez Alvarado. “Fundamentals of planarian regeneration”. In: *Annu. Rev. Cell Dev. Biol.* 20 (2004), pp. 725–757.
- [57] Volker Schmid et al. “Factors effecting manubrium-regeneration in hydromedusae (Coelenterata)”. In: *Development Genes and Evolution* 179.1 (1976), pp. 41–56.
- [58] Y-C James Lin, Nikita G Grigoriev, and Andrew N Spencer. “Wound healing in jellyfish striated muscle involves rapid switching between two modes of cell motility and a change in the source of regulatory calcium”. In: *Developmental Biology* 225.1 (2000), pp. 87–100.
- [59] Volker Schmid. “Regeneration in medusa buds and medusae of Hydrozoa”. In: *American Zoologist* 14.2 (1974), pp. 773–781.
- [60] Christian Weber. “Structure, histochemistry, ontogenetic development, and regeneration of the ocellus of *Cladonema radiatum* Dujardin (Cnidaria, Hydrozoa, Anthomedusae)”. In: *Journal of Morphology* 167.3 (1981), pp. 313–331.
- [61] Sebastian-Alexander Stamatidis, Katrine Worsaae, and Anders Garm. “Regeneration of the Rhopalium and the Rhopalial Nervous System in the Box Jellyfish *Tripedalia cystophora*”. In: *The Biological Bulletin* 234.1 (2018), pp. 000–000.
- [62] Michael J Layden, Fabian Rentzsch, and Eric Röttinger. “The rise of the starlet sea anemone *Nematostella vectensis* as a model system to investigate development and regeneration”. In: *Wiley Interdisciplinary Reviews: Developmental Biology* 5.4 (2016), pp. 408–428.

- [63] GE Lesh-Laurie, A Hujer, and P Suchy. “Polyp regeneration from isolated tentacles of *Aurelia scyphistomae*: a role for gating mechanisms and cell division”. In: *Coelenterate Biology: Recent Research on Cnidaria and Ctenophora*. Springer, 1991, pp. 91–97.
- [64] Thomas CG Bosch. “Why polyps regenerate and we don’t: towards a cellular and molecular framework for *Hydra* regeneration”. In: *Developmental biology* 303.2 (2007), pp. 421–433.
- [65] David A Gold and David K Jacobs. “Stem cell dynamics in Cnidaria: are there unifying principles?” In: *Development genes and evolution* 223.1-2 (2013), pp. 53–66.
- [66] Jarrod A Chapman et al. “The dynamic genome of *Hydra*”. In: *Nature* 464.7288 (2010), p. 592.
- [67] Nicholas H Putnam et al. “Sea anemone genome reveals ancestral eumetazoan gene repertoire and genomic organization”. In: *science* 317.5834 (2007), pp. 86–94.
- [68] Sebastian Baumgarten et al. “The genome of *Aiptasia*, a sea anemone model for coral symbiosis”. In: *Proceedings of the National Academy of Sciences* 112.38 (2015), pp. 11893–11898.
- [69] Chuya Shinzato et al. “Using the *Acropora digitifera* genome to understand coral responses to environmental change”. In: *Nature* 476.7360 (2011), p. 320.
- [70] Zachary K Stewart et al. “Transcriptomic investigation of wound healing and regeneration in the cnidarian *Calliactis polypus*”. In: *Scientific reports* 7 (2017), p. 41458.
- [71] Adam M Reitzel et al. “Genomic survey of candidate stress-response genes in the estuarine anemone *Nematostella vectensis*”. In: *The Biological Bulletin* 214.3 (2008), pp. 233–254.
- [72] Timothy Q DuBuc, Nikki Traylor-Knowles, and Mark Q Martindale. “Initiating a regenerative response; cellular and molecular features of wound healing in the cnidarian *Nematostella vectensis*”. In: *BMC biology* 12.1 (2014), p. 24.
- [73] Hendrik O Petersen et al. “A comprehensive transcriptomic and proteomic analysis of *hydra* head regeneration”. In: *Molecular biology and evolution* 32.8 (2015), pp. 1928–1947.
- [74] Guoshan Wang et al. “The physiological and molecular response of *Aurelia* sp. 1 under hypoxia”. In: *Scientific reports* 7.1 (2017), p. 1558.
- [75] Omer Choresch, Abdussalam Azem, and Yossi Loya. “Over-expression of highly conserved mitochondrial 70-kDa heat-shock protein in the sea anemone *Anemonia viridis*”. In: *Journal of Thermal Biology* 32.7-8 (2007), pp. 367–373.

- [76] Eneour Puill-Stephan et al. “Expression of putative immune response genes during early ontogeny in the coral *Acropora millepora*”. In: *PLoS One* 7.7 (2012), e39099.
- [77] Tanya Brown, David Bourne, and Mauricio Rodriguez-Lanetty. “Transcriptional activation of *c3* and *hsp70* as part of the immune response of *Acropora millepora* to bacterial challenges”. In: *PLoS One* 8.7 (2013), e67246.
- [78] Antonis Rokas et al. “Conflicting phylogenetic signals at the base of the metazoan tree”. In: *Evolution & development* 5.4 (2003), pp. 346–359.
- [79] Alys M Cheatle Jarvela and Leslie Pick. “Evo-Devo: Discovery of diverse mechanisms regulating development”. In: *Current topics in developmental biology*. Vol. 117. Elsevier, 2016, pp. 253–274.
- [80] Frédéric Delsuc, Henner Brinkmann, and Hervé Philippe. “Phylogenomics and the reconstruction of the tree of life”. In: *Nature Reviews Genetics* 6.5 (2005), p. 361.
- [81] Xing-Xing Shen, Chris Todd Hittinger, and Antonis Rokas. “Contentious relationships in phylogenomic studies can be driven by a handful of genes”. In: *Nature ecology & evolution* 1.5 (2017), p. 0126.
- [82] Scott A Nichols et al. “Early evolution of animal cell signaling and adhesion genes”. In: *Proceedings of the National Academy of Sciences* 103.33 (2006), pp. 12451–12456.
- [83] Brigitte Galliot et al. “Origins of neurogenesis, a cnidarian view”. In: *Developmental biology* 332.1 (2009), pp. 2–24.
- [84] TW Holstein, E Hobmayer, and Ulrich Technau. “Cnidarians: an evolutionarily conserved model system for regeneration?” In: *Developmental Dynamics* 226.2 (2003), pp. 257–267.
- [85] Ben-Zion Shilo. “The organizer and beyond”. In: *Cell* 106.1 (2001), pp. 17–22.
- [86] David J Duffy et al. “Wnt signaling promotes oral but suppresses aboral structures in *Hydractinia* metamorphosis and regeneration”. In: *Development* 137.18 (2010), pp. 3057–3066.
- [87] Hiroshi Watanabe et al. “Sequential actions of β -catenin and Bmp pattern the oral nerve net in *Nematostella vectensis*”. In: *Nature communications* 5 (2014), p. 5536.
- [88] Timothy Q DuBuc et al. “Hox genes pattern the primary body axis of an anthozoan cnidarian prior to gastrulation”. In: *bioRxiv* (2017), p. 219758.
- [89] Alexandru S Denes et al. “Molecular architecture of annelid nerve cord supports common origin of nervous system centralization in bilateria”. In: *Cell* 129.2 (2007), pp. 277–288.

- [90] William A Alaynick, Thomas M Jessell, and Samuel L Pfaff. “SnapShot: spinal cord development”. In: *Cell* 146.1 (2011), p. 178.
- [91] Patrick RH Steinmetz et al. “Six3 demarcates the anterior-most developing brain region in bilaterian animals”. In: *Evodevo* 1.1 (2010), p. 14.
- [92] Nagayasu Nakanishi, Volker Hartenstein, and David K Jacobs. “Development of the rhopalial nervous system in Aurelia sp. 1 (Cnidaria, Scyphozoa)”. In: *Development genes and evolution* 219.6 (2009), pp. 301–317.
- [93] H Yu Frank and William A Catterall. “The VGL-chanome: a protein superfamily specialized for electrical signaling and ionic homeostasis”. In: *Science Signaling* 2004.253 (2004), re15.
- [94] Emma C Baker et al. “Functional characterization of cnidarian HCN channels points to an early evolution of ih”. In: *PloS one* 10.11 (2015), e0142730.
- [95] Nagayasu Nakanishi et al. “Early development, pattern, and reorganization of the planula nervous system in Aurelia (Cnidaria, Scyphozoa)”. In: *Development genes and evolution* 218.10 (2008), pp. 511–524.
- [96] Hiroshi Watanabe, Toshitaka Fujisawa, and Thomas W Holstein. “Cnidarians and the evolutionary origin of the nervous system”. In: *Development, growth & differentiation* 51.3 (2009), pp. 167–183.
- [97] Cornelis JP Grimmelikhuijzen, Michael Williamson, and Georg N Hansen. “Neuropeptides in cnidarians”. In: *Canadian Journal of Zoology* 80.10 (2002), pp. 1690–1702.
- [98] George O Mackie. “Central neural circuitry in the jellyfish *Aequorea victoria*”. In: *Neurosignals* 13.1-2 (2004), pp. 5–19.
- [99] CJP Grimmelikhuijzen et al. “Neuropeptides in coelenterates: a review”. In: *Coelenterate Biology: Recent Research on Cnidaria and Ctenophora*. Springer, 1991, pp. 555–563.
- [100] Peter AV Anderson, Louise F Thompson, and Craig G Money Penny. “Evidence for a common pattern of peptidergic innervation of cnidocytes”. In: *The Biological Bulletin* 207.2 (2004), pp. 141–146.
- [101] CJP Grimmelikhuijzen. “Antisera to the sequence Arg-Phe-amide visualize neuronal centralization in hydroid polyps”. In: *Cell and tissue research* 241.1 (1985), pp. 171–182.
- [102] CJP Grimmelikhuijzen et al. “Isolation of $Glu-Leu-Leu-Gly-Gly-Arg-Phe-NH_2$ (Pol-RFamide), a novel neuropeptide from hydromedusae”. In: *Brain research* 475.1 (1988), pp. 198–203.
- [103] G Plickert. “Proportion-altering factor (PAF) stimulates nerve cell formation in *Hydractinia echinata*”. In: *Cell differentiation and development* 26.1 (1989), pp. 19–27.

- [104] Osamu Koizumi, Nobuko Sato, and Chieko Goto. “Chemical anatomy of hydra nervous system using antibodies against hydra neuropeptides: a review”. In: *Hydrobiologia* 530.1-3 (2004), pp. 41–47.
- [105] Dan-E Nilsson et al. “Advanced optics in a jellyfish eye”. In: *Nature* 435.7039 (2005), p. 201.
- [106] GI Matsumoto. “Observations on the anatomy and behaviour of the cubozoan *Carybdea rastonii* Haacke”. In: *Marine & Freshwater Behaviour & Phy* 26.2-4 (1995), pp. 139–148.
- [107] George Howard Parker. *The elementary nervous system*. Vol. 1920. JB Lippincott, 1919.
- [108] Theodore Bullock and G Adrian Horridge. “Structure and function in the nervous systems of invertebrates.” In: (1965).
- [109] Jane A Westfall and Carol F Elliott. “Ultrastructure of the tentacle nerve plexus and putative neural pathways in sea anemones”. In: *Invertebrate Biology* 121.3 (2002), pp. 202–211.
- [110] Brigitte Galliot and Manon Quiquand. “A two-step process in the emergence of neurogenesis”. In: *European Journal of Neuroscience* 34.6 (2011), pp. 847–862.
- [111] Detlev Arendt, Maria Antonietta Tosches, and Heather Marlow. “From nerve net to nerve ring, nerve cord and brain—evolution of the nervous system”. In: *Nature Reviews Neuroscience* 17.1 (2016), p. 61.
- [112] Magdalena Bezanilla, Jeanne M Wilson, and Thomas D Pollard. “Fission yeast myosin-II isoforms assemble into contractile rings at distinct times during mitosis”. In: *Current Biology* 10.7 (2000), pp. 397–400.
- [113] Nathan V Whelan et al. “Error, signal, and the placement of Ctenophora sister to all other animals”. In: *Proceedings of the National Academy of Sciences* 112.18 (2015), pp. 5773–5778.
- [114] Patrick RH Steinmetz et al. “Independent evolution of striated muscles in cnidarians and bilaterians”. In: *Nature* 487.7406 (2012), p. 231.
- [115] Lucas Leclère and Eric Röttinger. “Diversity of cnidarian muscles: function, anatomy, development and regeneration”. In: *Frontiers in cell and developmental biology* 4 (2017), p. 157.
- [116] Glen M Watson and Patricia Mire-Thibodeaux. “The cell biology of nematocysts”. In: *International review of cytology*. Vol. 156. Elsevier, 1994, pp. 275–300.
- [117] Timm Nüchter et al. “Nanosecond-scale kinetics of nematocyst discharge”. In: *Current Biology* 16.9 (2006), R316–R318.

- [118] William Farnsworth Loomis. “Glutathione control of the specific feeding reactions of hydra”. In: *Annals of the New York Academy of Sciences* 62.1 (1955), pp. 211–227.
- [119] Howard M Lenhoff, Wyrta Heagy, and Jean Danner. “Bioassay for, and characterization of, activators and inhibitors of the feeding response”. In: *Hydra: Research Methods*. Springer, 1983, pp. 443–451.
- [120] H Shimizu. “Feeding and wounding responses in Hydra suggest functional and structural polarization of the tentacle nervous system”. In: *Comparative Biochemistry and Physiology Part A: Molecular & Integrative Physiology* 131.3 (2002), pp. 669–674.
- [121] RICHARD N MARISCAL and HOWARD M LENHOFF. “The chemical control of feeding behaviour in *Cyphastrea ocellina* and in some other Hawaiian corals”. In: *Journal of Experimental Biology* 49.3 (1968), pp. 689–699.
- [122] Marcia J Loeb and Richard S Blanquet. “Feeding behavior in polyps of the Chesapeake Bay sea nettle, *Chrysaora quinquecirrha* (Desor, 1848)”. In: *The Biological Bulletin* 145.1 (1973), pp. 150–158.
- [123] Howard R Lasker, Jo Ann Syron, and William S Clayton Jr. “The feeding response of *Hydra viridis*: effects of prey density on capture rates”. In: *The Biological Bulletin* 162.3 (1982), pp. 290–298.
- [124] Miguel Vazquez Archdale and Kazuhiko Anraku. “Feeding behavior in scyphozoa, crustacea and cephalopoda”. In: *Chemical senses* 30.suppl_1 (2005), pp. i303–i304.
- [125] AN Spencer. “The physiology of a coelenterate neuromuscular synapse”. In: *Journal of comparative physiology* 148.3 (1982), pp. 353–363.
- [126] Brad J Gemmell et al. “Suction-based propulsion as a basis for efficient animal swimming”. In: *Nature communications* 6 (2015), p. 8790.
- [127] KE Feitl et al. “Functional morphology and fluid interactions during early development of the scyphomedusa *Aurelia aurita*”. In: *The Biological Bulletin* 217.3 (2009), pp. 283–291.
- [128] John H Costello and SP Colin. “Morphology, fluid motion and predation by the scyphomedusa *Aurelia aurita*”. In: *Marine Biology* 121.2 (1994), pp. 327–334.
- [129] John H Costello and SP Colin. “Flow and feeding by swimming scyphomedusae”. In: *Marine Biology* 124.3 (1995), pp. 399–406.
- [130] JO Dabiri et al. “Flow patterns generated by oblate medusan swimmers: in situ observation and analysis”. In: *J. Exp. Biol* 208 (2005), pp. 1257–1265.

- [131] JE Higgins III, MD Ford, and JH Costello. “Transitions in morphology, nematocyst distribution, fluid motions, and prey capture during development of the scyphomedusa *Cyanea capillata*”. In: *The Biological Bulletin* 214.1 (2008), pp. 29–41.
- [132] Kathrin P Lampert. “Cassiopea and Its Zooxanthellae”. In: *The Cnidaria, Past, Present and Future*. Springer, 2016, pp. 415–423.
- [133] Aki H Ohdera et al. “Upside-Down but Headed in the Right Direction: Review of the Highly Versatile Cassiopea xamachana System”. In: *Frontiers in Ecology and Evolution* 6 (2018), p. 35.
- [134] Christina Hamlet, Arvind Santhanakrishnan, and Laura A Miller. “A numerical study of the effects of bell pulsation dynamics and oral arms on the exchange currents generated by the upside-down jellyfish *Cassiopea xamachana*”. In: *Journal of Experimental Biology* 214.11 (2011), pp. 1911–1921.
- [135] Adam M Reitzel, Lars Behrendt, and Ann M Tarrant. “Light entrained rhythmic gene expression in the sea anemone *Nematostella vectensis*: the evolution of the animal circadian clock”. In: *PLoS One* 5.9 (2010), e12805.
- [136] Jay C Dunlap and Jennifer J Loros. “Making Time: Conservation of Biological Clocks from Fungi to Animals.” In: *Microbiology spectrum* 5.3 (2017).
- [137] Avni V Gandhi et al. “Melatonin is required for the circadian regulation of sleep”. In: *Neuron* 85.6 (2015), pp. 1193–1199.
- [138] Nicolas Dupont et al. “Diel vertical migration of the deep-water jellyfish *Periphylla periphylla* simulated as individual responses to absolute light intensity”. In: *Limnology and Oceanography* 54.5 (2009), pp. 1765–1775.
- [139] Cloe Taddei-Ferretti and Carlo Musio. “Photobehaviour of *Hydra* (Cnidaria, Hydrozoa) and correlated mechanisms: a case of extraocular photosensitivity”. In: *Journal of Photochemistry and Photobiology B: Biology* 55.2-3 (2000), pp. 88–101.
- [140] William D Hendricks, Christine A Byrum, and Elizabeth L Meyer-Bernstein. “Characterization of circadian behavior in the starlet sea anemone, *Nematostella vectensis*”. In: *PLoS One* 7.10 (2012), e46843.
- [141] AK Brady, JD Hilton, and PD Vize. “Coral spawn timing is a direct response to solar light cycles and is not an entrained circadian response”. In: *Coral Reefs* 28.3 (2009), pp. 677–680.
- [142] J Daniel Hilton et al. “Photoreception and signal transduction in corals: proteomic and behavioral evidence for cytoplasmic calcium as a mediator of light responsivity”. In: *The Biological Bulletin* 223.3 (2012), pp. 291–299.

- [143] Matan Oren et al. “Profiling molecular and behavioral circadian rhythms in the non-symbiotic sea anemone *Nematostella vectensis*”. In: *Scientific reports* 5 (2015), p. 11418.
- [144] Aisling K Brady, Kevin A Snyder, and Peter D Vize. “Circadian cycles of gene expression in the coral, *Acropora millepora*”. In: *PLoS One* 6.9 (2011), e25072.
- [145] Adam M Reitzel, Ann M Tarrant, and Oren Levy. *Circadian clocks in the cnidaria: environmental entrainment, molecular regulation, and organismal outputs*. 2013.
- [146] Rafael Peres et al. “Developmental and light-entrained expression of melatonin and its relationship to the circadian clock in the sea anemone *Nematostella vectensis*”. In: *EvoDevo* 5.1 (2014), p. 26.
- [147] CN Mundy and RC Babcock. “Role of light intensity and spectral quality in coral settlement: Implications for depth-dependent settlement? 1”. In: *Journal of Experimental Marine Biology and Ecology* 223.2 (1998), pp. 235–255.
- [148] Benjamin M Mason and Jonathan H Cohen. “Long-wavelength photosensitivity in coral planula larvae”. In: *The Biological Bulletin* 222.2 (2012), pp. 88–92.
- [149] O Levy et al. “Light-responsive cryptochromes from a simple multicellular animal, the coral *Acropora millepora*”. In: *Science* 318.5849 (2007), pp. 467–470.
- [150] Eiichi Shoguchi et al. “A genome-wide survey of photoreceptor and circadian genes in the coral, *Acropora digitifera*”. In: *Gene* 515.2 (2013), pp. 426–431.
- [151] Hiroshi Suga, Volker Schmid, and Walter J Gehring. “Evolution and functional diversity of jellyfish opsins”. In: *Current Biology* 18.1 (2008), pp. 51–55.
- [152] C Torres-Farfan et al. “Maternal melatonin effects on clock gene expression in a nonhuman primate fetus”. In: *Endocrinology* 147.10 (2006), pp. 4618–4626.
- [153] Brittney Jung-Hynes, Russel J Reiter, and Nihal Ahmad. “Sirtuins, melatonin and circadian rhythms: building a bridge between aging and cancer”. In: *Journal of pineal research* 48.1 (2010), pp. 9–19.

Chapter 2

SELF-REPAIRING ESSENTIAL SYMMETRY IN JELLYFISH

2.1 Abstract

What happens when an animal is injured and loses important structures? Some animals simply heal the wound, whereas others are able to regenerate lost parts. In this study, we report a previously unidentified strategy of self-repair, where moon jellyfish respond to injuries by reorganizing existing parts, and rebuilding essential body symmetry, without regenerating what is lost [1]. Specifically, in response to arm amputation, the young jellyfish of *Aurelia aurita* rearrange their remaining arms, recenter their manubria, and rebuild their muscular networks, all completed within 12 hours to 4 days. We call this process symmetrization. We find that symmetrization is not driven by external cues, cell proliferation, cell death, and proceeded even when foreign arms were grafted on. Instead, we find that forces generated by the muscular network are essential. Inhibiting pulsation using muscle relaxants completely, and reversibly, blocked symmetrization. Furthermore, we observed that decreasing pulse frequency using muscle relaxants slowed symmetrization, whereas increasing pulse frequency by lowering the magnesium concentration in seawater accelerated symmetrization. A mathematical model that describes the compressive forces from the muscle contraction, within the context of the elastic response from the mesoglea and the ephyra geometry, can recapitulate the recovery of global symmetry. Thus, self-repair in *Aurelia* proceeds through the reorganization of existing parts, and is driven by forces generated by its own propulsion machinery. We find evidence for symmetrization across species of jellyfish (*Chrysaora pacifica*, *Mastigias sp.*, and *Cotylorhiza tuberculata*).

2.2 Introduction

Animals are capable of a broad array of self-repair mechanisms - the daily maintenance of cellular components, tissues, and organs are all forms of self-repair [2, 3]. As described in the introduction, there are two general classes of self-repair: wound healing and regeneration. These processes have been well studied in a number of vertebrate and invertebrate models [4–7].

However, it difficult to generalize about the role of self-repair. Some examples appear adaptive (*e.g.*, lizard tail or starfish arm regeneration after the intentional loss of these structures through autotomy). However, species closely related to those that regenerate, living in similar contexts, can show staggering differences in regenerative ability [8]. Further, some animals lose their regenerative ability as they develop (*e.g.*, tadpoles [6]), while others maintain their ability as sexually mature animals (*e.g.*, axolotl [5]). Self-repair appears to span the spectrum from adaptive and utilitarian to unintended or otherwise unexplainable, and there appears to be similar diversity at the mechanistic level [9].

It has been hypothesized that certain examples of regeneration are epiphenomena, linked pleiotropically to adaptations more useful than regeneration [10–12]. For example, cardiomyocytes in zebrafish re-utilize core signaling pathways (*e.g.*, FGF) to regenerate heart structures that are surgically removed, which to some extent may be adaptive, though it is hard to imagine a scenario in nature when the animal would survive a wound that removes half of its heart [13, 14]. However, regeneration is also often inextricably linked to the future usability of the reformed structure. For example, amputated amphibian limbs will not regenerate without innervation [15], nor will annelid worms regenerate anteriorly if the ventral nerve cord has been removed [16]. This utilitarian imperative seems to prevent the wasteful allocation of limited resources on useless regenerating structures [10]. It is with an eye towards these theories that we approached studying self-repair in *Aurelia aurita* ephyrae. We were particularly interested in this young free swimming stage because of their dependence on radial symmetry for their overall functionality. We asked if jellyfish

have a means to recover this functional symmetry, and the implications of these findings could connect to theories that address the varying rationale for self-repair abilities in animals.

The moon jelly, *Aurelia aurita*, is one of the most plentiful jellyfish in oceans across the world (Fig. 2.1A). Ranging from tropical seas to subarctic regions, from the open ocean to brackish estuaries, the moon jelly occupies diverse habitats [17–19]. The moon jelly varies greatly in size, from a few centimeters to a foot [17, 20, 21]. Transition into medusa may proceed over 1 month in the laboratory (with abundant feeding), or longer in the wild. The ephyra stage is hardy and can withstand months of starvation [22]. *Aurelia* can even thrive in dirty, polluted, acidified, warm, and oxygen poor waters [23–26]. Presently, jelly blooms have been increasing in size and frequency worldwide, which has been interpreted as a troubling sign of a disturbed ocean ecosystem [27], pitt2014jellyfish).

Injury is common in marine invertebrates. Examining 105 studies, Lindsay [29] showed that, at any given time, about 33–47% of the benthic fauna is injured. Some cited studies recorded entire starfish populations with at least one injured arm. Injury may be due to numerous factors, including partial predation, autotomy, cannibalism, competitive interaction, and human activities. Jellyfish have many known predators. A well-studied group of predators are the sea turtles (*e.g.*, the leatherback and the loggerhead; Fig. 2.1C). Juvenile sea turtles have been observed biting into foot-wide jellyfish, and adults gorge on an average of 261 jellyfish per day [30]. In addition, over 124 species of fish, 11 species of birds, several species of shrimps, sea anemones, corals, and crabs are reported to assail *Aurelia* [31–34]. Barnacles have been reported to catch and digest newly strobilated ephyrae [35].

Here, we ask how *Aurelia* responds to injuries. Marine invertebrates are known for their regenerative ability. Reported cases of regenerating marine organisms include jellyfish, sponges, corals, ctenophores, sea anemones, clams, polychaetes, starfish, and brittlestars [29, 36–41]. Isolated striated muscle from hydromedusae can transdifferentiate to regenerate various cell types [42]. The polyps of *Aurelia*,

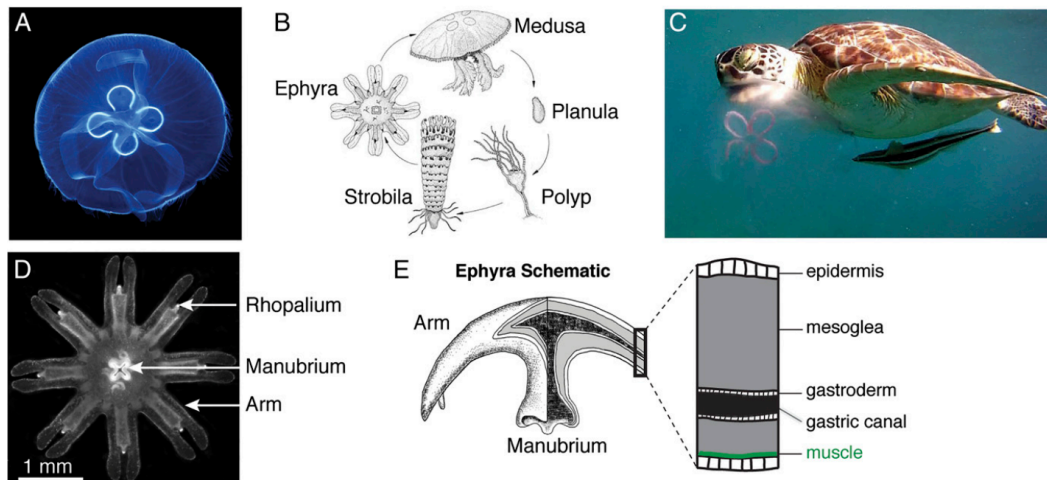


Figure 2.1: Life cycle and anatomy of *Aurelia aurita*. (A) Adult *Aurelia*. The blue color is due to lighting. Image courtesy of Wikimedia Commons/Hans Hillewaert. Image © Hans Hillewaert. (B) *Aurelia* life cycle. Fertilized eggs develop into larval planulae, which settle and develop into polyps. Seasonally, or in the right conditions, the polyps metamorphose into strobilae and release free-swimming, juvenile jellyfish (a process called strobilation). The young jellyfish, called ephyrae, grow into medusae in 3–4 wk. Reprinted with permission from ref. [28]. (C) A juvenile green sea turtle preying on *Aurelia* at Playa Tamarindo, Puerto Rico. Image courtesy of R. P. van Dam. (D) An *Aurelia* ephyra has eight radially symmetrical arms, surrounding the manubrium at the center. At the end of each arm is a light- and gravity-sensing organ, called rhopalium. (E) The epithelium of ephyra is composed of two cell layers, the ectoderm-derived epidermis that faces the outer side and the endoderm-derived gastrodermis that lines the gastric cavity. Between the two layers is the gelatinous, viscoelastic mesoglea. Embedded in the subumbrellar side (mouth side) is the coronal muscle (green).

and a number of other species, can regenerate tentacles, stolons, and hydrants [43–46], and an entire polyp can regrow from a single polyp tentacle [47]. In this study, we investigated the repair capacity in the free-swimming forms of *Aurelia* and discovered that *Aurelia* have evolved a fast strategy of self-repair, one that does not involve regenerating lost body parts.

2.3 *Aurelia* rapidly reorganize their remaining arms and recover radial symmetry after amputation

To study how the free-swimming forms of *Aurelia* respond to injuries, we chose to examine the ephyrae, the discrete symmetry of which gave us clear morphological markers to follow (Fig. 2.1D). Newly strobilated ephyrae are typically 3–5 mm in diameter (Movie S2.1). They have a disk-shaped body, with eight symmetrical

arms. Also called lobes, lappets, or tentaculocytes by other authors, these arms form a swimming apparatus in the ephyrae. Viscous boundary layers of fluid form between the arms to create a hydrodynamically continuous paddling surface [48]. Symmetric pulsation of the arms generates fluid flow that facilitates propulsion and prey capture [49, 50]. As ephyrae grow into medusae, bell tissues grow between the arms, replacing a viscous bell with a physical one.

At the end of each arm is a sensory organ, called rophalium, which contains ocelli, chemosensory pits, and a statocyst [36]. At the center of the body is the manubrium, a muscular channel connecting the mouth to the gastrovascular cavity. The stomach is surrounded by an epithelium composed of two cells layers, the outer-facing epidermis (containing the stinging cells) and the gastrodermis lining the stomach (Fig. 2.1E). Between the two cells layers is the mesoglea, a viscoelastic, jelly-like substance composed predominantly of fibrous proteins and water [51].

We conducted the amputation experiments in the following way. Freshly strobilated ephyrae were anesthetized and amputated using a homemade razor knife (Fig. 2.2A and Materials and Methods). Ephyrae were immediately returned to artificial seawater (ASW) to recover. Muscle contractions typically resumed within minutes. Fig. 2.2 B and C shows a typical progression of recovery. The three-armed and five-armed pieces here were cut from an individual ephyra. The process commenced within minutes. The wound at the cut site closed within the first hours. The arms gradually spread further apart, as the manubrium relocated to the center of the body. Within 18 h in this experiment, we observed fully symmetrical three-armed and five-armed ephyrae.

We call this process “symmetrization” to denote the recovery of radial symmetry, rather than regeneration of precise initial body parts, *e.g.*, the missing arms. Symmetrization was observed across amputation schemes. Fig. 2.2D shows symmetrical ephyrae that recovered from injury with two, three, four, five, six, and seven arms. Symmetrization even proceeded in grafting experiments: a foreign arm grafted onto a cut tetramer led to the formation of a fivefold symmetrical ephyra

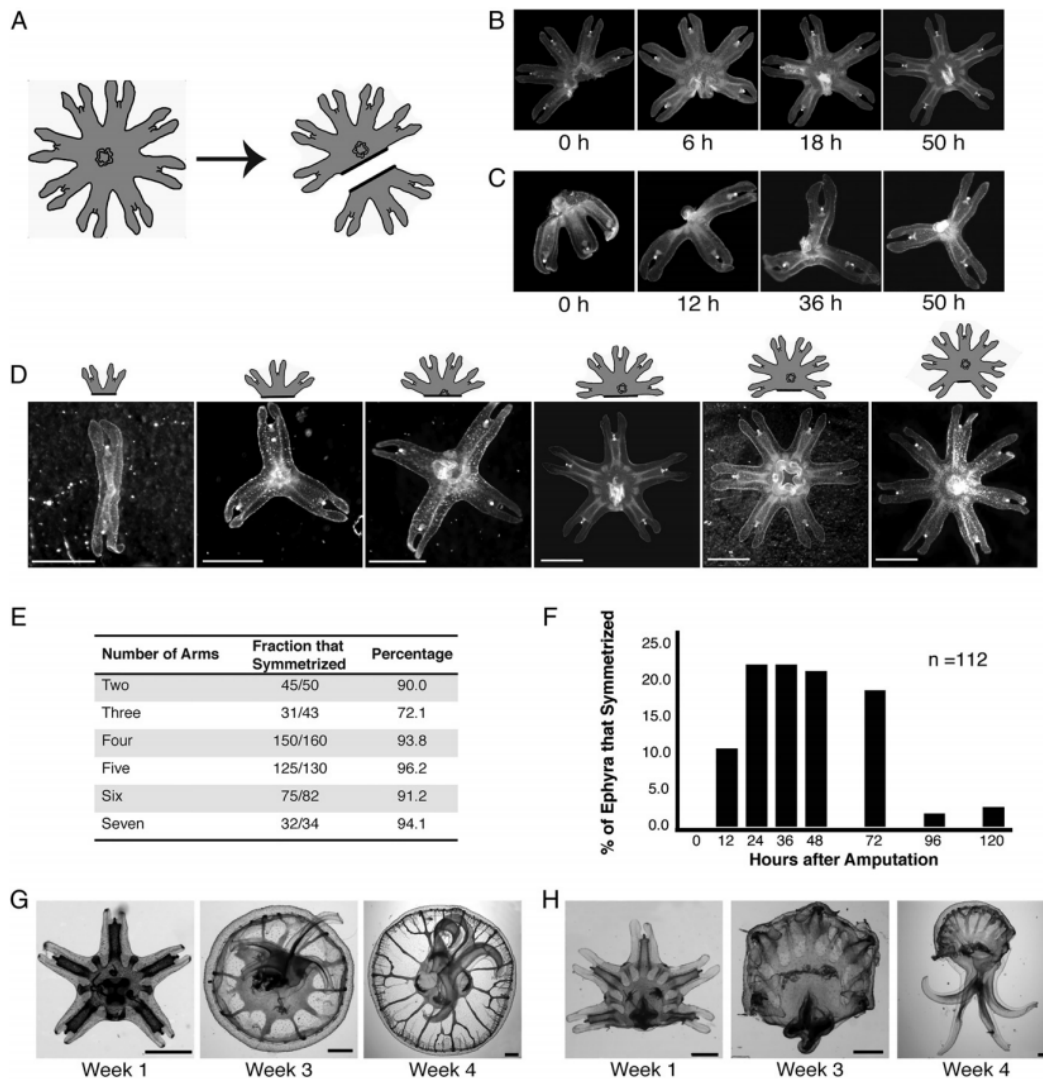


Figure 2.2: *Aurelia ephyra* reorganize existing arms to regain radial symmetry. (A) An example of amputation schemes used in the study. Cuts were performed across the body using a razor blade. (B and C) A three-armed and five-armed piece amputated from a single ephyra. Within 2 d, neither regenerated the lost arms. Instead, each reorganized to reform radial symmetry. (D) Symmetrization was observed with two, three, four, five, six, and seven arms. The cartoons indicate the initial forms after amputation. (E) Percentage of symmetrization across amputation schemes. The ephyrae in the amputation experiments were 1–3 d old (after strobilation) and were examined daily for 4 d. (F) Progression of symmetrization. In this experiment, we counted the number of ephyrae that symmetrized at the indicated time. Data were collected from dimers, tetramers, pentamers, and hexamers. There is a slight trend in the recovery speed across amputation scheme. The 12-h recovery is typical for dimers. Symmetrical tetramers and pentamers often started appearing by day 1 onward, as analyzed in more detail in Fig. 2.5H. (G and H) Ephyrae in these experiments were tracked individually for 1 mo, fed daily, and imaged every 2–3 d. (G) Pentamers that symmetrized continued growing into mature medusa ($n = 19$). (H) Pentamers that did not symmetrize grew abnormally with oversized manubria ($n = 10$). (Scale bar in each photograph: 1 mm.)

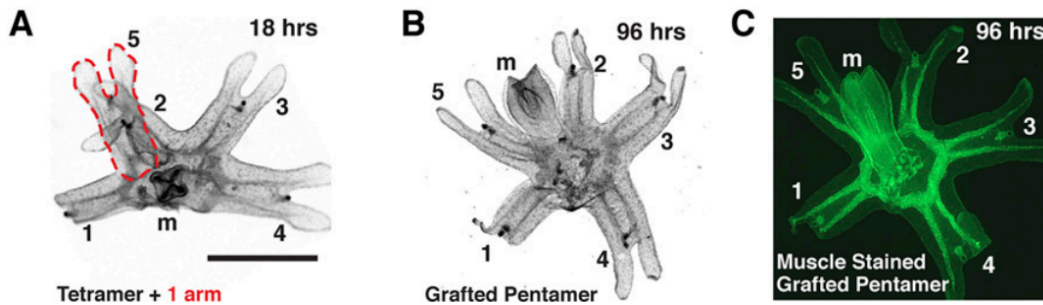


Figure 2.3: Symmetrization proceeded with foreign arms. (A) In this experiment, the ephyra was cut in half. Subsequently, an arm from another ephyra (outlined in red) was grafted to the tetramer, between arm 1 and 2. “m” indicates the manubrium. Grafting was performed by pinning the ephyra segments next to each other on an agarose plate (1% agarose, made with artificial seawater). Pinning was done using cactus spines (ones from columnar *Espostoa* sp. worked best). The ephyrae were kept pinned overnight (~12 h), unpinned the next morning, and allowed to recover in artificial seawater. (B) By 4 d, the patchwork ephyra had become symmetrical. The grafted arm is outlined in red. The location of grafting looked smooth, and the ephyra had healed without obvious scarring. The extra arm was incorporated seamlessly into the host tetramer. The resulting patchwork pentamer was symmetrical and pulsed synchronously. (C) Phalloidin staining shows that the axisymmetrical muscle was rebuilt, and muscle from the extra arm was connected seamlessly into the host ephyra (we discuss the muscle network in more detail in the main text and in Fig. 2.5)

(Fig. 2.3A-C).

Symmetrization occurred at high frequency (Fig. 2.2E). We amputated hundreds of ephyrae and observed frequency of symmetrization ranging from 72% to 96% across amputation schemes. In the ephyrae that did not symmetrize, the cut wounds simply closed, with little traces of the initial injury. The speed of recovery varied, but ephyrae typically symmetrized within 12 h to 4 d (Fig. 2.2F).

We tested whether ephyrae that regained radial symmetry could continue developing. Two- and three-armed ephyrae, which have no manubrium for feeding, did not develop further, and typically died within 2 wk. We observed pronounced effects in ephyrae with four to six arms. Ephyrae that reformed symmetry matured into medusae; developed gonads, full bells, and oral arms (Fig. 2.2E; $n = 19$); and showed active swimming (Movie S2.2). Ephyrae that remained asymmetrical developed shrunken bells and disproportionately large manubria (Fig. 2.2F; $n = 10$), and remained sunken at the bottom of the aquaria (Movie S2.2). These results suggest that regaining radial symmetry facilitates further development of injured ephyrae into adult medusae.

2.4 Symmetrization phenocopies developmental variation

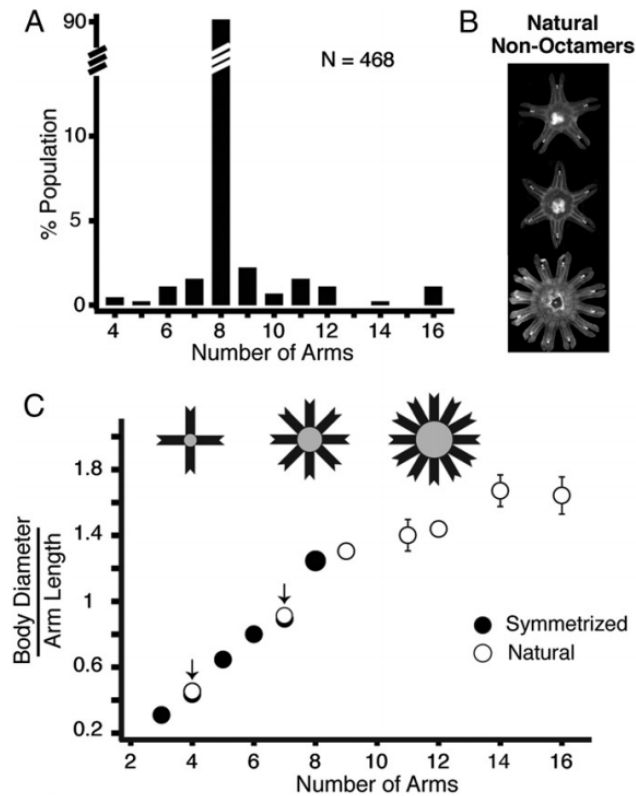


Figure 2.4: Symmetrization phenocopies developmental variation. (A) Nonoctamers form 9.5% of the *Aurelia* population in our laboratory. Ephyrae were scored immediately upon strobilation. This histogram come from multiple strobilae in a single strobilation round. A single strobila may produce 10–20 ephyrae, with variable numbers of arms. (B) A natural pentamer, hexamer, and dodecamer. (C) White circles: body size of natural ephyrae. Black circles: body size of ephyrae from symmetrization. Both plotted as a function of the arm number. The arrows indicate where there are both black and white circles overlapping. Body size was measured as the diameter (the gray region in the ephyra cartoons). We normalized body diameter to arm length (black regions of the ephyra cartoons), to account for variation across ephyrae. The ephyrae also grew in size over time; to account for this, we characterized the growth curve and normalized all measurements to 1-d-old ephyrae (Materials and Methods). A total of 46 ephyrae was measured to generate this plot. Error bars are SD from more than three ephyrae. Some error bars are not seen because they are smaller than the circles.

Interestingly, radially symmetrical nonoctamers have been observed in *Aurelia* populations in the wild [52–54], as well as cited by William Bateson [55] as an example of meristic variation, and they are not rare. Scoring freshly strobilated ephyrae, we observed that 9.5% of the ephyrae in our laboratory population are nonoctamers (Fig. 2.4A), consistent with a previous study in marine aquaria [56]. The natural nonoctamers range from having 4 to 16 arms and are capable of ma-

turing into medusae. These natural nonoctamers look indistinguishable from those recovering from the amputation experiments (Fig. 2.4B). Furthermore, we found that, in ephyrae, the body size scales with the number of arms and that this scaling is conserved between the natural and the amputated ephyrae (Fig. 2.4C). The conserved scaling is remarkable because the ephyrae were simply cut in the amputation experiments and the amount of body lost was variable, suggesting an active geometric regulation. These results show that symmetrization produces physiologically relevant morphologies, recapitulating those generated by developmental variation.

2.5 Symmetrization is not driven by cell proliferation, cell death, or muscle reconnection

Next, we investigated the mechanism that drives the recovery of radial symmetry. We did not find obvious requirement for global external input. Symmetrization proceeded in stagnant or moving water, in light or dark, and even when the ephyrae were pinned upside down. Symmetrization also occurred when the ephyrae were reared alone or in groups. Neither did we see an obvious global organizer within the body. As Fig. 2.2C shows, ribbons of two or three arms, missing the majority of the central body, recovered symmetry. Finally, symmetrization is not simply driven by wound closure. The wound closed within hours, preceding symmetry reformation. Moreover, the wound also closed in amputated ephyrae that did not symmetrize.

We next investigated other classes of mechanisms that could explain symmetrization. One possibility was that symmetrization might be driven by localized cell proliferation that could push the arms apart (Fig. 2.5A). Local cell proliferation in the *Drosophila* wing disk can generate global tension that rapidly drives changes in tissue shape [57, 58]. To mark cell proliferation, we used 5-ethynyl-2'-deoxyuridine (EdU), a thymidine analog that gets incorporated into newly synthesized DNA [59]. Fig. 2.5B shows EdU staining in the cut tetramers with no obvious localized patterns (the green EdU stain here reflects the cumulative DNA synthesis over 4 d). We saw similar staining in the uncut ephyrae (Fig. 2.6A). Denser stain was seen in the

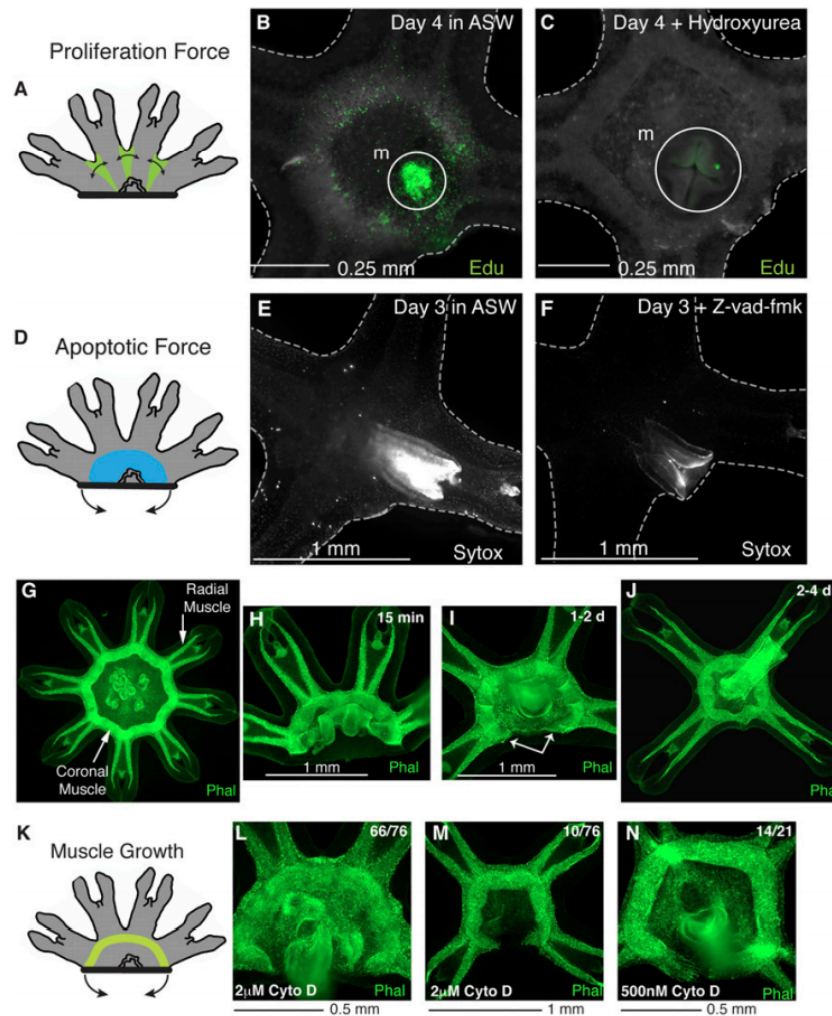


Figure 2.5: Symmetrization is not driven by cell proliferation, cell death, or muscle reconnection. (A–D) Is symmetrization driven by cell proliferation? (A) Localized cell proliferation (*e.g.*, in the green regions) may push the arms apart. (B) EdU stain (green) in a symmetrized tetramer, showing cumulative signal over 4 d. (C) EdU stain was abolished in the presence of 20 μM hydroxyurea. In this experiment, the cut ephyrae were incubated in EdU with or without 20 μM hydroxyurea for 4 d. The solution was refreshed daily. Ephyrae were fixed and stained on day 4 (Materials and Methods). (D–F) Is symmetrization driven by cell death? (D) Localized cell death (*e.g.*, in the blue region) may pull the arms into the cut site. (E) Sytox stain (white) in a symmetrized ephyra 3 d after amputation. (F) Sytox stain was abolished in the presence of a caspase inhibitor (100 μM Z-vad-fmk). Cut ephyrae were incubated in the inhibitor for 3 d, and then stained with Sytox (Materials and Methods). (G–J) Symmetrization is accompanied by reconnection of coronal muscle. (G) Staining of the musculature in an uncut ephyra. Muscle was visualized using phalloidin–Alexa Fluor 488 (Materials and Methods). (H–J) Staining of muscle in symmetrizing ephyrae. Ephyrae were fixed and stained at 15 min (H), 1 d (I), and 3 d after amputation (J). White arrows in K indicate the extending edges of the muscle. (K–N) Is symmetrization driven by muscle reconnection? (K) Reconnection of muscle (green) may pull the arms along. (L–N) Ephyrae were amputated, incubated in 2 μM (L–M) or 500 nM (N) cytochalasin D for 4 d, and then stained with phalloidin–Alexa Fluor 488

manubrium (circled) and rophalia. Moreover, when we blocked cell proliferation using 20 μM hydroxyurea, the EdU stain was largely abolished (Fig. 2.5C), and symmetrization progressed fully, and at a normal pace ($n = 40$). We observed the same results using another inhibitor of cell proliferation, 5-fluoroacil (10 μM ; $n = 40$).

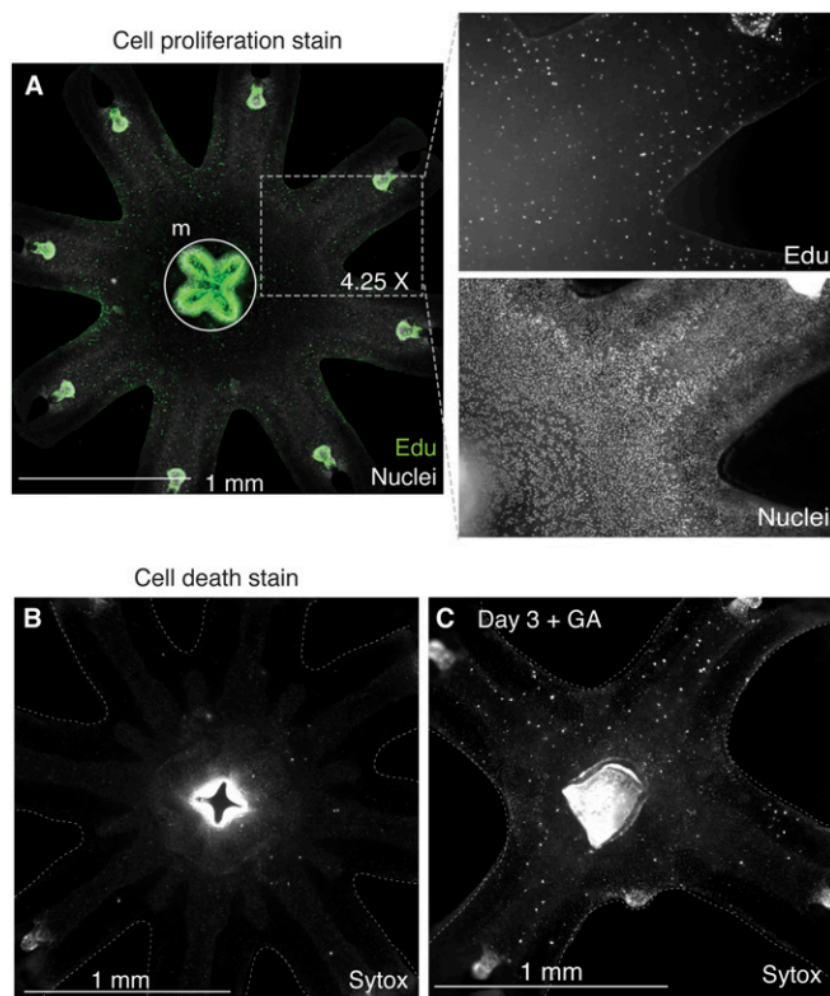


Figure 2.6: Cell proliferation and cell death stains. (A) EdU stain (green) in an uncut ephyrae. Total nuclei were stained using Hoechst (white). The magnified regions show the EdU and nuclear stain separately. The circle indicates the manubrium. (B) Sparse baseline Sytox stain (white) in an uncut ephyra. (C) Sytox stain was increased in the presence a caspase inducer (100 nM gambogic acid; $n = 19$ of 20). In this experiment, cut ephyrae were incubated in the chemicals for 1–3 d, and then stained with Sytox (Materials and Methods). The 1 μM gambogic acid was lethal to ephyrae, giving us an upper limit.)

Alternatively, symmetrization may be driven by localized cell death, creating a negative pressure space that pulls the arms around the body (Fig. 2.5D). Apoptosis

in *Drosophila* embryogenesis can produce forces that pull in neighboring cells [60]. We assessed cell death using Sytox, a DNA-binding dye that does not cross intact cell membranes and therefore only stains cells with compromised membranes, a proxy for dying cells. As a positive control, we saw high Sytox stain when we fixed the ephyrae (hence permeabilizing all cells), and when we treated the ephyrae with an apoptosis inducer (100 nM gambogic acid; Fig. 2.6; n = 19 of 20). Fig. 2.5E shows that there was little staining in the cut tetramers. We saw similarly little stain in uncut ephyrae (Fig. 2.6A). We stained every 24 h after amputation and did not see an increase in Sytox staining during symmetrization. High Sytox stain was seen in the manubrium and rophalia; both are regions of high EdU staining, indicating these are areas of high cell turnover. Finally, when we treated the ephyrae with a caspase inhibitor (100 μ M Z-vad-fmk), the Sytox stain was largely reduced (Fig. 2.5F, n = 17 of 20), and still symmetrization progressed normally.

Thus, neither cell proliferation nor cell death seems to play a significant role in driving the recovery of body symmetry. Symmetrization appears to be primarily driven by the reallocation of existing cells and tissues. What might be other sources of force that could mediate rebalancing of existing body parts? A prominent structure in the ephyrae is the striated musculature network [36, 60, 61]. Phalloidin staining in Fig. 2.5G shows actin enriched in the muscle, revealing the axisymmetrical architecture of the ephyra musculature, with a coronal ring in the central body, and radial rays extending into each arm. Fig. 2.5H shows a freshly cut tetramer, where the halved manubrium and the blunt muscle ends can be seen at the edge of the wound. Fig. 2.5I show how the ends of the coronal muscle gradually extended toward each other as the ephyrae symmetrized (see arrows), and reconnected to reform axisymmetrical musculature (Fig. 2.5J).

We asked whether the musculature network plays a role in symmetrization. First, we tested the idea that perhaps the muscle reconnection itself pulls the arms along into symmetrical positions (Fig. 2.5K). To block muscle reconnection, we treated the cut ephyrae with cytochalasin D, which inhibits actin polymerization.

Pretreatment with cytochalasin D (for 1 d before amputation) blocked the wound closure, and the ephyrae died. This suggests that wound closure requires actin dynamics and that wound closure is a necessary first step in symmetrization, even though it does not drive symmetrization because the wound also closes normally in unsymmetrized ephyrae. To avoid the lethal effects, in subsequent experiments, ephyrae were amputated first and then immediately incubated in cytochalasin D. Treated ephyra continued pulsing and feeding (as also observed in [62]), and the wound closed normally. At high doses of cytochalasin D (2 μ M), the vast majority of ephyrae failed to symmetrize (Fig. 2.5L; n = 66 of 76). Similar effects were observed with other actin inhibitors, dihydro-cytochalasin B (n = 20 of 20) at 750 nM and latrunculin A at 60 nM (n = 19 of 20).

The lower dose, however, is more revealing. At 500 nM, cytochalasin D treatment blocked reconnection of the coronal muscle (Fig. 2.5N), despite which the ephyrae often symmetrized (n = 14 of 21). In fact, we also observed this with 2 μ M cytochalasin D, but at a lower percentage (Fig. 2.5M; n = 10 of 76). Muscle reconnection therefore does not fully explain symmetrization, because ephyrae could symmetrize normally without it. We seem to have disentangled two effects here. The higher doses of cytochalasin D may reveal the more nonspecific effects on actin cytoskeleton beyond the muscle cells, possibly suggesting a role for actin dynamics in tissue repositioning (as has been proposed in other systems [63, 64]). The lower doses of cytochalasin D showed that actin polymerization is necessary for the reconnection of the coronal muscle but that this can be decoupled from, and more importantly does not drive, symmetrization.

2.6 Symmetrization is driven by muscle contractions in the propulsion machinery

To determine forces upstream of muscle reconnection, we turned to the muscle function itself. The jellyfish muscle network generates contractile forces that drive bell pulsation. This generates fluid flow that facilitates propulsion and prey capture

[48–50, 65]. Muscle filaments are located in the basal extension of the epitheliomuscular cells, embedded in the subumbrellar mesoglea, and receive inputs from the surrounding diffuse nervous systems and ganglionic pacemakers [36, 66]. To inhibit muscle contraction, we tested a number of muscle relaxants that were soluble in seawater (*e.g.*, tricaine, bezoncaine, urethane), and most of them were fatal within a day. However, two muscle relaxants, menthol and magnesium chloride, proved to be gentle enough: the ephyra remained alive in the anesthetics for >3 wk. Both anesthetics have been used in a number of studies in marine invertebrates [67–69] and are thought to modulate the excitation–contraction coupling by blocking voltage-gated ion channels [70, 71] that transmit electrical stimuli to the muscle.

In 400 μM menthol, all treated ephyrae were motionless and failed to symmetrize (Fig. 2.7A; $n = 60$ of 60). The arms remained asymmetrical, the manubrium remained at the edge, and the cut muscle remained blunt (Fig. 2.7B). The effect was reversible: ephyrae removed from menthol resumed symmetrization (Fig. 2.7C; $n = 20$ of 20). We observed the same complete inhibition of symmetry recovery with 2.5% (wt/vol) MgCl_2 ($n = 20$ of 20). Because motionless ephyrae could not feed effectively, we confirmed that all control-starved ephyrae symmetrized appropriately ($n = 20$ of 20). Thus, inhibiting muscle contraction completely blocked symmetrization. This argues that forces generated by muscle contraction during pulsation are necessary for symmetrization.

How might forces from muscle contraction drive the recovery of radial symmetry? To understand this, we consider muscle contraction in the context of its roles in propulsion. A stroke cycle in jellyfish consists of alternating fast muscle contraction (the power stroke), followed by a slow elastic response from the gelatinous mesoglea (the recovery stroke) (Fig. 2.7D; Movie S2.1 shows an ephyra swimming in seawater) [65, 72, 73]. Activation of the axisymmetric musculature produces symmetric bell contraction and a forward thrust. Recovery stroke, powered by the elastic aspects of the mesoglea, brings the bell to its original shape and generates a secondary thrust in the process. In ephyra, where there are discontinuous arms, a

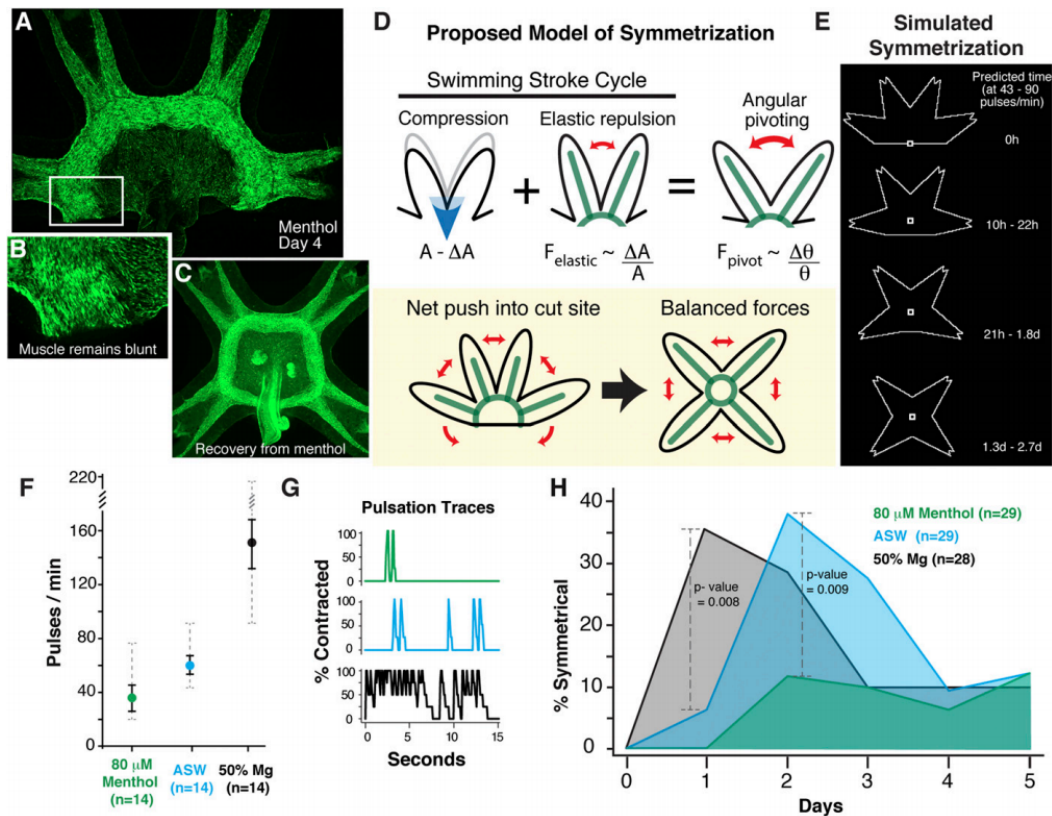


Figure 2.7: Symmetrization is driven by muscle contraction in the propulsion machinery. (A–C) Inhibiting muscle contraction blocks symmetrization. (A) Amputated ephyrae were incubated in 400 μM menthol for 4 d, and then stained with phalloidin. All treated ephyrae failed to symmetrize ($n = 60$ of 60). (B) A magnified view shows that the cut muscle remained blunt in the presence of menthol. (C) Ephyrae removed from menthol (after 4 d) resumed and completed symmetrization within 4 d ($n = 20$ of 20). (D and E) Proposed model of symmetrization. (D) A swimming stroke consists of muscle contraction, which generates compression, followed by elastic response from the mesoglea. We propose that, in the amputated ephyrae, this leads to angular pivoting into the cut site, as there is less bulk resistance. With repeated cycles of compression and elastic repulsion, the arms gradually relax into a more symmetrical state, until the forces are rebalanced. (E) Mathematical simulation of the symmetrization of a tetramer, taking into account the compression generated by the muscle contraction, the elastic response, and the ephyra geometry (see Supporting Information for details of the model). The predicted time of symmetrization is computed based on the pulsation frequency measured in seawater (Fig. 2.7F). (F–H) Frequency of muscle contraction dictates the speed of symmetrization. (F) Incubation in reduced MgCl_2 (50% of the normal seawater) increased the frequency of muscle contraction, whereas incubation in 80 μM menthol decreased the frequency of muscle contraction. The dashed gray line shows the full range of the data, whereas the black lines indicate 95% confidence intervals. (G) Sample traces of ephyra pulsation in normal seawater (blue), reduced magnesium (black), and 80 μM menthol (green). Frequency of muscle contraction was counted by hand from time-lapse movies taken at 15 fps. A single pulse typically takes 0.5 s. Full contraction was when the ephyrae fully closed in, and partial contraction was when the arms only contracted halfway. (H) Cut ephyrae were incubated in normal seawater (blue), seawater with reduced MgCl_2 (black), or 80 μM menthol (green), and scored every day for symmetrization.

continuous paddling surface is generated by viscous, overlapping boundary layers between the symmetrically arranged arms [48].

In such an interlinked system where the symmetry of the arm and muscle architecture is essential for driving propulsion, loss of symmetry would be immediately sensed through imbalance in the interacting forces. In uncut ephyrae, muscle contraction produces an axisymmetric compression that is balanced in all directions. In amputated ephyrae, where the geometric balance is disrupted, the asymmetrical compression from muscle contraction, followed by the elastic response, may intuitively produce a net angular pivoting of the arms into the cut site, where there is less opposing bulk (Fig. 2.7D). This is akin to squeezing an elastic ball at one end and producing a protrusion on the other side. With each cycle of compression and elastic repulsion, the arms may then relax to a new stable state. Through repetition of this cycle, the arms may gradually ratchet into the cut site, until the morphology is geometrically rebalanced (Fig. 2.7D).

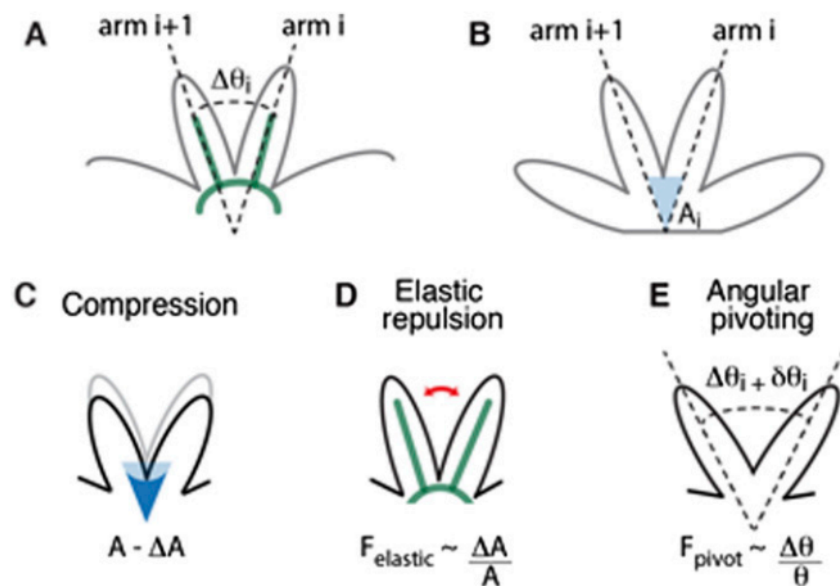


Figure 2.8: **Model geometry and coordinate.** (A) We consider a $\Delta\theta_i$, the angular span between arm i and arm $i + 1$. (B) The corresponding body area is denoted as A_i . Muscle contraction compresses the body by ΔA (C) and generates an elastic response (D), which in turn leads to angular pivoting of the arms (E).

To test this intuitive model, we built a mathematical model that considers forces

generated by the muscle contraction and the mesoglea elastic response, in the context of ephyra geometry (Fig. 2.8A-E). The dimensions of the ephyrae were measured directly, and the elastic and tensile modulus of the body were obtained from previous biomechanic studies[51, 74]. Simulation of the model (Fig. 2.7E and Movie S2.3) shows that interactions between these local forces can indeed recover global symmetry. Not only does the model recapitulate the symmetry recovery but it also captures the timescale of symmetry recovery, predicting a recovery time of 1.3–2.7 d (see Supporting Information for detailed calculation). The force–balance model makes a prediction: the speed of symmetrization is proportional to the frequency of muscle contraction. If the ephyrae pulse more often, they will symmetrize faster.

To test the model prediction, we use gentle perturbations to modulate the frequency of muscle contraction in the ephyrae. Muscle contraction can be stimulated by reducing magnesium concentration in seawater, as was also observed in ref. [75]. Fig. 2.7 F–H shows that a 50% reduction in magnesium ions (referred to as “reduced Mg”) increased the frequency of contraction in ephyrae (shown in black; also see Movie S2.4, with the control in Movie S2.4). Under this increased frequency of muscle contraction, symmetrization proceeded faster (Fig. 2.7H; $n = 28$). Within a day, 36% of ephyrae in reduced Mg symmetrized, higher than the 7% in ASW (P value < 0.01). In the parallel experiment, we slowed down muscle contraction by treating ephyrae with 80 μ M menthol. Under this condition, the ephyrae pulsed less frequently (shown in green in Fig. 2.7 F–H and Movie S2.4) and symmetrized more slowly (Fig. 2.7H; $n = 29$). By day 2, only 14% of ephyrae symmetrized in 80 μ M menthol, compared with 38% in ASW (P value < 0.01). As predicted by the model, the speed of symmetrization indeed correlates with the frequency of muscle contraction. Higher frequency of muscle contraction delivers more work per unit time and drives faster symmetrization.

Moreover, the simple model captures the orders of magnitude of the observed symmetrization time. In reduced Mg, they pulse 92–215 per min (Fig. 2.7F), which predicts a symmetrization time of 13 h to 1.25 d (see Supporting Information

for detailed calculation). This corresponds nicely with the observed peak at day 1 in reduced Mg (Fig. 2.7H). In 80 μM menthol, they pulse 20–76 per min (Fig. 2.7F), which the model predicts would have a symmetrization time of 1.5–5.8 d, corresponding to the broad spread we see in the menthol experiment (Fig. 2.7H).

The correlation between pulsation rate and symmetrization speed supports the idea that muscle contraction plays a dominant role in driving symmetrization. One potential caveat here is that menthol and magnesium may also affect ion flow in nonmuscle cells. To further confirm the specific role of muscle contraction, we used two different inhibitors of skeletal muscle myosin II, N-benzyl-p-toluene sulfonamide (BTS) and 2,3-butanedione monoxime (BDM) [76, 77]. Similar to those treated with menthol and reduced Mg, the myosin-inhibited ephyrae were also incapable of pulsing and survived for over a week in the treatment. We saw no symmetrization in ephyrae incubated in 150 μM BTS (n = 40 of 40) or 25 mM BDM (n = 40 of 40), as shown in Fig. 2.9. Examining phalloidin staining in these ephyrae showed blunt coronal muscle on the cut edge, indistinguishable from those incubated in 400 μM menthol (compare Fig. 2.9 to Fig. 2.7).

Finally, might recovering symmetry, rather than precise body parts, be a more general strategy across Scyphozoa? The Scyphozoa class in Cnidaria encompasses some 200 extant species, the majority of which undergo an ephyra stage. Despite the morphological diversity of the adult medusae, the ephyrae across species are incredibly similar, in anatomy, in musculature, and in size (most known ephyrae range between 3 and 5 mm; ref. [53]). Indeed, we observed symmetrization in *Chrysaora pacifica*, *Mastigias sp.*, and *Cotylorhiza tuberculata* (Fig. 2.10). Halved ephyrae of these species did not regenerate lost arms, but reorganized and regained radial symmetry within 1–4 d. Together with our observations in *Aurelia*, this suggests that symmetrization is present across two major orders of the Scyphozoa (order Semaestomeae and Rhizostomeae).

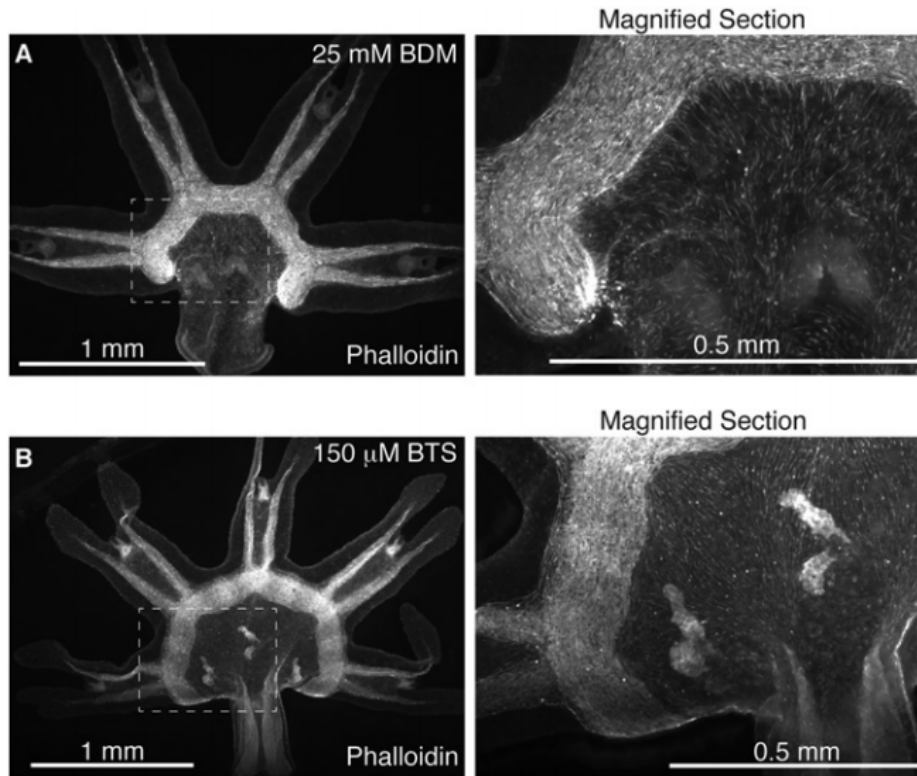


Figure 2.9: Inhibitors of skeletal myosin II blocks symmetrization. In this experiment, the ephyrae were cut, and then incubated in (A) 2,3-butanedione monoxime (BDM) (25 mM) or (B) N-benzyl-p-toluene-sulfonamide (BTS) (150 mM). In both inhibitors, the ephyrae did not pulse and remained asymmetrical throughout the 4-d treatment, and the coronal muscle remained blunt ($n = 40$ of 40 for BDM; $n = 40$ of 40 for BTS). The phalloidin staining was performed on day 4 after amputation.

2.7 Discussion

We describe in this study a strategy of self-repair in jellyfish, where, in response to severe injuries, *Aurelia* ephyrae do not regenerate lost parts or simply close the wound; rather, the organisms reorganize existing parts and recover body symmetry. The absence of regeneration of arms is interesting in light of the fact that *Aurelia* is capable of regeneration—*Aurelia* polyps can regenerate from a single polyp tentacle [47]. It appears that rapidly regaining body symmetry, rather than precise body parts, may be more critical in the free-swimming ephyrae.

Radial symmetry in jellyfish is essential for propulsion, and it is interesting that the propulsion machinery intrinsically facilitates both sensing the loss of symmetry,

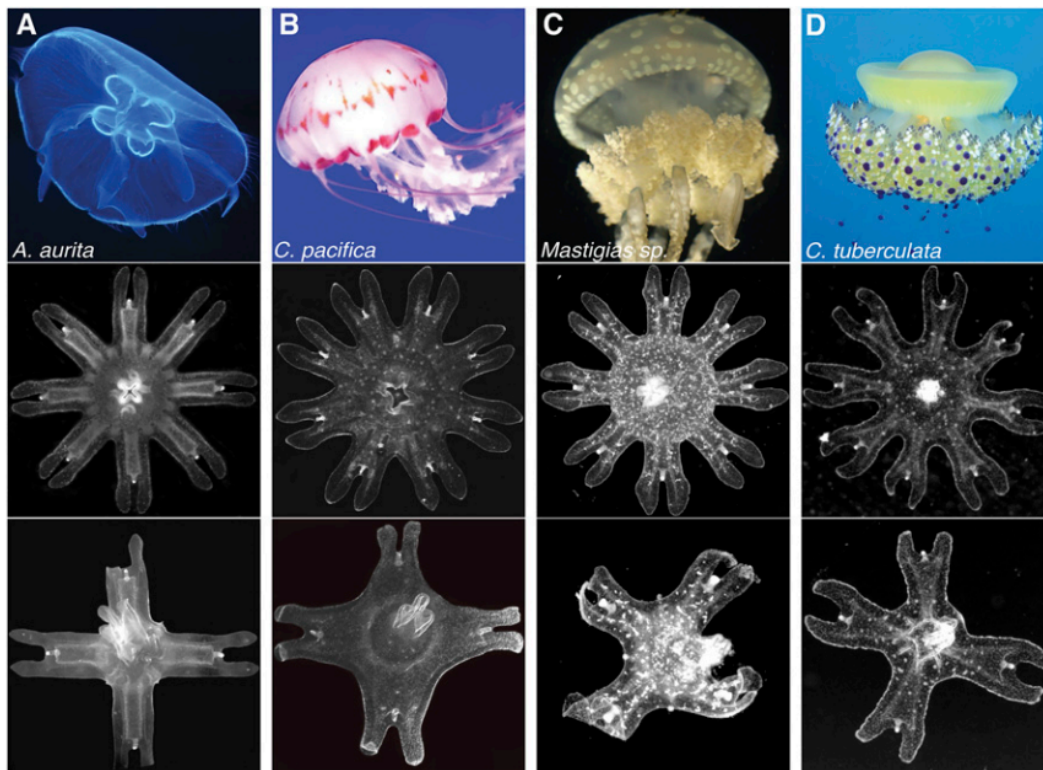


Figure 2.10: Symmetrization was observed across four species of Scyphozoan jellyfish. (A) The moon jellyfish *Aurelia aurita*. Image courtesy of Wikimedia Commons/Hans Hillewaert. Image © Hans Hillewaert. (B) The sea nettle *Chrysaora pacifica*. Image courtesy of Sofi Quinodoz. (C) The lagoon jellyfish *Mastigias* sp. Image courtesy of Wikimedia Commons/Captmondo. (D) The Mediterranean jellyfish *Cotylorhiza tuberculata*. Image courtesy of Wikimedia Commons/Antonio Sontuoso. For each column, row 1 shows the adult medusa, row 2 shows the uncut ephyra, and row 3 shows the symmetrized tetramer from amputation. Freshly strobilated ephyrae were cut in half and allowed to recover in seawater. Symmetrized tetramers were observed within 4 d in all species.

and the repair of symmetry. Symmetrization does not require making new cells or losing cells through programmed death. Instead, it is clear from our work that mechanical forces play the dominant role in this self-repair process. Rather than activating a special module, self-repair in jellyfish uses constitutive physiological machinery. It will be interesting next to investigate the molecular underpinnings that transmit forces from muscle contraction into tissue reorganization. Our data indicate the roles of actin polymerization. As mechanical forces and cytoskeletal dynamics are increasingly implicated in morphogenesis, symmetrization in *Aurelia* with discrete geometry, clear morphological readout, and amenability to molecular tools, may emerge as a model system for probing such questions. Moreover, we

observed that a given polyp generated ephyrae with a variable number of arms. It will be interesting to investigate whether mechanical forces play a role during development to maintain symmetry and facilitate the generation of natural variation.

The lack of an increase in cell proliferation during symmetrization partially brings to mind wound healing in the hydromedusa *Polyorchis penicillatus* [78], which relies on cell migration rather than cell proliferation for wound closure, as well as morphallaxis in *hydra*, in which lost structures are regenerated without increase in cell proliferation [7, 40, 79, 80]. Our study therefore suggests a potentially interesting pattern: there is evidence of three strategies of self-repair in cnidarians that do not require cell proliferation: one for simple wounding healing (*P. penicillatus*), another to restore lost parts (in *Hydra*), and now one that restores functional symmetry without restoring lost parts (in *Aurelia*).

Our findings also connect to the theories surrounding the role of self-repair across animals. In essence, symmetrization appears to fulfill the utilitarian imperative - when the arms are made dysfunctional, their reorganization does not occur. Simultaneously, symmetrization could be the unintended positive outcome, an epiphenomenon, of wound healing and mechanical forces operating in a viscoelastic material, combining to form an adaptive self-repair program. It is difficult to know how symmetrization came to be, but there is no question that ephyrae that fail to symmetrize do not thrive.

Two points have not been explicitly addressed in our model. First, the ratchet aspect of symmetrization. Over hours or days, the arms gradually move into the cut site, until symmetry is fully regained. The mesoglea is a viscoelastic material that produces an elastic response over short timescales but behaves like a viscous fluid over longer time periods [51, 74, 81, 82]. Therefore, the ephyrae behaves like an elastic object in responding to fast muscular compression, and we speculate that the viscous aspect of the mesoglea may then help relax the organism to a new state with the arms slightly repositioned into the cut site. Symmetrization relies as much on the force-generating muscle machinery as on the material properties of the

reorganized tissues. Second, it is striking that, in all of our amputation experiments, the recovering ephyrae remained planar. One way we successfully broke planarity was by removing the manubrium altogether. These ephyrae recovered to a bilaterally symmetrical fan shape (Fig. 2.11A), or a spiral shape (Fig. 2.11B). The manubrium, lined with muscle and connected to the body through a dense actin-rich network, may plausibly act as a source of rigid planarity.

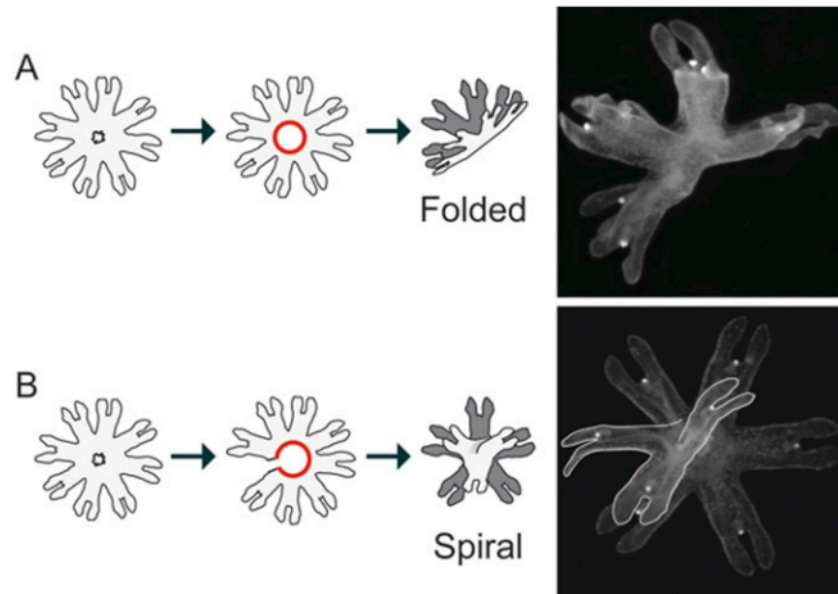


Figure 2.11: Removing the manubrium broke planarity. (A) Punching out the manubrium led the ephyrae to adopt a fan shape. We used a P200 pipette tip to make a clean hole and removed the entire manubrium. (B) Punching out the manubrium and linearizing the ribbon led the ephyrae to adopt a spiral shape, with threefold symmetry stacked on fivefold symmetry. The new symmetry was observed within 1–4 d after amputation. The ephyrae pulsed synchronously and remained alive for over 3 wk until the experiment was ended.

Our study suggests a different framework to reinterpret previously reported lack of regeneration in other marine invertebrates. In Hydrozoa, Hargitt suggested in 1897 that injured hydromedusae (*Gonionemus vertens*) did not regenerate but instead recast themselves into “a morphological equivalent of their original form” [83]. In Ctenophores, Coonfield noted in 1936 that, although ~50% of ctenophores (*Mnemiopsis sp.*) regenerated after quartering, the other 50% did not regenerate but rather “rounded up and behaved as normal animals” [84]. Our work establishes the lack of regeneration in Scyphozoa, demonstrates reorganization to recover body

symmetry as an active process that facilitates growth and development, and presents the underlying mechanism. Symmetrization is an agile strategy: it proceeds from various starting conditions, it uses constitutive physiological machinery, and it is fast and plausibly energy conserving (as it does not require new cells). It will be interesting to test whether symmetrization has evolved as a parallel or alternative strategy to regeneration across radially symmetrical animals.

Finally, beyond biology, the finding of a self-repair strategy that is mechanically driven may inspire biomimetic materials and technologies that aim to self-repair functional geometries, without regenerating precise shapes and forms.

2.8 Materials and Methods

ASW preparation

ASW is prepared at 32 ppt from prepared from Instant Ocean mix using deionized water. For experiments in Fig. 2.7, magnesium-free ASW was made using recipe 4 in table 3A in the Marine Biological Laboratory Recipe Book [85] and was mixed with regular ASW from the same recipe book to vary magnesium concentration.

Jellyfish Nursery

Aurelia aurita polyps were obtained from the Cabrillo Marine Aquarium (San Pedro, CA) and strobilated in the laboratory. Polyps, ephyrae and medusae were reared at 54 °F in Kreisel tanks (Midwater Systems and ones we built in the laboratory). The colony was fed daily with brine shrimps (*Artemia nauplii*) enriched with *Nannochloropsis* algae. Polyps were occasionally fed L-type rotifers (*Brachionus plicatilis*). To induce strobilation, we used temperature or chemical induction. For temperature-induced strobilation, polyps growing at 54 °F were moved to 68 °F for 2–3 wk, and then returned to 54 °F. Strobilation typically occurred 2–3 wk after. For chemical-induced strobilation, we used the recent finding in ref. [86]. Polyps were incubated in 50 mM 5-methoxy-2-methyl-indole (Sigma; M15451) at

68 °F and replaced daily. Strobilation typically occurred 1 wk after. *Chrysaora pacifica*, *Mastigas sp.*, and *Cotylorhiza sp.* polyps were obtained from the Monterey Bay Aquarium (Monterey, CA). *C. pacifica* was reared at 54 °F, and the other species at 68 °F. *C. pacifica* and *Mastigas sp.* strobilation happened naturally in the laboratory. Strobilation in *Cotylorhiza sp.* was induced using 50 mM 5-methoxy-2-methyl-indole at 68 °F.

Amputations were performed using a single-edged industrial razor blade. Ephyrae were anesthetized using 0.08% MS-222 or 400 µM menthol. Each ephyra was anesthetized for 2–5 min, amputated, and then returned to ASW. Recovering ephyrae were maintained in an HAG rotator (FinePCR), altered to continually rotate 50-mL Falcon tubes at 7–10 rpm. Ten to 20 ephyrae were placed in each tube. Feeding was performed daily unless otherwise noted. For quick chemical screenings, ephyrae were reared in six-well plates.

Treatment with Inhibitors or Activators

For each treatment, we first screened a wide range of doses to determine the effective doses. Ephyrae were amputated, and then placed in ASW with the inhibitor or activator, at the concentration indicated below. Solutions were changed daily. Ephyrae were tracked between 4 and 14 d. Ephyrae were not fed during the treatment, and we confirmed that starved ephyrae symmetrized at the same rate as fed ephyrae. Specifically, hydroxyurea (Sigma; H8627) was used at 20 µM, 5-fluorouracil (Sigma; F6627) at 10 µM, Z-vad-fmk (APEX-BIO; A1902) at 100 µM, gambogic acid (Sigma; G8171) at 100 nM, menthol (Sigma; M2772) at 80–400 µM, cytochalasin D (Sigma; C8278) at 500 nM to 2 µM, dihydrocytochalasin B (Sigma; D1641) at 750 nM, latrunculin A (Sigma; L5168) at 60 nM, BTS (Millipore; 203895) at 150 µM, and BDM (Sigma; B0753) at 25 mM.

Staining Protocol

All steps were performed at room temperature, unless indicated otherwise. Nuclei were stained using Hoechst 33342 (Sigma; B2261) at 1:10 concentration, and 30-min incubation in the dark. For costaining, Hoechst staining was done at the end of the procedure before imaging. Actin was stained using Alexa Fluor 488 Phalloidin (Life Technologies; A12379) at 1:20 concentration. Ephyrae were first anesthetized. This step ensured that the ephyrae would not curl when they were fixed. Ephyrae were next fixed in 3.7% (vol/vol) formaldehyde for 15 min, washed in PBS, permeabilized in 0.5% Triton/PBS for 5 min, washed in PBS, and then blocked using 3% (wt/vol) BSA for 1–2 min. Ephyrae were then incubated in 1:20 phalloidin solution (in PBS) for 1–2 h in the dark, washed in PBS, and imaged.

Dead cells were stained using Sytox Orange (Life Technologies; S34861). Ephyrae were incubated in 1:1,000 Sytox solution (in ASW) for 30 min in the dark at room temperature, and then thoroughly washed with ASW and immediately imaged.

Proliferating cells were stained using Click EdU Alexa Fluor 594 (Life Technologies; C10339) according to the protocol, with the following modifications: Ephyrae were incubated in 15 mL of 1:1,000 EdU in ASW, in the dark, for 24–96 h. In the following steps, a total volume of 10 mL was used in each step. Ephyrae were washed in ASW for 1 h, fixed in 3.7% (vol/vol) formaldehyde/PBS for 15 min, washed in PBS, blocked with 3% (wt/vol) BSA/PBS, permeabilized in 0.5% Triton X-100/PBS for 20 min, and washed in PBS. Ephyrae were then placed in 500 μ L of the Click-iT reaction mixture, incubated for 30 min in the dark, followed by washes, and were immediately imaged.

Except for Sytox, all stained ephyrae could be stored in PBS at 4 °C in the dark, for at least 2 wk without significant loss in signal.

Imaging

Dark-field, bright-field, and fluorescent ephyrae were imaged using the Zeiss AxioZoom.V16 stereo zoom microscope equipped with an AxioCam HR 13-megapixel camera, and processed using the Zen software. Optical sectioning of the thick samples and removal of out-of-focus light scattering were performed using the Apo-Tome.2 module. To facilitate imaging, ephyrae were typically imaged anesthetized in MS-222 or menthol. Coverslips were sometime used to hold ephyrae in place for better image quality. Movies were captured using CamStudio.

Allometry Measurement and Age Correction

For each data point, at least three ephyrae were measured. For every ephyra, the body diameter and three arm lengths were measured. Body diameter was measured by fitting a circle to the body (Fig. 2.12). Arms were measured to the intersection of the body and the arm. Ephyrae increase in size over time. To account for this, we characterized the growth in body diameter with age. With this correlation, we normalized all measurements to 1-d-old ephyrae.

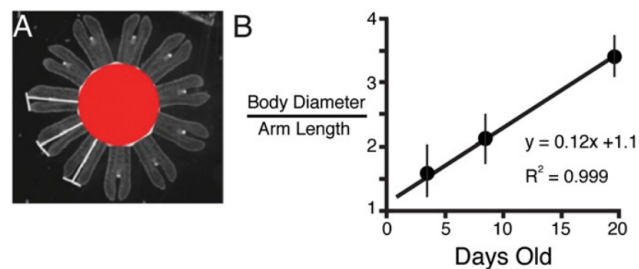


Figure 2.12: **Correlation of age and size.**(A) Line indicates arm length. Red area indicates the body. (B) Body size increases linearly with age. Error bars were from more than three biological replicates and technical replicates.

Ephyrae Grafting

To generate grafted ephyrae, ephyrae segments must heal together. This was achieved by pinning the ephyrae segments next to each other and allowing them to heal together for ~12 h. Ephyrae were pinned on 10-mL Petri dishes filled halfway

with 1% agarose/ASW. These dishes were allowed to cool and were then filled with ASW. A donor ephyrae was anesthetized in 400 μ M menthol in ASW, and arms were amputated and stored in menthol ASW until grafting. Host ephyrae were then halved in menthol ASW to produce nonsymmetrical tetramer ephyrae. The host ephyrae were then pinned on an agarose dish, to which an arm was then pinned. Pinning was accomplished using cactus spines from *Espostoa mirabilis*. Ephyrae were kept pinned overnight (~12 h) in ASW. The next day, they were unpinned and allowed to recover.

Muscle Contraction Modulation. Menthol (Sigma; M2772) was dissolved in ASW to make 20–400 μ M working solutions. MgCl₂ at 2.5% (wt/vol) was prepared in ASW. Magnesium-free ASW was made using recipe 4 in table 3A in ref. [AswBB] and was diluted in ASW to make 1:1 to 1:10 final working concentrations. Ephyrae were amputated in an anesthetic and maintained in ASW plus inhibitor for 4 d in six-well plates or rotisserie. For recovery experiments, we waited for 4 d, and then ephyrae were moved back to ASW.

2.9 Supporting Information

A Mathematical Model Describing Forces in Jellyfish Propulsion Captures the Recovery of Global Symmetry

How does muscle contraction drive symmetry recovery? Here, placing muscle contraction in the context of its function in propulsion and the ephyra geometry, we show that consideration of forces that normally operate in propulsion can explain the recovery of radial symmetry in injured ephyrae.

Mathematical Formulation

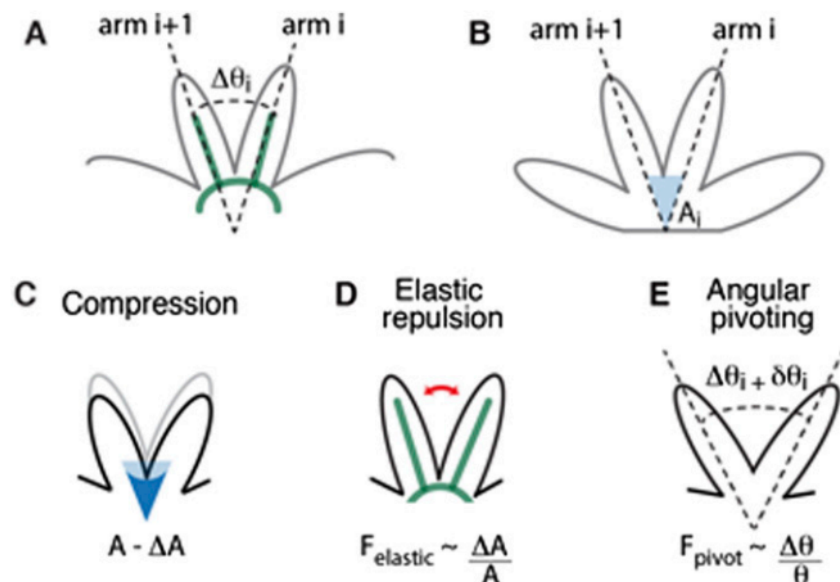


Figure 2.9: Model geometry and coordinate. (A) We consider a $\Delta\theta_i$, the angular span between arm i and arm $i + 1$. (B) The corresponding body area is denoted as A_i . Muscle contraction compresses the body by ΔA (C) and generates an elastic response (D), which in turn leads to angular pivoting of the arms (E).

The components of the model are established properties of swimming pulsation (contraction and elastic response) and parameters measured directly in ephyrae (body dimensions, frequency of contraction, and percentage change of body area in response to muscle contraction). We model the angular movement of each arm with respect to the geometrical center of the body. Fig. 2.8 illustrates the model coordinates. $\Delta\theta_i$ is the angular span between the i th arm and the $(i + 1)$ th arm (Fig.

2.8A), where the corresponding body area is denoted as A_i (Fig. 2.8B). Contraction leads to a change in the body area, ΔA (Fig. 2.8C), which in turns generates an elastic response, described using the Hooke's law:

$$F_{elastic} = k_C \frac{\Delta A}{A_i},$$

[S1]

where k_C is the elastic modulus of the body materials. This elastic force results into angular pivoting of the arms (Fig. 2.8D), as there is less resistance in the amputated site:

$$F_{pivot} = k_T \frac{\delta \theta}{\Delta \theta_i},$$

[S2]

where k_T is the tensile modulus of the body. Combining Eqs. S1 and S2, we have the force balance on the i th arm:

$$k_C \frac{\delta A}{A_i} = k_T \frac{\delta \theta}{\Delta \theta_i}.$$

[S3]

The new steady-state angle $\Delta \theta_i$ after every contraction cycle can be described analytically by integrating Eq. S2:

$$\theta_{i,new} = \theta_{i,old} \left(e^{\frac{k_C}{k_T} \times \frac{\Delta A}{A_i}} - 1 \right) + \theta_{i,old}.$$

[S4]

Simulation.

To solve the model, we estimated some parameters directly in the ephyrae: the body diameter was set at 1 mm, arm length was set at 1 mm, and the swimming contraction (coded as a sinusoidal function) was set at $\sim 0.5\text{--}4$ pulses per s (see measurements in Fig. 2.7F and G). The compressive elastic modulus of the body, k_C , was set at 20 Pa (based on measurements in refs. [74] and [51]). The tensile modulus of the body, k_T , was set at 1 MPa (based on measurement in ref. [74]). Movie S2.3 (www.youtube.com/watch?v=VpWf74BkAbE&feature=youtu.be) shows the resulting model simulation. Every cycle of contraction and elastic recoil generates a net push into the cut site. With every cycle, the ephyra relaxes into a new stable configuration where the arms go slightly into the cut site. This continues until spacing between the arms is rebalanced. Matlab codes are available upon request. Thus, the mathematical model consisting of known mechanical properties of swimming pulsation can recapitulate the recovery of global symmetry. Furthermore, the mathematical model also recapitulates the timescale of symmetry recovery. Eq. S4 gives the angular pivoting per cycle as follows:

$$\frac{\theta_{i,new} - \theta_{i,old}}{\theta_{i,old}} = \left(e^{\frac{k_C}{k_T} \times \frac{\Delta A}{A_i}} - 1 \right) \Delta N, \quad [\text{S5}]$$

where N is the number of contraction cycles. Because $\frac{k_C}{k_T}$ is small ($\sim 10^{-5}$), Eq. S5 can be approximated as follows:

$$\frac{d\theta_i}{\theta_i} = \left(e^{\frac{k_C}{k_T} \times \frac{\Delta A}{A_i}} - 1 \right) dN. \quad [\text{S6}]$$

Then, for a tetramer, the total number of cycles N required to change $\Delta\theta_i$ from $\frac{\pi}{4}$ (the initial configuration) to $\frac{\pi}{2}$ (the final symmetrized configuration) is as follows:

$$N\left(e^{\frac{k_C}{k_T} \times \frac{\Delta A}{A_i}} - 1\right) = \int_{\frac{\pi}{4}}^{\frac{\pi}{2}} \frac{d\theta_i}{\theta_i} = \ln 2.$$

[S7]

The time T to recover symmetry can therefore be analytically derived as follows:

$$T = \frac{\Delta \ln 2}{\left(e^{\frac{k_C}{k_T} \times \frac{\Delta A}{A_i}} - 1\right)} \approx 47 \Delta t \text{ hours.}$$

where ΔT is the period of a contraction cycle (in seconds), or the inverse of frequency (in pulses per s). The estimated pulse frequency of an ephyra swimming in artificial seawater is 0.7–1.5 pulses/s (Fig. 2.7 E–G). Eq. S8 then predicts a symmetrization time ranging from 1.3 d – 2.7 d, which corresponds to what we typically observed in ephyra (Fig. 2.2F).

The frequency of the contraction cycle effects the elastic and viscous moduli, though for *Aurelia*, their frequency of muscle contractions is such that their mesoglea is much more elastic than viscous [51]. We tested our model for the effect of contraction frequency within the range we observed, from 1/1.5 - 1/1.7 pulses per second, and variations in the elastic modulus, varying from 10 - 50 pascals, described in ref. [51]. To recover symmetry, variation in pulsation alone produces a range of 1.3 to 2.9 days, while the elastic modulus alone produces a range of 0.8 to 4 days. Together, using the extremes for both pulse frequency and the elastic modulus, we find a range of 0.5 to 6 days. This represents a scenario where the two values are fully correlated. We also tried a different approach where we assumed that these ranges represented 95% of the observed variability, i.e. 2 standard deviations of a normal distribution. In this case, 95% of the resulting symmetry times fall within 0.6 to 4 days. This approach assumes the two variables are fully independent, and hence we see a lower final variability. Importantly, the scenarios we tested indicate that our model recapitulates the observed range in symmetrization speeds.

2.10 Supplemental Movies

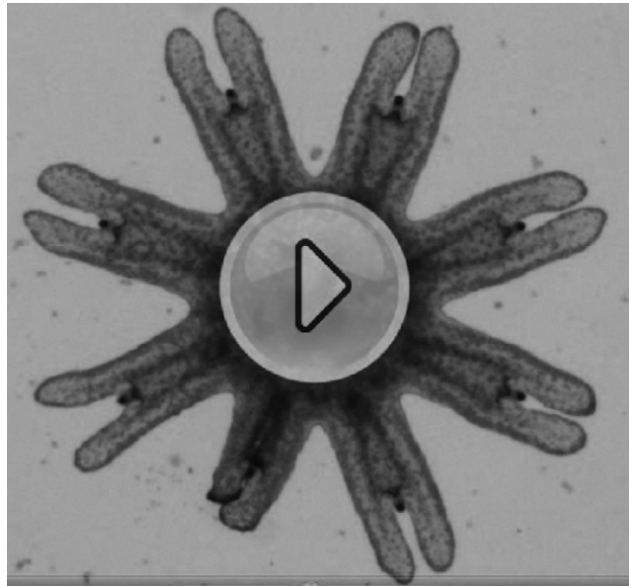


Figure Movie S1: An *Aurelia* ephyra swimming in seawater. A 1-d-old ephyra. The movie is in real time. The movie can also be viewed through the following YouTube link: www.youtube.com/watch?v=fdFkjwWrI-U&feature=youtu.be.

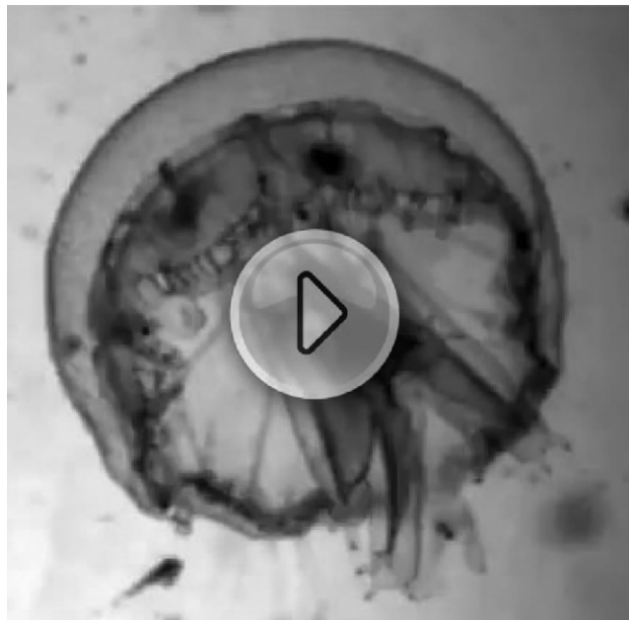


Figure Movie S2: An *Aurelia* ephyra swimming in seawater. A 1-d-old ephyra. The movie is in real time. The movie can also be viewed through the following YouTube link: www.youtube.com/watch?v=fdFkjwWrI-U&feature=youtu.be.

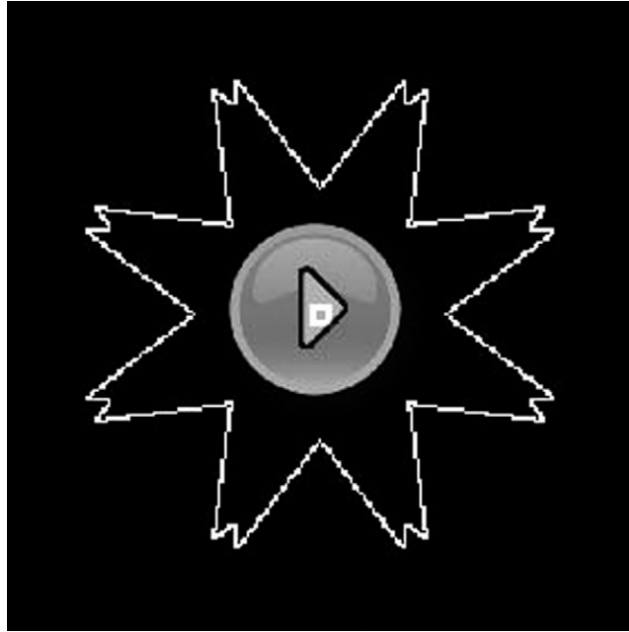


Figure Movie S3: Simulation of a tetramer symmetrizing using our mathematical model. Every cycle of contraction and elastic recoil generates a net push into the cut site. With every cycle, the ephyra relaxes into a new stable configuration where the arms go slightly into the cut site. This continues until spacing between the arms is rebalanced. Matlab codes are available upon request. The movie can also be viewed through the following YouTube link: www.youtube.com/watch?v=VpWf74BkAbE&feature=youtu.be.

References

- [1] Michael J Abrams et al. “Self-repairing symmetry in jellyfish through mechanically driven reorganization”. In: *Proceedings of the National Academy of Sciences* 112.26 (2015), E3365–E3373.
- [2] Jian-Kan Guo and Lloyd G Cantley. “Cellular maintenance and repair of the kidney”. In: *Annual review of physiology* 72 (2010), pp. 357–376.
- [3] Jennifer L Shadrach and Amy J Wagers. “Stem cells for skeletal muscle repair”. In: *Philosophical Transactions of the Royal Society of London B: Biological Sciences* 366.1575 (2011), pp. 2297–2306.
- [4] Jamie I Morrison et al. “Salamander limb regeneration involves the activation of a multipotent skeletal muscle satellite cell population”. In: *The Journal of cell biology* 172.3 (2006), pp. 433–440.
- [5] Jeremy P Brookes and Phillip B Gates. *Mechanisms underlying vertebrate limb regeneration: lessons from the salamander*. 2014.

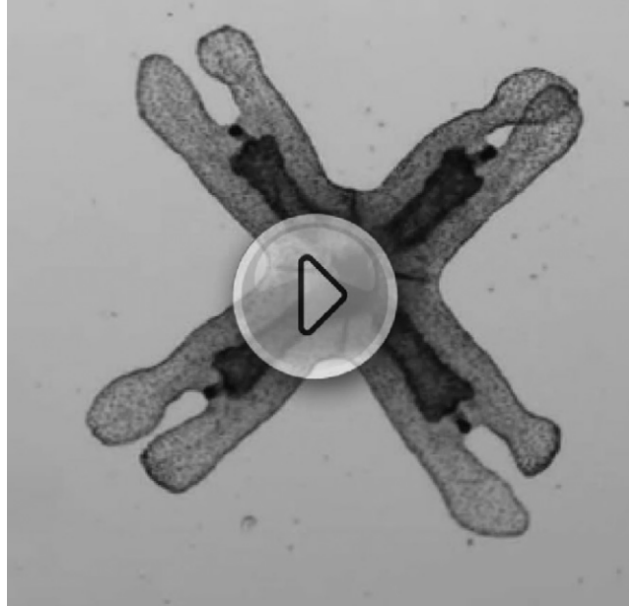


Figure Movie S4: Frequency of muscle contraction dictates the speed of symmetrization. The movies are in real time. Part 1: Tetramer swimming in seawater. Part 2: Tetramer swimming in seawater with reduced $MgCl_2$ (50% of the concentration in normal seawater). Part 3: Tetramer swimming in seawater with $80 \mu M$ menthol. The movie can also be viewed through the following YouTube link: www.youtube.com/watch?v=DxrNW0qcWy4&feature=youtu.be..

- [6] Yaoyao Chen, Nick R Love, and Enrique Amaya. *Tadpole tail regeneration in Xenopus*. 2014.
- [7] Peter W Reddien and Alejandro Sánchez Alvarado. “Fundamentals of planarian regeneration”. In: *Annu. Rev. Cell Dev. Biol.* 20 (2004), pp. 725–757.
- [8] Thomas R Gawriluk et al. “Comparative analysis of ear-hole closure identifies epimorphic regeneration as a discrete trait in mammals”. In: *Nature communications* 7 (2016), p. 11164.
- [9] Elly M Tanaka and Peter W Reddien. “The cellular basis for animal regeneration”. In: *Developmental cell* 21.1 (2011), pp. 172–185.
- [10] Richard J Goss. “The evolution of regeneration: adaptive or inherent?” In: *Journal of Theoretical Biology* 159.2 (1992), pp. 241–260.
- [11] Elly M Tanaka and Patrizia Ferretti. “Considering the evolution of regeneration in the central nervous system”. In: *Nature Reviews Neuroscience* 10.10 (2009), p. 713.
- [12] Siiri E Iismaa et al. “Comparative regenerative mechanisms across different mammalian tissues”. In: *NPJ Regenerative medicine* 3.1 (2018), p. 6.
- [13] Kenneth D Poss, Lindsay G Wilson, and Mark T Keating. “Heart regeneration in zebrafish”. In: *Science* 298.5601 (2002), pp. 2188–2190.

- [14] Junji Itou et al. “Migration of cardiomyocytes is essential for heart regeneration in zebrafish”. In: *Development* 139.22 (2012), pp. 4133–4142.
- [15] Charles S Thornton. “Amphibian limb regeneration and its relation to nerves”. In: *American zoologist* 10.2 (1970), pp. 113–118.
- [16] M AVEL. “L’influence du syst: me nerveux sur la rrgn&ation chez les urodrles et les oligochrtes”. In: *Bull. Soc. zool. Fr* 86 (1961), p. 464483.
- [17] Niels Jørn Olesen, Kristian Frandsen, and Hans Ulrik Riisgård. “Population dynamics, growth and energetics of jellyfish *Aurelia aurita* in a shallow fjord”. In: *Marine Ecology Progress Series* (1994), pp. 9–18.
- [18] Keats Conley and Shin-ichi Uye. “Effects of hyposalinity on survival and settlement of moon jellyfish (*Aurelia aurita*) planulae”. In: *Journal of experimental marine biology and ecology* 462 (2015), pp. 14–19.
- [19] Werner Schroth et al. “Speciation and phylogeography in the cosmopolitan marine moon jelly, *Aurelia* sp”. In: *BMC Evolutionary Biology* 2.1 (2002), p. 1.
- [20] William M Graham and Ryan M Kroutil. “Size-based prey selectivity and dietary shifts in the jellyfish, *Aurelia aurita*”. In: *Journal of Plankton Research* 23.1 (2001), pp. 67–74.
- [21] Jennifer E Purcell, WM Graham, and Henri J Dumont. *Jellyfish Blooms: Ecological and Societal Importance: Ecological and Societal Importance: Proceedings of the International Conference on Jellyfish Blooms, Held in Gulf Shores, Alabama, 12-14 January 2000*. Vol. 155. Springer Science & Business Media, 2001.
- [22] Zhilu Fu et al. “Body size reduction under starvation, and the point of no return, in ephyrae of the moon jellyfish *Aurelia aurita*”. In: *Marine Ecology Progress Series* 510 (2014), pp. 255–263.
- [23] Rodrigo Almeda et al. “Effects of crude oil exposure on bioaccumulation of polycyclic aromatic hydrocarbons and survival of adult and larval stages of gelatinous zooplankton”. In: *PLoS One* 8.10 (2013), e74476.
- [24] Amanda K Winans and Jennifer E Purcell. “Effects of pH on asexual reproduction and statolith formation of the scyphozoan, *Aurelia labiata*”. In: *Hydrobiologia* 645.1 (2010), pp. 39–52.
- [25] Erik V Thuesen et al. “Intragel oxygen promotes hypoxia tolerance of scyphomedusae”. In: *Journal of Experimental Biology* 208.13 (2005), pp. 2475–2482.
- [26] Hiroshi Miyake, Kenji Iwao, and Yoshiko Kakinuma. “Life history and environment of *Aurelia aurita*”. In: *South Pacific Study* 17.2 (1997), pp. 273–285.

- [27] Anthony J Richardson et al. “The jellyfish joyride: causes, consequences and management responses to a more gelatinous future”. In: *Trends in ecology & evolution* 24.6 (2009), pp. 312–322.
- [28] RC Brusca and GJ Brusca. *Invertebrates Sinauer Associates Sunderland*. 1990.
- [29] Sara M Lindsay. “Frequency of injury and the ecology of regeneration in marine benthic invertebrates”. In: *Integrative and comparative biology* 50.4 (2010), pp. 479–493.
- [30] Kylie A Pitt and Cathy H Lucas. *Jellyfish blooms*. Springer, 2014.
- [31] Daniel Pauly et al. “Jellyfish in ecosystems, online databases, and ecosystem models”. In: *Hydrobiologia* 616.1 (2009), pp. 67–85.
- [32] Mary Needler Arai. “Predation on pelagic coelenterates: a review”. In: *Journal of the Marine Biological Association of the United Kingdom* 85.3 (2005), pp. 523–536.
- [33] DG Fautin and WK Fitt. “A jellyfish-eating sea anemone (Cnidaria, Actiniaria) from Palau: *Entacmaea medusivora* sp. nov.” In: *Hydrobiologia*. Vol. 216. 1. Springer. 1991, pp. 453–461.
- [34] John Berryman. “Predation of *Sagartiogeton laceratus* upon *Aurelia aurita* in shallow water”. In: *Journal of the Marine Biological Association of the United Kingdom* 64.3 (1984), pp. 725–725.
- [35] Harold N Cones and Dexter S Haven. “Distribution of *Chrysaora quinquecirrha* in the York River”. In: *Chesapeake Science* 10.2 (1969), pp. 75–84.
- [36] Mary N Arai. *A functional biology of Scyphozoa*. Springer Science & Business Media, 2012.
- [37] Wilfried F Hoppe. “Growth, regeneration and predation in three species of large coral reef sponges”. In: *Marine Ecology Progress Series* (1988), pp. 117–125.
- [38] George T Hargitt. “Regeneration in hydromedusae”. In: *Archiv für Entwicklungsmechanik der Organismen* 17.1 (1903), pp. 64–91.
- [39] Charles R Stockard. “Studies on tissue growth. III”. In: *An experimental study of the rate of regeneration of *Cassiopea xamachana**. Publication 103 (1908).
- [40] TH Morgan. *Regeneration New York*. 1901.
- [41] Nanette E Chadwick and Y Loya. “Regeneration after experimental breakage in the solitary reef coral *Fungia granulosa* Klunzinger, 1879”. In: *Journal of Experimental Marine Biology and Ecology* 142.3 (1990), pp. 221–234.

- [42] Volker Schmid and Hansjürg Alder. “Isolated, mononucleated, striated muscle can undergo pluripotent transdifferentiation and form a complex regenerate”. In: *Cell* 38.3 (1984), pp. 801–809.
- [43] Sonia N Steinberg. “The regeneration of whole polyps from ectodermal fragments of scyphistoma larvae of *Aurelia aurita*”. In: *The Biological Bulletin* 124.3 (1963), pp. 337–343.
- [44] WA Müller, G Plickert, and S Berking. “Regeneration in Hydrozoa: distal versus proximal transformation in *Hydractinia*”. In: *Roux’s archives of developmental biology* 195.8 (1986), pp. 513–518.
- [45] Florence Peebles. “Further experiments in regeneration and grafting of hydroids”. In: *Archiv für Entwicklungsmechanik der Organismen* 14.1-2 (1902), pp. 49–64.
- [46] TH Morgan. “Further experiments on the regeneration of *Tubularia*”. In: *Archiv für Entwicklungsmechanik der Organismen* 13.4 (1901), pp. 528–544.
- [47] Georgia E Laurie-Lesh and R Corriel. “Scyphistoma regeneration from isolated tentacles in *Aurelia aurita*”. In: *Journal of the Marine Biological Association of the United Kingdom* 53.4 (1973), pp. 885–894.
- [48] KE Feitl et al. “Functional morphology and fluid interactions during early development of the scyphomedusa *Aurelia aurita*”. In: *The Biological Bulletin* 217.3 (2009), pp. 283–291.
- [49] BK Sullivan, CL Suchman, and JH Costello. “Mechanics of prey selection by ephyrae of the scyphomedusa *Aurelia aurita*”. In: *Marine Biology* 130.2 (1997), pp. 213–222.
- [50] JE Higgins III, MD Ford, and JH Costello. “Transitions in morphology, nematocyst distribution, fluid motions, and prey capture during development of the scyphomedusa *Cyanea capillata*”. In: *The Biological Bulletin* 214.1 (2008), pp. 29–41.
- [51] Camille Gambini et al. “Micro- and macrorheology of jellyfish extracellular matrix”. In: *Biophysical journal* 102.1 (2012), pp. 1–9.
- [52] Edward T Browne. “On the variation of the tentaculocysts of *Aurelia aurita*”. In: *QJ Microsc Sci* 37 (1895), pp. 245–251.
- [53] Edward T Browne. “Variation in *Aurelia aurita*”. In: *Biometrika* 1.1 (1901), pp. 90–108.
- [54] Alfred Goldsborough Mayer. *Medusae of the world: The Hydromedusae*. Vol. 1. Carnegie institution of Washington, 1910.
- [55] William Bateson. “Materials for the Study of Variation”. In: (1894).

- [56] Lisa-ann Gershwin. “Clonal and population variation in jellyfish symmetry”. In: *Journal of the Marine Biological Association of the United Kingdom* 79.6 (1999), pp. 993–1000.
- [57] Yanlan Mao et al. “Differential proliferation rates generate patterns of mechanical tension that orient tissue growth”. In: *The EMBO journal* 32.21 (2013), pp. 2790–2803.
- [58] A Wagoner Johnson and Brendan Harley. *Mechanobiology of cell-cell and cell-matrix interactions*. Springer Science & Business Media, 2011.
- [59] Adrian Salic and Timothy J Mitchison. “A chemical method for fast and sensitive detection of DNA synthesis in vivo”. In: *Proceedings of the National Academy of Sciences* 105.7 (2008), pp. 2415–2420.
- [60] Xiang Teng and Yusuke Toyama. “Apoptotic force: active mechanical function of cell death during morphogenesis”. In: *Development, growth & differentiation* 53.2 (2011), pp. 269–276.
- [61] Patrick RH Steinmetz et al. “Independent evolution of striated muscles in cnidarians and bilaterians”. In: *Nature* 487.7406 (2012), p. 231.
- [62] Janna C Nawroth et al. “A tissue-engineered jellyfish with biomimetic propulsion”. In: *Nature biotechnology* 30.8 (2012), p. 792.
- [63] Carl-Philipp Heisenberg and Yohanns Bellaiche. “Forces in tissue morphogenesis and patterning”. In: *Cell* 153.5 (2013), pp. 948–962.
- [64] Daniel J Marston and Bob Goldstein. “Actin-based forces driving embryonic morphogenesis in *Caenorhabditis elegans*”. In: *Current opinion in genetics & development* 16.4 (2006), pp. 392–398.
- [65] WB Gladfelter. “Structure and function of the locomotory system of the Scyphomedusa *Cyanea capillata*”. In: *Marine Biology* 14.2 (1972), pp. 150–160.
- [66] Nagayasu Nakanishi, Volker Hartenstein, and David K Jacobs. “Development of the rhopalial nervous system in *Aurelia* sp. 1 (Cnidaria, Scyphozoa)”. In: *Development genes and evolution* 219.6 (2009), pp. 301–317.
- [67] Richard S Blanquet and Gavin P Riordan. “An ultrastructural study of the subumbrellar musculature and desmosomal complexes of *Cassiopea xamachana* (Cnidaria: Scyphozoa)”. In: *Transactions of the American Microscopical Society* (1981), pp. 109–119.
- [68] John H Norton et al. “An evaluation of some relaxants for use with pearl oysters”. In: *Aquaculture* 144.1-3 (1996), pp. 39–52.
- [69] HOWARD L GILLARY. “Electrical potentials from the regenerating eye of *Strombus*”. In: *Journal of experimental biology* 107.1 (1983), pp. 293–310.

- [70] Christelle Gaudioso et al. “Menthol pain relief through cumulative inactivation of voltage-gated sodium channels”. In: *Pain* 153.2 (2012), pp. 473–484.
- [71] WJ Fawcett, EJ Haxby, and DA Male. “Magnesium: physiology and pharmacology.” In: *British journal of anaesthesia* 83.2 (1999), pp. 302–320.
- [72] Brad J Gemmell et al. “Passive energy recapture in jellyfish contributes to propulsive advantage over other metazoans”. In: *Proceedings of the National Academy of Sciences* 110.44 (2013), pp. 17904–17909.
- [73] Brad J Gemmell et al. “Suction-based propulsion as a basis for efficient animal swimming”. In: *Nature communications* 6 (2015), p. 8790.
- [74] William M Megill, John M Gosline, and Robert W Blake. “The modulus of elasticity of fibrillin-containing elastic fibres in the mesoglea of the hydromedusa *Polyorchis penicillatus*”. In: *Journal of Experimental Biology* 208.20 (2005), pp. 3819–3834.
- [75] Walter E Schwab. “The ontogeny of swimming behavior in the scyphozoan, *Aurelia aurita*. I. Electrophysiological analysis”. In: *The Biological Bulletin* 152.2 (1977), pp. 233–250.
- [76] Tom H Cheung et al. “Maintenance of muscle stem-cell quiescence by microRNA-489”. In: *Nature* 482.7386 (2012), p. 524.
- [77] Hideo Higuchi and Shigeru Takemori. “Butanedione monoxime suppresses contraction and ATPase activity of rabbit skeletal muscle”. In: *The Journal of Biochemistry* 105.4 (1989), pp. 638–643.
- [78] Y-C James Lin, Nikita G Grigoriev, and Andrew N Spencer. “Wound healing in jellyfish striated muscle involves rapid switching between two modes of cell motility and a change in the source of regulatory calcium”. In: *Developmental Biology* 225.1 (2000), pp. 87–100.
- [79] Kiyokazu Agata, Yumi Saito, and Elizabeth Nakajima. “Unifying principles of regeneration I: Epimorphosis versus morphallaxis”. In: *Development, growth & differentiation* 49.2 (2007), pp. 73–78.
- [80] Jörg Wittlieb et al. “Transgenic Hydra allow in vivo tracking of individual stem cells during morphogenesis”. In: *Proceedings of the National Academy of Sciences* 103.16 (2006), pp. 6208–6211.
- [81] R McN Alexander. “Visco-elastic properties of the mesogloea of jellyfish”. In: *Journal of experimental Biology* 41.2 (1964), pp. 363–369.
- [82] M Edwin Demont and John M Gosline. “Mechanics of jet propulsion in the hydromedusan jellyfish, *Polyorchis penicillatus*: II. Energetics of the jet cycle”. In: *Journal of experimental biology* 134.1 (1988), pp. 333–345.
- [83] Charles W Hargitt. “Recent experiments on regeneration”. In: *Zoological Bulletin* 1.1 (1897), pp. 27–34.

- [84] BR Coonfield. “Regeneration in *Mnemiopsis leidyi*, Agassiz”. In: *The Biological Bulletin* 71.3 (1936), pp. 421–428.
- [85] Biological Bulletin Compendium. *ARTIFICIAL SEAWATERS - KEY*. 2018.
URL: <http://comm.archive.mbl.edu/BiologicalBulletin/COMPENDIUM/CompTab2.html> (visited on 05/01/2018).
- [86] Björn Fuchs et al. “Regulation of polyp-to-jellyfish transition in *Aurelia aurita*”. In: *Current Biology* 24.3 (2014), pp. 263–273.

*Chapter 3***SLEEP IN JELLYFISH****3.1 Abstract**

Do all animals sleep? Sleep has been observed in many vertebrates, and there is a growing body of evidence for sleep-like states in arthropods and nematodes [1–5]. Here we show that sleep is also present in Cnidaria [6–8], an earlier-branching metazoan lineage. Cnidaria and Ctenophora are the first metazoan phyla to evolve tissue-level organization and differentiated cell types, such as neurons and muscle [9–15]. In Cnidaria, neurons are organized into a non-centralized radially symmetric nerve net [11, 13, 15–17] that nevertheless shares fundamental properties with the vertebrate nervous system: action potentials, synaptic transmission, neuropeptides, and neurotransmitters [15–20]. It was reported that cnidarian soft corals [21] and box jellyfish [22, 23] exhibit periods of quiescence, a requirement for sleep-like states. Within Cnidaria, the upside-down jellyfish *Cassiopea spp.* displays a quantifiable pulsing behavior, allowing us to perform long-term behavioral tracking. Monitoring of *Cassiopea* pulsing activity for consecutive days and nights revealed behavioral quiescence at night that is rapidly reversible, as well as a delayed response to stimulation in the quiescent state. When deprived of nighttime quiescence, *Cassiopea* exhibited decreased activity and reduced responsiveness to a sensory stimulus during the subsequent day, consistent with homeostatic regulation of the quiescent state. Together, these results indicate that *Cassiopea* has a sleep-like state, supporting the hypothesis that sleep arose early in the metazoan lineage, prior to the emergence of a centralized nervous system [24].

3.2 Introduction

Sleep has long been a curiosity - Aristotle remarked upon the lack of alarm exhibited by sleeping animals and their tendency to sleep at night in his *Inquires*

into Animals [25]. Sleep-like states have been behaviorally defined in a diverse array of animals, from worms to flies and fish to humans [1–5] (Figure 3.1A). Sleep among these animals shows remarkable similarity in its genetic and pharmacological control, which supports the hypothesis that sleep was present in the common ancestor of these bilaterians over 600 million years ago [23, 26], though the function sleep plays in these animals is not well understood.

The behaviors associated with sleep have been recognized since the 1930s [28], and are now widely accepted as the set of criteria that appear to define the features of sleep that are indicative of its core functions [29–33]. Sleep-like states can be defined by three behavioral characteristics [6, 7, 30], and to exemplify these characteristics we use the zebrafish sleep system. The first is behavioral quiescence, typically a reversible period of decreased motor activity (3.1B). Second, a reduced responsiveness to stimuli during the quiescent state, suggesting that the sensory and motor systems are less active (Figure 3.1C) [34]. Third, the homeostatic regulation of sleep, is most evident when sleep is deprived, there is an intense buildup of a drive to sleep, even during normally wakeful periods (the section after sleep deprivation in Figure 3.1D). Homeostatic behaviors, such as feeding, are tightly regulated and serve important functions, leading to the suggestion sleep acts as a restorative period during which the animal recovers from the adverse effects of wakefulness [6, 35, 36]. Layered on top of these behaviors in certain animals are distinct physiological processes. For example, the development and use of the electroencephalogram (EEG) revealed that electrical patterns relate to the physiologically distinct states of rapid eye movement (REM) and non-REM sleep [35, 37, 38]. However, these may represent species-specific attributes, and for our purposes, are not considered defining characteristics of a sleep-like state.

The obvious disadvantages of sleep, a period in which animals cannot eat, mate or defend against predators, must be balanced by the positive functions of sleep. It has been hypothesized that sleep must play important restorative roles, perhaps replenishing the pools of macromolecules used during wakeful activities throughout

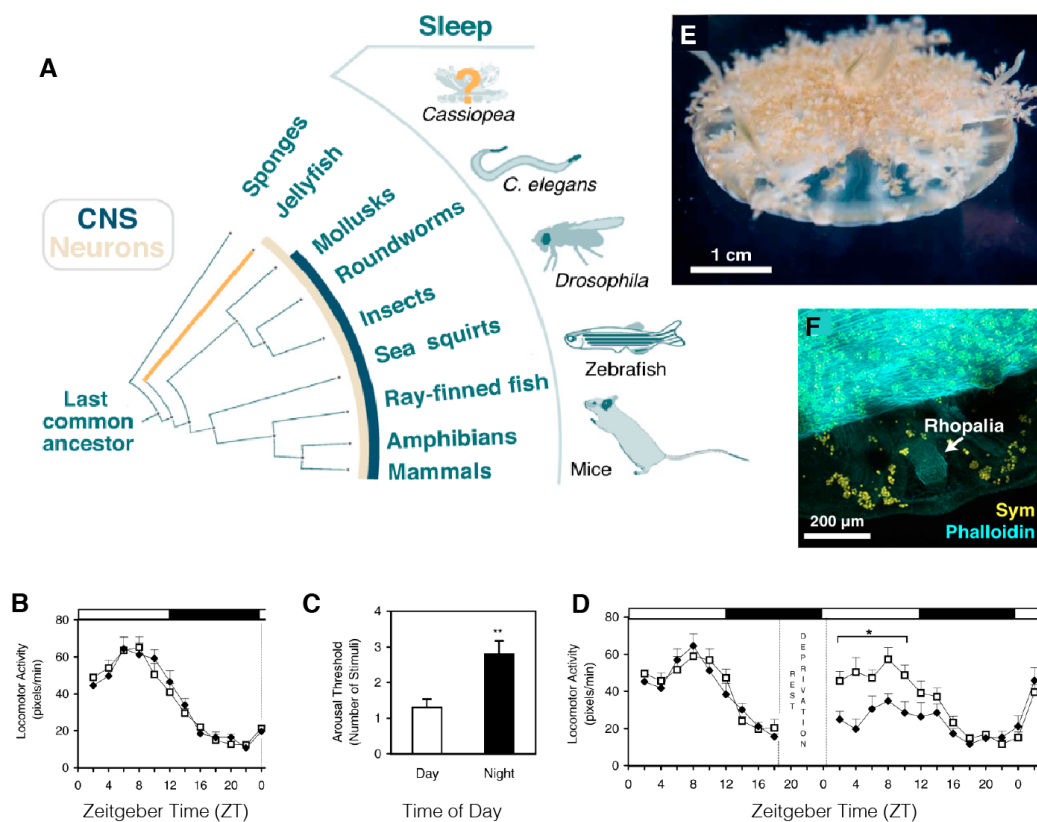


Figure 3.1: The phylogenetic prevalence and behavioral components of sleep-like states (A) Phylogenetic tree schematic highlighting animals in which sleep behavior has been described, the presence of neurons (tan), and the emergence of a centralized nervous system (dark blue). See boxed key. (B-D) Daily variation in locomotor activity and arousal threshold in larval zebrafish maintained in constant darkness and a compensatory reduction in locomotor activity and increase in arousal threshold following rest deprivation. Zeitgeber time (ZT) and horizontal white/black bars indicate subjective day versus subjective night, according to 12:12 light–dark cycle prior to the beginning of recording, with ZT0 corresponding to lights on time. Each data point represents mean \pm S.E.M. group locomotor activity for preceding 2 h of recording (pixels per minute). N = 560 for each group. (B) behavioral quiescence observed during subjective night (ZT12–ZT24). (C) Arousal threshold increased at night; measured in constant darkness during subjective day (ZT3–5) or subjective night (ZT15–17); N=520 for each group. White bars – control; striped bars – rest deprivation. N520 for each group. *,0.05; **P,0.01. modified from [27]. (D) Homeostatic regulation of sleep; rest deprivation was scheduled during subjective night (ZT0–ZT6). Closed diamonds – rest deprivation group, open squares – control group. (E) An image of the upside-down jellyfish *Cassiopea*. (F) Higher-magnification view of *Cassiopea* with labeled actin-rich muscle (phalloidin stain; cyan), autofluorescent *Symbiodinium* (yellow), and a rhopalia, the sensory organ that controls pulsing, which is free of *symbiodinium*.

the body, and more specifically for the optimal function of neural processes [6, 39–41]. The fact that rats and flies die if they are chronically deprived of sleep [42, 43] also emphasizes the essential function sleep must play. While the physiological

importance of sleep is evident, we lack understanding of its complex mechanistic underpinnings. By defining a behavioral sleep-like state in an early branching animal lineage that does not have a centralized nervous system we may reduce the complexity of the state and perhaps lay the foundation for further comprehension of its mechanistic regulation.

One of the first metazoan phyla to evolve tissue-level organization and differentiated cell types, such as neurons and muscle [9–15], is Cnidaria (described in Chapter 1). Neurons in these animals are organized into a non-centralized radially symmetric nerve net [11, 13, 15–17] that nevertheless shares fundamental properties with the vertebrate nervous system: action potentials, synaptic transmission, neuropeptides, and neurotransmitters [15–20]. It was also reported that cnidarian soft corals [21] and box jellyfish [22, 23] exhibit periods of quiescence, a requirement for sleep-like states. Additionally, several cnidarians have quantifiable circadian behaviors and have biological clock components [44–46], often associated with sleep-like states. However, the baseline activity of most cnidarians is difficult to assess (they either move too much or not enough). From our other projects we were aware of another cnidarian, the upside-down jellyfish, *Cassiopea*, which has a unique upside-down pulsing behavior suitable for quantification. Initial anecdotal observations indicated this pulsing activity responded to changes in light conditions. Together, this prompted us to ask whether a sleep-like state is present in *Cassiopea*.

Cassiopea are found throughout the tropics in shallow ocean waters and mudflats (Figure 3.1E) [47, 48]. Like other jellyfish, *Cassiopea* are dimorphic, with an asexually reproducing polyp stage, and a sexual medusae stage. The young medusae, called ephyrae, are no more than a few millimeters in diameter, but these quickly develop to mature jellyfish over a couple months. In the wild these animals can grow to ~30cm in diameter, generally have brown bodies and bushy tentacles, though occasionally they can be darkly pigmented. These jellyfish are not particularly venomous, allowing for easy handling.

They are capable of swimming, but rarely do so and rather remain with their

bell down against a surface, hence their name, the upside-down jellyfish (Figure 3.1E; Figure 3.2A; Figure 3.3A; Movie S1) [47, 48]. *Cassiopea*, like coral and sea anemones, have a photosynthetic obligate endosymbiote, *Symbiodinium* (*SYM* in Figure 3.1F), which have good access to light because of *Cassiopea*'s unique upside-down pulsing behavior.

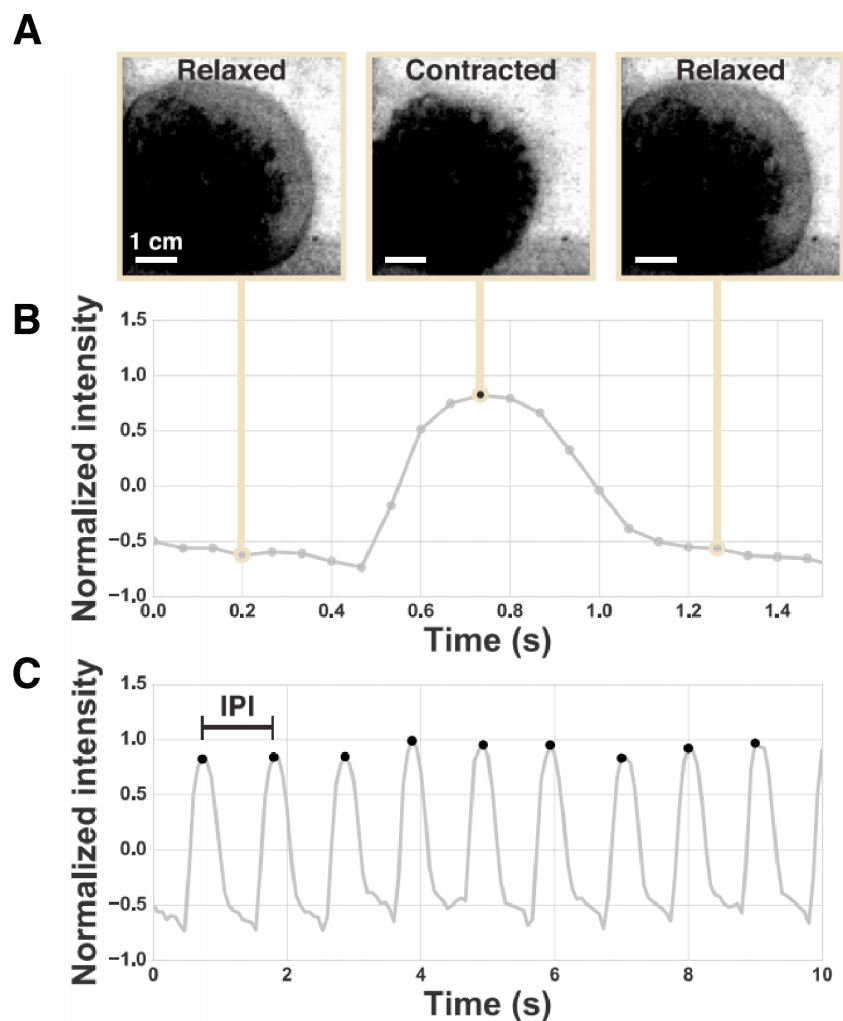


Figure 3.2: The Pulsing Behavior of the Upside-Down Jellyfish, *Cassiopea* spp., Is Trackable (A-C) As *Cassiopea* pulse, the relaxation and contraction of the bell causes a corresponding change in average pixel intensity. Pulsing behavior was tracked by measuring this change in pixel intensity within the region of interest. (A) Representative frames and (B) corresponding normalized pixel intensities for one pulse event. The local maximum in the pulse trace was used to count pulse events. (C) A 10 second recording of one jellyfish shows multiple pulsing events. The interpulse interval (IPI) was calculated as the time between the maxima. See also Figures 3.2 and 3.3 and Movie S1.

Cassiopea continuously pulse by relaxing and contracting their bell at a rate of about 1 pulse per second (Figure 3.2A). This pulsing behavior generates fluid cur-

rents that facilitate vital processes such as filter feeding, circulation of metabolites, expulsion of byproducts, and gamete dispersion [47, 49]. The pulsing behavior is controlled by light- and gravity-sensing organs called rhopalia (Figure 3.1F) [11, 13]. This stationary pulsing behavior makes *Cassiopea* a suitable jellyfish for behavioral tracking. Before we could ask whether the cnidarian jellyfish *Cassiopea* exhibits the core behavioral characteristics of sleep, we had to develop a system for long-term behavioral analysis. To track behavior in *Cassiopea*, we designed an imaging system (Figures 3.3C–F) for counting the pulses of individual jellyfish over successive cycles of day and night, defined as a 12 hr period when the light is on or off, respectively. As *Cassiopea* pulse, the relaxation and contraction of the bell causes a corresponding change in average pixel intensity, which was measured for each frame of the recording, producing a pulse trace (Figure 1D). Pulse events were counted using the peak of the pulse trace, and the inter-pulse interval (IPI) was calculated as the time between the peaks (Figure 3.2A–C and Figure 3.4).

3.3 Continuous tracking of *Cassiopea* reveals pulsing quiescence at night

We observed that *Cassiopea* pulse less at night than during the day (Figure 3.4; Data S1). To quantify this difference in pulsing frequency, we tracked the pulsing behavior of 23 jellyfish over six consecutive days and nights (Figure 3.4C). We define “activity” as the total number of pulses in the first 20 min of each hour. Although individual jellyfish showed different basal activity levels (Figure 3.4C), all showed a large decrease in mean activity (32%) at night (781 ± 199 pulses/20 min, mean \pm SD) compared to the day ($1,155 \pm 315$ pulses/20 min, mean \pm SD; Figures 3.4C and E). To determine whether fast- and slow-pulsing jellyfish change their activity to a similar degree, we normalized activity of individual jellyfish by their mean day activity. Despite variations in basal activity, the relative change from day to night was similar between jellyfish (Figure 3.4D). Jellyfish activity decreased throughout the first 3–6 hr of the night, with the lowest activity occurring 6–12 hr after the day-to-night transition. Pulsing activity peaked upon feeding, occurring on the fourth hour of each day (Figures 3.4C and D). To ensure that day feeding does not cause

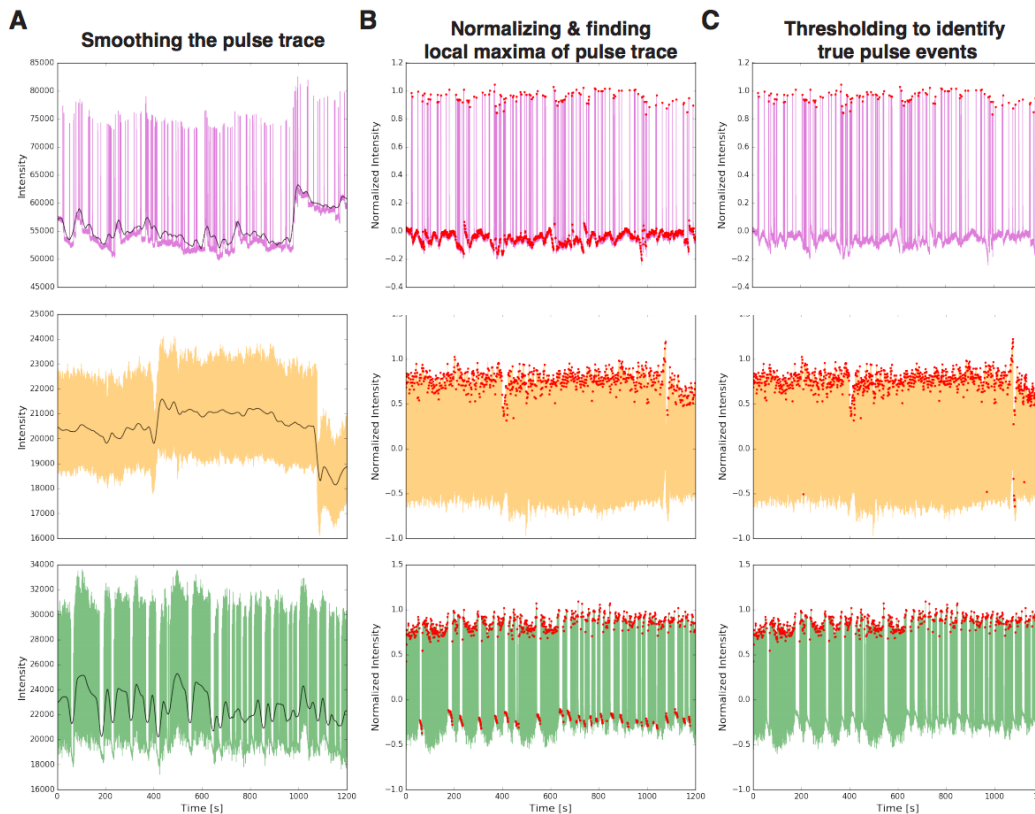


Figure 3.4: Processing the jellyfish pulse-trace data to count pulse events, Related to Figure 1. Each color represents data from a different jellyfish (pink, orange, and green). (A) Smoothing the pulse-trace for normalization. Black line represents the smoothed trace for a 20 min recording. (B) Normalized pulsing traces for three different jellyfish with local maxima indicated by red dots. Many local maxima are detected within pauses in activity due to noise (small fluctuations in intensity), which are removed by thresholding. (C) Thresholding to identify local maxima at pulsing peaks. Pulsing peaks are indicated by red dots. For more details see the ‘*Cassiopea* behavioral tracking’ section of the Materials and Methods.

tribute to this lengthening of the IPI: (1) the mode of the IPI distribution is longer at night than during the day, and (2) night pulsing is more often interrupted by pauses of variable length. These pauses are seen as a tail in the IPI frequency distribution (Figure 3.4B; 95th percentile of night IPI frequency distribution (gray) is 13.9 s). Such long pauses are rarely seen during the day (Figure 3.4B; 95th percentile of day IPI frequency distribution (yellow) is 2.5 s). This pause behavior may be analogous to long rest bouts observed in *Drosophila* and zebrafish, which are suggested to be periods of deep quiescence with reduced responsiveness to stimuli [1, 50].

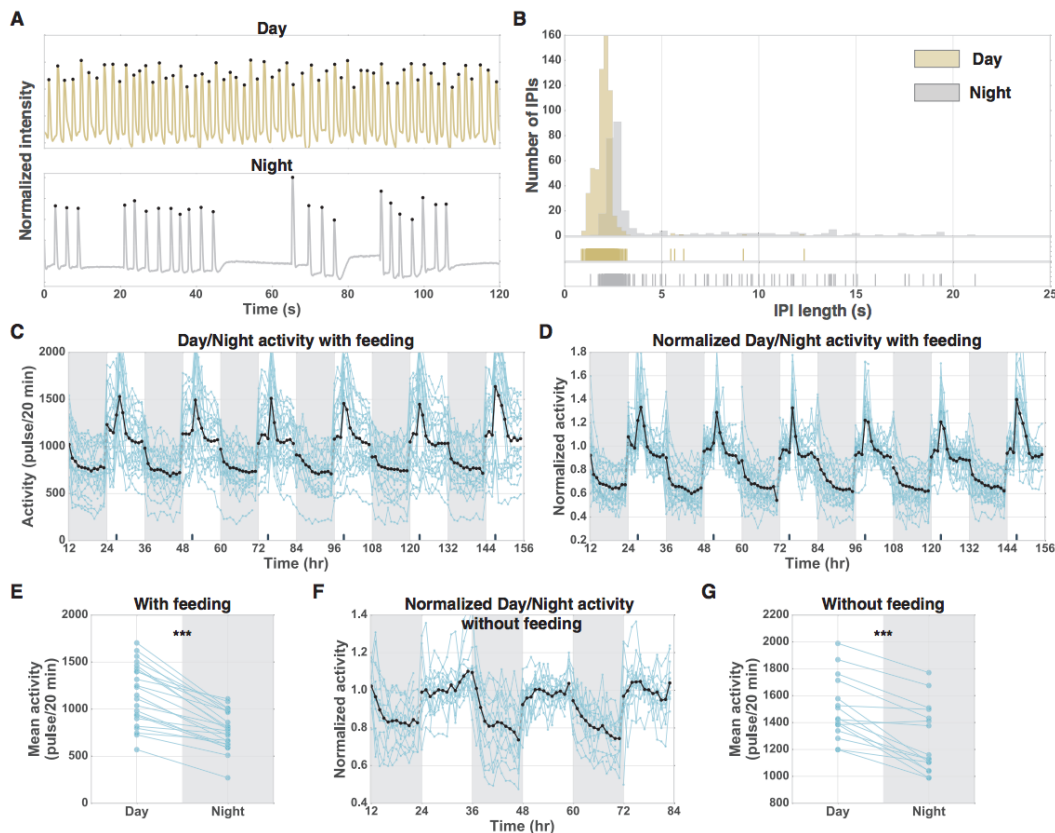


Figure 3.5: Continuous Tracking of *Cassiopea* Reveals Pulsing Quiescence at Night (A) Pulsing traces for individual jellyfish during day and night over 120 s. (B) The distribution of IPI length for a 12 hr day and a 12 hr night for the same jellyfish shown in (A). Tick marks below the distribution show each IPI length during the day and night. This highlights the long-pause events, which are more common at night (Figure S3A; Data S1). (C–G) Each blue line corresponds to a single jellyfish. The black line indicates the mean activity of all jellyfish. Dark-gray shading indicates night periods. Dark tick marks on the x axis indicate the time of feeding. (C) Baseline activity (pulses/20 min) of 23 jellyfish tracked for 6 days from four laboratory replicates. (D) Normalized baseline activity for jellyfish shown in (C), where each jellyfish is normalized by its mean day activity. (E) Mean day activity versus mean night activity for each jellyfish over the 6 day experiment shown in (C). Two-sided paired t test, day versus night, $p = 6 \times 10^{-9}$. (F) Normalized baseline activity without feeding of 16 jellyfish tracked over 3 days from two laboratory replicates, where each jellyfish is normalized by its mean day activity. (G) Mean day activity versus mean night activity for each jellyfish over the 3 day experiment shown in (F). Two-sided paired t test, day versus night, $p = 10^{-5}$. *** $p < 10^{-3}$. See also Figure S3.

3.4 *Cassiopea* show reduced responsiveness to a sensory stimulus at night

To test whether *Cassiopea* exhibit reduced responsiveness to stimuli during their nighttime-quiescent state, we designed an experiment to deliver a consistent arousing stimulus to the jellyfish. We observed in our nursery that *Cassiopea* prefer staying on solid surfaces as is found in nature. If *Cassiopea* are released into the

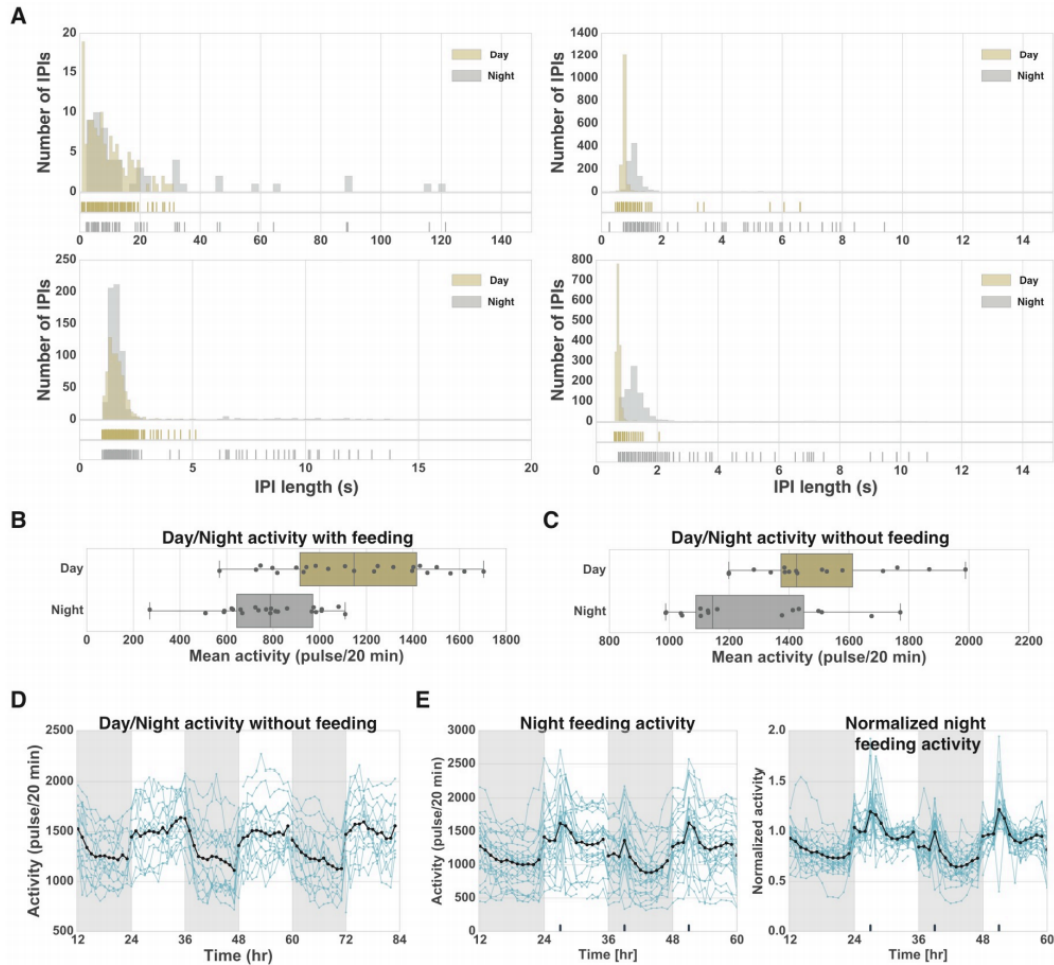


Figure 3.6: *Cassiopea* pulsing quiescence at night (A) Distribution of IPI length for four *Cassiopea* during the day (yellow) and night (gray) showing each IPI event. Tick marks below the distributions show each IPI length during the day (yellow) and night (gray). The ticks highlight the long-pauses that are more common at night for all jellyfish (Data S1). Box plot of *Cassiopea* day and night pulsing activity with feeding (B), and without feeding (C). Each dot represents a single jellyfish, mean activity is calculated over 6 (feeding, B) or 3 (without feeding, C) days and nights. For D and E each blue line corresponds to a single jellyfish. The black line indicates the mean activity of all jellyfish. Dark gray shading indicates night periods. (D) Day and night activity of *Cassiopea* without feeding. Baseline activity (pulses/20 min) without feeding of 16 jellyfish tracked over three days. (E) Feeding induced arousal rapidly reverses the night quiescent state. Dark tick marks on x-axis indicate time of feeding. Activity (pulses/20 min) and normalized activity of 30 jellyfish tracked over two day/nights from six laboratory replicates. Jellyfish were fed 4 hours into each day and 4 hours into the second night.

water column, they quickly reorient and move to the bottom of the tank. We used placement into the water column as a stimulus to compare responsiveness during the night versus the day. *Cassiopea* were put inside a short PVC pipe with a screen bottom (Figure 3.6A). This was lifted to a fixed height, held for 5 min to allow the

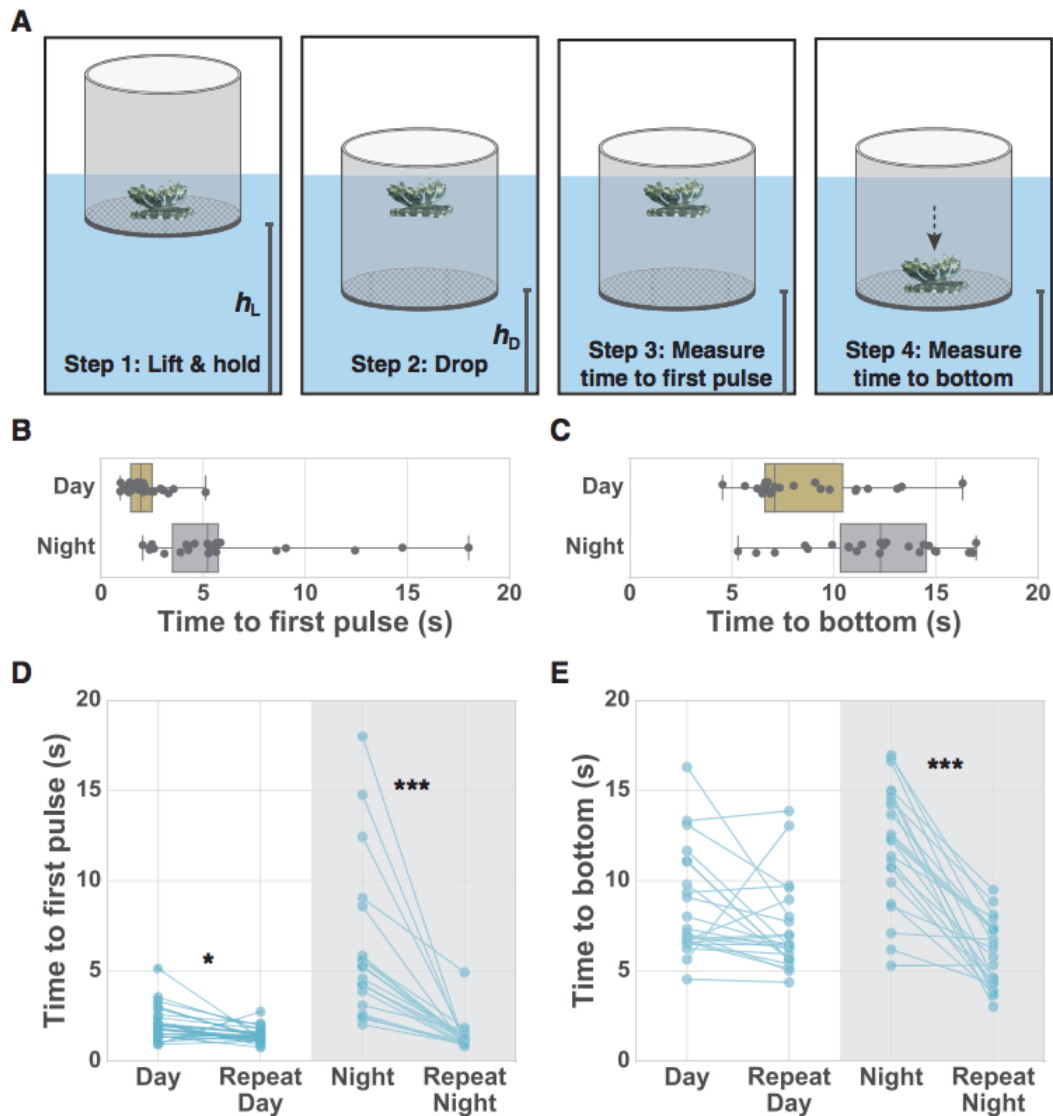


Figure 3.7: *Cassiopea* Show Reduced Responsiveness to a Sensory Stimulus at Night. (A) Schematic of experiment to test sensory responsiveness. Jellyfish were lifted and held at a fixed height (h_L) and then dropped to a fixed height (h_D). h_L and h_D were kept constant throughout experiments. (B and C) Boxplots of time to first pulse after drop (B) for 23 jellyfish and time to reach bottom after drop (C) for 23 jellyfish during the day and night. Dots represent individual jellyfish collected from two laboratory replicates. Two-sided unpaired t test, day versus night, (B) $p < 10^{-4}$ and (C) $p = 5 \times 10^{-4}$. (D) Time to first pulse after initial drop and after perturbation for both day and night for 23 jellyfish. (E) Time to reach bottom after initial drop and after perturbation for both day and night for 23 jellyfish. A two-way ANOVA was performed for data shown in (D) and (E), followed by post hoc comparisons between experimental groups using Bonferroni post test (* $p < 5 \times 10^{-2}$, *** $p < 10^{-3}$). For the time to first pulse, a two-sided unpaired t test (B) and two-way ANOVA (D) were performed after log transformation (Materials and Methods).

jellyfish to acclimate, and then rapidly lowered, placing the jellyfish free-floating into the water column. We then scored the time it took for the jellyfish to first pulse

and the time to reach the screen bottom (Figure 3.6; Methods and Methods). At night, the jellyfish showed an increase in the time to first pulse and the time to reach bottom compared to during the day (time to first pulse: day 2.1 ± 0.9 s versus night 5.9 ± 4.0 s; time to reach bottom: day 8.6 ± 2.9 s versus night 12.0 ± 3.2 s; mean \pm SD; $n = 23$ animals) (Figures 3.5B and C). This increased latency in response to stimulus indicates that *Cassiopea* have reduced responsiveness to stimulus during the night.

To determine whether the increased latency at night is rapidly reversible, we initiated a second drop within 30 s of the first drop, that is, after the jellyfish have been aroused. Reversibility was tested during both the day and night for 23 jellyfish. During the night, there is a large decrease in the time to first pulse and time to reach the bottom after the second drop when compared to the first drop (Figures 3.6D and E). During the day and night, the time to first pulse and time to bottom after the second drop were indistinguishable, demonstrating that after perturbation, animals have similar arousal levels during the day and night. These results indicate that *Cassiopea* have rapidly reversible reduced responsiveness to a stimulus during the night.

3.5 *Cassiopea* quiescence displays homeostatic rebound

To test whether *Cassiopea* nighttime quiescence is homeostatically regulated, we deprived jellyfish of behavioral quiescence for either 6 or 12 hr using a mechanical stimulus (Figure 3.7). The stimulus consisted of a brief (10 s) pulse of water every 20 min, which caused a transient increase in pulsing activity (Movie S2). This increase in pulsing activity lasts for approximately 5 min after the 10 s pulse of water. Thus, the perturbation disrupts quiescence for approximately 25% of the perturbation period (either 6 hr or 12 hr). When the perturbation was performed during the last 6 hr of the night (Figure 3.7A), we observed a significant decrease in activity (12%) during the first 4 hr of the following day relative to the pre-perturbation day (mean of first 4 hr of pre-perturbation day: $1,146 \pm 232$ pulses/20 min; compared

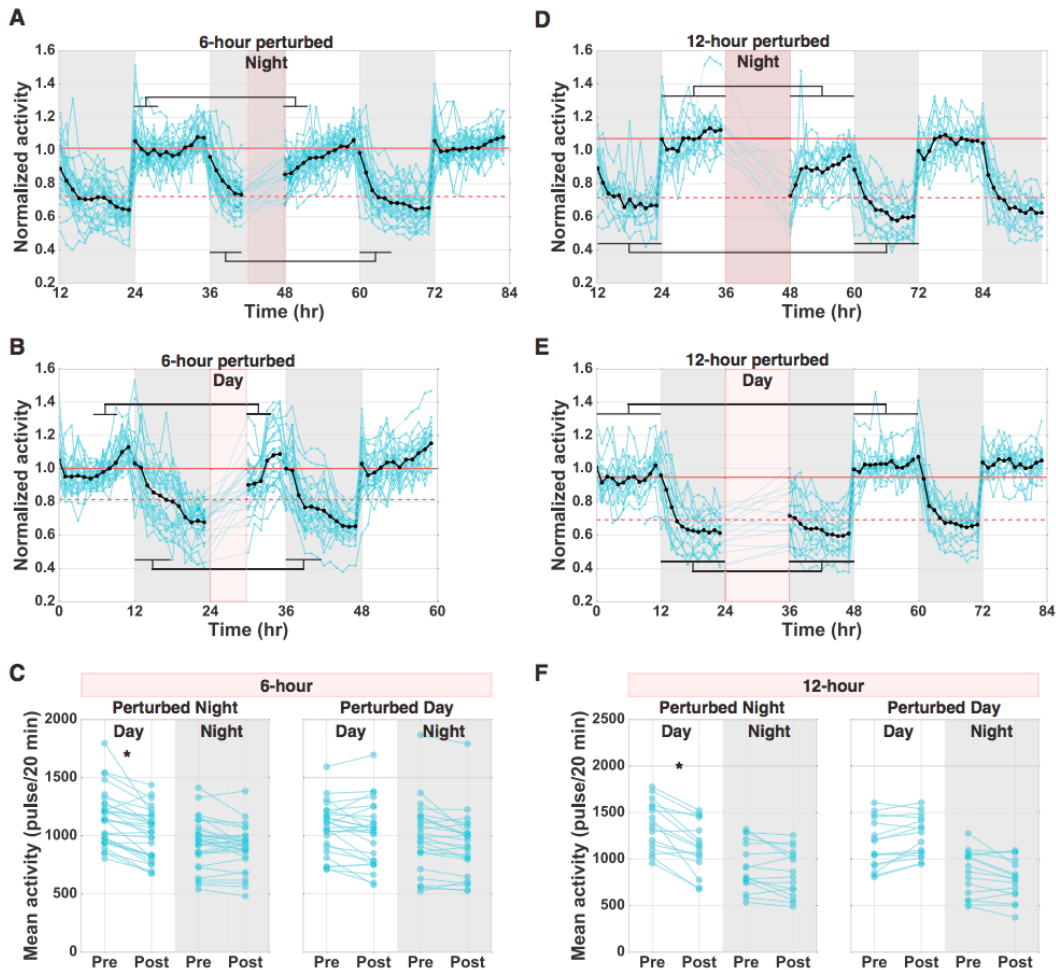


Figure 3.8: Homeostatic Rebound in *Cassiopea*. Each blue line corresponds to a single jellyfish. The black line indicates the mean activity of all jellyfish. Dark-gray shading indicates night periods. Maroon shading indicates perturbation periods with 10 s water pulses every 20 min. Jellyfish were exposed to different perturbation lengths (6 or 12 hr) at different times (day or night). The normalized activity of all jellyfish tracked over multiple days is plotted. Maroon horizontal lines show the mean activity of pre-perturbation day (solid) and pre-perturbation night (dashed). (A) Perturbation of 30 jellyfish for the last 6 hr of the night. (B) Perturbation of 26 jellyfish for the first 6 hr of the day. (C) Mean day and night activity pre- and post-perturbation for experiments shown in (A) and (B). (D) Perturbation of 16 jellyfish for an entire 12 hr night. (E) Perturbation of 16 jellyfish for an entire 12 hr day. (F) Mean day and night activity pre- and post-perturbation for experiments shown in (D) and (E). Black-horizontal lines in (A), (B), (D), and (E) indicate the windows of time used for calculating pre- and post perturbation means shown in (C) and (F) for both the night (bottom lines) and day (top lines). For the 6 hr experiments, we compared the first 4 hr of the post-perturbation day to the equivalent time pre-perturbation and also compared the first 6 hr of post-perturbation night to the equivalent time pre-perturbation. For the 12 hr experiments, we compared the full 12 hr days and nights pre- and post-perturbation. Two-way ANOVA followed by post hoc comparisons between experimental groups using Bonferroni post test, $*p < 5 \times 10^{-2}$. Both day and night 6 hr perturbation experiments include data from four laboratory replicates. Both day and night 12 hr perturbation experiments include data from two laboratory replicates. See also Figure 3.8 and Movie S2.

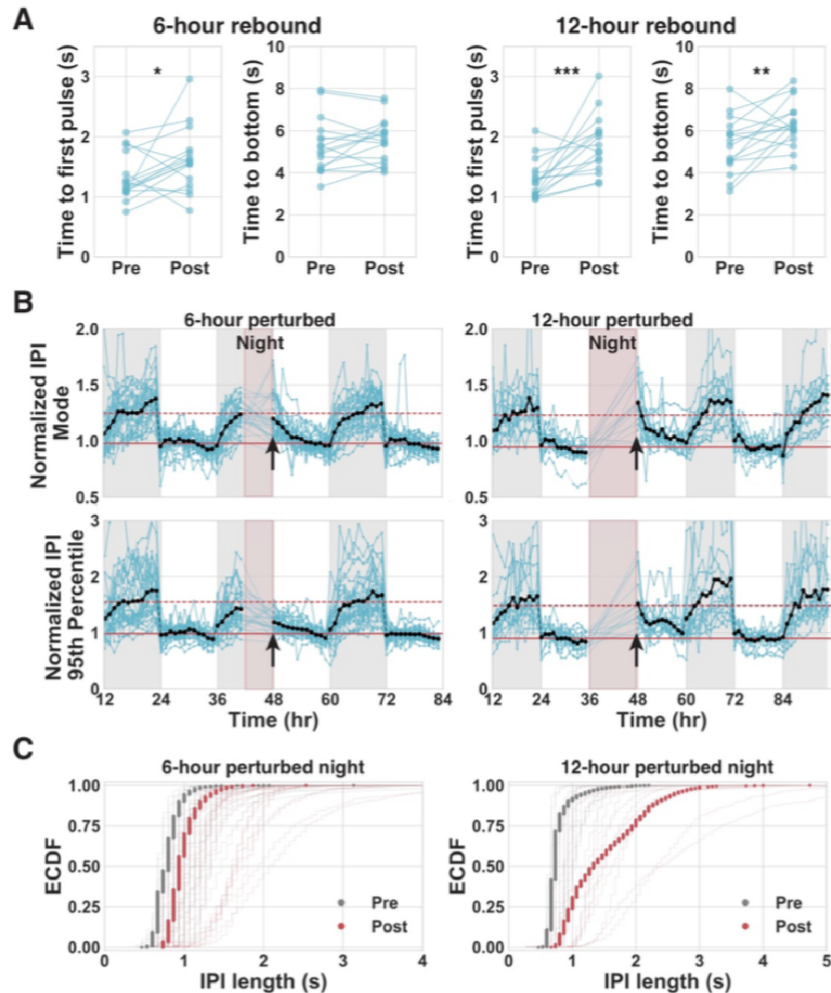


Figure 3.9: Regulation of quiescence in *Cassiopea*. Each blue line corresponds to a single jellyfish. The black line indicates the mean activity of all jellyfish. Dark gray shading indicates night periods. (A) Sensory responsiveness was tested during periods of decreased activity before (pre) and after (post) either the 6-hour or 12-hour perturbation periods (10 s water pulses every 20 min) using the assay described in Figure 3. Time to first pulse after drop and time to reach bottom after drop were measured during the day pre or post perturbation. After perturbation (post), an increased response latency was observed. Two-sided paired t-test, pre versus post, $*P < 5 \times 10^{-2}$, $**P < 10^{-2}$, $***P < 10^{-3}$. (B) Maroon horizontal lines show the mean activity of pre-perturbation day (solid) and pre-perturbation night (dashed). Maroon shading indicates perturbation periods with 10 s water pulses every 20 min. In these experiments jellyfish were exposed to different perturbation lengths (either 6 or 12 hours) during the night. Plotted here is the normalized mode and 95th percentile of the IPI length for all jellyfish tracked over multiple days. Perturbation of either 30 jellyfish for the last 6 hours of the night or 16 jellyfish for an entire 12-hour night. For both the 6-hour and 12-hour perturbation there is an increase in the mode and 95th percentile of the IPI length after perturbation (black arrowhead). (C) Empirical cumulative distribution function (ECDF) of daytime IPI length for all jellyfish pre (gray) and post (maroon) perturbation (thin lines, single jellyfish; dots, all jellyfish). Jellyfish exhibited increased IPI lengths after perturbation compared to before perturbation. These results suggest that the increased quiescence observed in Figure 3.4 results from both a decreased frequency of pulsing and an increase in the length of pause events.

to post-perturbation day: $1,008 \pm 210$ pulses/20 min; mean \pm SD; $n = 30$ animals; Figure 3.7C). This period of decreased activity is due to both decreased pulsing frequency (increased mode of IPI length) and increased pause length (increase in the IPI length 95th percentile) (Figures 3.8B and C). This result is consistent with an increased sleep drive after sleep deprivation. After a single day of decreased activity, the jellyfish return to baseline levels of day and night activity. Similar results were observed after an entire night of perturbation (12 hr; Figure 3.7D), with a large decrease in activity (17%) throughout the following day (mean of 12 hr of pre-perturbation day: $1,361 \pm 254$ pulses/20 min; compared to post-perturbation day: $1,132 \pm 263$ pulses/20 min; mean \pm SD; $n = 16$ animals; Figure 3.7F). The decrease in activity caused by the 12 hr perturbation was larger than that of the 6 hr perturbation, indicating that the amount of sleep rebound is dependent on the level of sleep deprivation. During periods of decreased activity after either the 6 hr or 12 hr perturbation, we also observed increased response latency to a sensory stimulus (Figure 3.8A), indicating a sleep-like state.

If the reduced activity after nighttime perturbation is due to sleep deprivation rather than muscle fatigue, then applying the perturbation during the day, when *Cassiopea* are much less quiescent, should not result in reduced activity. To distinguish between sleep deprivation and muscle fatigue, we performed the 6 or 12 hr mechanical stimulus experiments during the day (Figures 3.7B and E). We observed no significant difference between pre- and post- perturbation activity levels (Figures 3.7C and F), indicating that the rebound response is specific to deprivation of nighttime quiescence. Taken together, these results demonstrate that *Cassiopea* have a nighttime-quiescent state that is homeostatically controlled.

3.6 Nighttime quiescence in *Cassiopea* may be under circadian regulation

In many animals, sleep is regulated by both homeostatic and circadian systems [35], but this is not always the case [4–7, 51]. For instance, the nematode *C. elegans* exhibits a developmentally regulated sleep state, and adult *C. elegans* show a non-

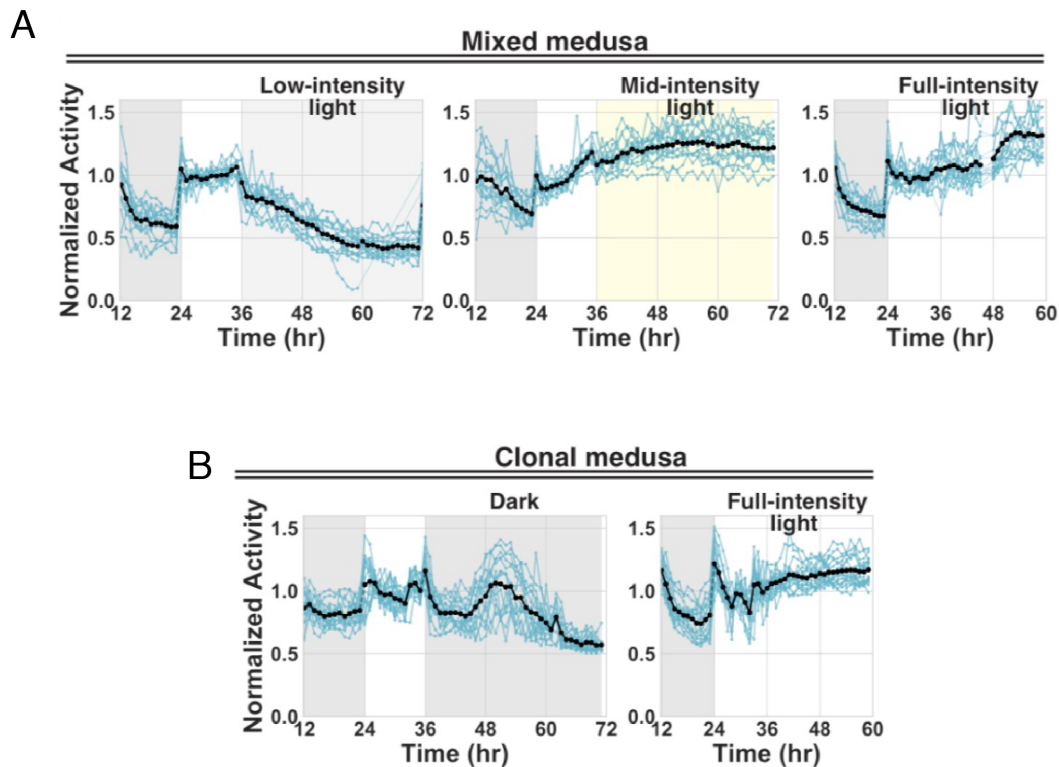


Figure 3.10: Monitoring activity with different light or dark conditions suggests that nighttime quiescence may be under circadian regulation in *Cassiopea*, Related to Figure 3.7. Each blue line corresponds to a single jellyfish. The black line indicates the mean activity of all jellyfish. Dark gray shading indicates night periods. (A) Prolonged light exposure of *Cassiopea* shows no circadian cycling. 16 jellyfish were exposed to either 36-hours of continuous low-intensity light (light-gray shading) from hour 36 to hour 72, 36-hours of continuous mid-intensity light (yellow shading) from hour 36 to hour 72, or 36-hours of continuous full-intensity light from hour 24 to hour 60. Each experiment represents two laboratory replicates using a mixed population of *Cassiopea* spp. (B) Prolonged exposure to dark conditions of jellyfish shows circadian cycling when using a clonal population of medusa (*Cassiopea xamachana*), see Methods. 16 jellyfish were exposed to dark conditions from hour 36 to hour 72 or full-intensity light from hour 24 to hour 60. With this clonal population of jellyfish, circadian cycling of behavior is only observed for constant dark conditions and not constant full-intensity light conditions, consistent with results seen in the mixed population of *Cassiopea* shown in (D).

circadian stress-induced-sleep state [4, 5, 52]. A fully functioning circadian system is also not essential for sleep to occur; animals with null mutations of circadian rhythm genes still sleep, though sleep timing is altered [51]. To test whether nighttime quiescence in *Cassiopea* is regulated by a circadian rhythm, we first entrained the jellyfish for 1 week in a normal 12 hr:12 hr light/dark cycle and then shifted them to constant lighting conditions for 36 hr. We tested low-intensity ~ 0.5 photosynthetic photon flux [PPF]), mid-intensity (\sim PPF), and full-intensity (~ 200

PPF) light, as well as dark (Figure 3.9A and B). If jellyfish activity is regulated by a circadian rhythm, cycling activity should persist in the absence of entraining stimuli, such as light. We observed no circadian oscillation of jellyfish activity under any of the constant-light conditions (Figure 3.9A). However, we did observe circadian oscillation of activity in constant-dark conditions (Figure 3.9B). This result suggests that the quiescent state may be under circadian regulation. *Cassiopea* display the key behavioral characteristics of a sleep-like state: a reversible quiescent state with reduced responsiveness to stimuli and both homeostatic and possibly circadian regulation. To our knowledge, our finding is the first example of a sleep-like state in an organism with a diffuse nerve [7, 8], suggesting that this behavioral state arose prior to the evolution of a centralized nervous system.

3.7 *Cassiopea* activity is depressed in the presence of deeply conserved sleep promoting molecules

Though at least 600 million years of evolution separate cnidarians from bilaterians [10–15, 53], many aspects of the nervous system are conserved, including neuropeptides and neurotransmitters [15–20]. One such conserved molecule, melatonin [54], promotes sleep in diurnal vertebrates, including zebrafish [50] and humans [55], and induces quiescence in invertebrates [56]. We observed that melatonin induces a reversible decrease in activity in *Cassiopea* during the day in a concentration-dependent manner (Figures 3.10A-C), suggesting that melatonin has a conserved quiescence-inducing effect in *Cassiopea*. Pyrilamine, a histamine H1 receptor antagonist that induces sleep in vertebrates [57], also induces concentration dependent quiescence in *Cassiopea* (Figure 3.10A). These results suggest that at least some mechanisms involved in vertebrate sleep may be conserved in *Cassiopea*.

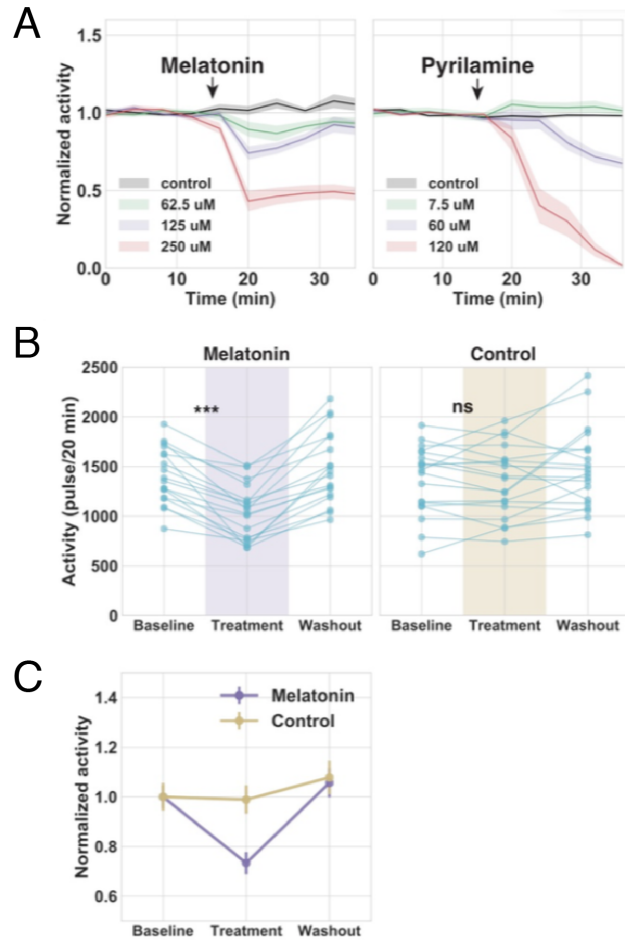


Figure 3.11: *Cassiopea* exhibit a decrease in activity in response to melatonin and pyrilamine exposure during the day. Each blue line corresponds to a single jellyfish. The black line indicates the mean activity of all jellyfish. Dark gray shading indicates night periods. (A) Treatment with either pyrilamine or melatonin effects pulsing activity. The colored lines represent different concentrations of compounds tested. Activity was monitored before and after treatment. Time of treatment is indicated by a black arrow. Both melatonin and pyrilamine induce a concentration-dependent decrease in pulsing activity. (B) Activity of 18 *Cassiopea* exposed to 125 μM melatonin solubilized in ethanol compared to 19 *Cassiopea* treated with ethanol vehicle control from four laboratory replicates. *Cassiopea* were monitored for 20 min before (baseline), during (treatment), and after (washout) either melatonin or vehicle treatment. Two-sided paired t test, before/during melatonin treatment: $P = 4 \times 10^{-7}$, and before/during vehicle treatment: $P = 7 \times 10^{-1}$. *** $P < 10^{-3}$, ns not significant (ns) $P > 5 \times 10^{-2}$. (C) Comparison of the normalized mean activity between the melatonin and control treatment. Error-bars represent the standard error of the mean.

3.8 Discussion

Although future studies are required to test whether other cnidarians sleep, field studies showing behavioral quiescence, diel vertical migration, and swimming speeds that vary with diel period [21–23, 58] suggest that a sleep-like state may not

be specific to *Cassiopea*. A cnidarian sleep-like state could result from either divergent or convergent evolution. The observation of behaviorally and mechanistically conserved sleep-like states across the animal kingdom [6, 7] strongly supports the possibility for an early-rooted sleep state rather than many instances of convergent evolution. It has been hypothesized that sleep has multiple functions, including synaptic homeostasis, regulation of neurotransmitters, repair of cellular damage, removal of toxins, memory consolidation, and energy conservation [7], although the ancestral role and selective advantage of sleep remains elusive. Our discovery of a sleep-like state in an ancient metazoan phylum suggests that the ancestral role of sleep is rooted in basic requirements that are conserved across the animal kingdom. The ancestral function of sleep may be revealed by further study of early-branching metazoa.

3.9 Materials and Methods

Experimental model and subject details

Cassiopea spp. medusae used in this study were originally collected from the Florida Keys. For the majority of the experiments, a collection of multiple *Cassiopea* species were used (Figure 3.1A and B). For the experiments shown in Figures 3.8A, 3.9B, and 3.10F, a young (2-4 months old) clonal population of medusa were used (*Cassiopea xamachana*). This clonal polyp line was generated in Monica Medina's lab at Pennsylvania State University and raised at Caltech in the Goentoro Lab.

Cassiopea were reared in artificial seawater (ASW, Instant Ocean, 30-34 ppt) at pH 8.1-8.3, 26-28 ° C with a 12 hr day/night cycle. During the day, 450 and 250 W light sources were used to generate 200-300 PPF (Photosynthetic Photon Flux, a measurement of light power between 400 and 700 nm). To limit waste buildup, the *Cassiopea* aquarium was equipped with a refugium (*Chaetomorpha* algae aquaculture), a protein skimmer (Vertex Omega Skimmer), carbon dosing bio-pellets (Bulk Reef Supply), activated carbon in a media reactor (Bulk Reef Supply), and a UV sterilizer (Emperor Aquatics 25 W). Waste products were kept at

or below the following levels: 0.1 ppm ammonia, 5 ppb phosphorus, 0 ppm nitrite, and 0 ppm nitrate.

Cassiopea were fed daily with brine shrimp (*Artemia nauplii*, Brine Shrimp Direct) enriched with *Nannochloropsis* algae (Reed Mariculture), and they were fed oyster roe once per week (Reed Mariculture). *Cassiopea* were group housed in a 60 gallon holding tank. Animals were randomly assigned to experimental groups. Medusae between 3-6 cm in diameter were used for experiments.

***Cassiopea* genotyping**

Cassiopea is a genus with many species that have not been classified. All of our experiments were performed with *Cassiopea* spp. of a range of sizes, ages, sex and morphologies (Figure 3.2A and B). To assess the diversity of *Cassiopea* spp. within our population we genotyped several animals by amplification and sequencing of the Mitochondrial cytochrome c oxidase I (COI). Genomic DNA extractions were performed as described [59]. Jellyfish fragments, about 2 mm of tissue from the tentacles, were placed in 400 mL DNA extraction buffer (50% w/v guanidinium isothiocyanate; 50 mM Tris pH 7.6; 10 mM EDTA; 4.2% w/v sarkosyl; 2.1% v/v β -mercaptoethanol). Samples were incubated at 72C for 10 min, centrifuged at 16,000 g for 5 min, and the resulting supernatant mixed with an equal volume of isopropanol and incubated at -20C overnight. The DNA was precipitated by centrifugation at 16,000 g for 15 min and the DNA pellet washed in 70% ethanol and resuspended and stored in water.

Amplification of COI was performed using primers designed by Folmer et al. [60], which amplify a 710 base pair fragment of COI across the broadest array of invertebrates. COI primers:

LCO1490 forward primer: 5' -ggtaacaaatcataaagatattgg-3' HC02198 reverse primer: 5' -taaacttcagggtgaccaaataatca-3'

Amplifications were performed under the following PCR conditions: 2 min at 92C, 30 cycles of 94° C for 30 s, 55°C for 30 s and 72°C for 45 s, with a final 72°C

extension for 7 min. Amplification products were then TOPO-cloned using OneTaq (NEB) and sequenced.

Multiple sequence alignment of *Cassiopea spp.* COI sequences were generated using Clustal Omega software. Sequences were aligned with each other (see Figure 3.2B), and to the previously identified cryptic species *Cassiopea ornata*, *Cassiopea andromeda*, and *Cassiopea frondosa* [48]. The level of identity between these sequences is presented in Figure 3.2B. Of the 15 *Cassiopea spp.* sequenced there were 8 identical COI sequences and 7 COI sequences with 45%–90% identity.

***Cassiopea* behavioral tracking**

Individual jellyfish were placed into 700 mL square clear plastic containers (cubbies), with white sand bottoms, in 10 gallon glass tanks (Figure 3.2C–F). Eight containers can fit in each tank, so eight jellyfish can be simultaneously recorded per tank. Tanks were housed inside Sterilite utility cabinets (65 cm W x 48 cm L x 176 cm H) with a door to eliminate ambient light in the recording setup. During the 12 hr day (lights on) tanks were illuminated with 24-inch florescent lamps, each containing four florescent bulbs that provide a combination of wavelengths optimized for photosynthesis in water: two 24 W, 6000 K Mid-day lights, and two 24 W Actinic lights (Gieseemann), which combined provided 200-300 PPF. During the 12 hr night (lights off) low-intensity red-LEDs were used to illuminate jellyfish to enable visualization. For all jellyfish recordings we used Unibrain 501b cameras above the tank running Firei software capturing at 15 frames per second. Camera aperture and Firei settings were adjusted to increase the contrast between jellyfish and background. Recordings were saved directly onto hard drives.

Jellyfish were acclimated in the recording tank in their cubbies for 2-3 days before starting recordings. 24 hr recordings were taken for successive days (7 am – 7 pm) and nights (7 pm – 7 am), unless otherwise indicated. *Cassiopea* were fed each day at 10:30 am, 3.5 hr after the lights turn on. Each jellyfish received 5 mL of 16 g/L brine shrimp. For each circadian rhythm experiment a different

light condition was left on for 36 hr: dark conditions, low-intensity light conditions (an array of white-LED lights, 0-0.5 PPF), mid-intensity light conditions (two 24 W, 6000 K Mid-day lights, 75-150 PPF), or full light conditions (two 24 W, 6000 K Mid-day lights, and two 24 W Actinic lights, 200-300 PPF). For 6 hr and 12 hr rebound experiments the mechanical stimulus (Movie S2) was applied for 10 s every 20 min.

All analysis was done using open-source packages in the SciPy ecosystem [61, 62]x. To monitor jellyfish activity, pulsing information was extracted from the individual frames of each recording. Approximately 648,000 frames were collected every 12 hr. To quantify pulsing activity, we processed the first 18,000 frames of every hour (20 min). As *Cassiopea* pulse, the relaxation and contraction of the bell causes a corresponding change in average pixel intensity. To measure this change in average pixel intensity we drew a rectangular region of interest (ROI) around each jellyfish (Figure 3.1D and Figure 3.2F). A user manually selected a ROI around each of the eight jellyfish in the first and last of the 18,000 frames. This was done so that the selected ROI accounts for any movement of the jellyfish. To control for noise from oscillations in ambient lighting, we perform background subtraction using a similarly sized ROI containing no jellyfish.

We analyzed pixel intensity data, and identified pulse events and inter-pulse intervals (IPI) in a four-step process. **Step 1:** Gaussian smoothing of the mean intensity over time to eliminate high frequency oscillations (Figure 3.3A). This smoothed trace was used to account for large movements in the mean intensity due to jellyfish translational movement within the selected ROI. **Step 2:** Normalization of the mean intensity values with the max mean intensity and the smoothed mean intensity:

$$T^n = \frac{T_r^{naw} - T_s^n mooth}{T_{max} - T_s^n mooth}$$

Where T_{raw} is the raw intensity trace, T_{smooth} is the smoothed trace generated in Step 1, T_{max} is maximum intensity across the raw trace, and n is the index of

each frame of the recording. **Step 3:** find the indices (time) of local maxima and minima in the normalized trace. Because of noise in the pulsing trace there is a high rate of false positives when finding local maxima and minima (Figure 3.3B). We have used a set of criteria to identify a true pulse event from the local maxima and local minima. Step 4: identifying pulses from local maxima and minima (Figure 3.3C). A local maximum can be defined as a pulse peak if it meets two criteria. First, it must be above a set threshold (to eliminate local maxima due to noise in pause regions of the pulse trace). Second, it must be above a set distance from the next local maxima (to prevent double counting of a single pulse). The standard deviation of the Gaussian smoothing, the threshold level, and the minimum distance between pulses can all be changed from one jellyfish to another. For all data analysis these parameter values were optimized to quantify pulsing events for each animal.

We calculated the total number of pulses and the IPI for each 20 min time bin. With some jellyfish the difference in pixel intensity from the contracted to non-contracted state was not big enough to easily identify pulsing above the noise. These jellyfish were excluded from analysis. During the 20 min recordings jellyfish would occasionally move out of the selected ROI. We would then exclude that 20 min recording for that jellyfish from the analysis. In compiling data to generate activity versus time plots we excluded jellyfish that we could not analyze for more than three 20 min recordings during a 12 hr day or night period.

For the arousal assay we designed an experiment to systematically test this sensory responsiveness. *Cassiopea* respond to being placed in the water column by rapidly orienting themselves and moving toward a stable surface. For the experimental system, *Cassiopea* were placed inside a 20 cm tall, 12 cm diameter, PVC pipe with a 53 mm filter screen bottom, called a *Cassiopea* dropper (CD). The experiment consists of four steps, as seen in the four panels in Figure 3.6A. Step 1, the jellyfish were placed on the screen bottom of the CD, which was positioned two cm below the water surface (hL) and were acclimated for five min. At night jellyfish took less than five min to return to quiescence after being placed in the CD. Step 2,

the CD was then “dropped” to a set depth (18 cm from the surface, hD). This action leaves the jellyfish free-floating, two cm below the water surface. Step 3, the time to first pulse was measured. Step 4, the time to reach bottom was measured. To determine if the nighttime arousal latency is reversible, a second drop experiment was performed within 30 s of the initial drop. The CD was returned to two cm below the water surface, but instead of waiting for five min, steps 2 and 3 were performed immediately. Time to first pulse and time to bottom are not completely independent measures, though there is also not a perfect correlation. A jellyfish could pulse quickly but be delayed in reaching the bottom due to, for example, inactivity after the first pulse.

***Cassiopea* staining and imaging**

Actin was stained using Alexa Fluor 488-Phalloidin (ThermoFisher A12379). Jellyfish were anesthetized in ice-cold 0.8 mM menthol/ ASW, and then fixed in 4% formaldehyde on ice for 45 min. Fixed jellyfish were permeabilized in 0.5% Triton/PBS for 2 hr and blocked using 3% BSA for 1 hr. They were then incubated in 1:100 Phalloidin solution in 0.5% Triton/PBS, for 18-24 hr in the dark at 4 C [63]. Stained jellyfish were mounted in refractive index matching solution [64] and imaged using a LSM 780 confocal microscope (Zeiss).

***Cassiopea* staining and imaging**

Quantification and Statistical analysis

The following statistical tests were used: two-sided paired Student’s t tests, two-sided unpaired Student’s t tests, and two-way ANOVA with Bonferroni posttest. We performed D’Agostino’s omnibus K2 normality test on all datasets to assess whether or not to reject the null hypothesis that all values were sampled from a population that follows a Gaussian distribution. For paired values, we tested if the pairs were sampled from a population where the difference between pairs follows a Gaussian distribution. Experimental groups that were statistically compared were

tested for equal variance. The normality tests showed that all datasets were approximately Gaussian distributed with the exception of the time to first pulse arousal data. The time to first pulse data also showed grounds for rejecting the null hypothesis that there was equal variance between experimental groups. Tests of the log transformed time to first pulse data showed that the transformed data was approximately Gaussian distributed with equal variance between experimental groups, validating the use of standard two-way ANOVA and unpaired t tests on the transformed data. Statistical tests were performed using either statistical functions from the SciPy ecosystem or GraphPad Prism (version 6.04 for Windows, GraphPad Software, San Diego California USA, <http://www.graphpad.com>). No statistical methods were used to predetermine sample size. For these experiments we performed at least two laboratory replicates within our recording setup, which is limited to 8 jellyfish. Investigators were not blinded to allocation during experiments and outcome assessment. No specific method for randomization was used.

DATA AND SOFTWARE AVAILABILITY

Code used for tracking jellyfish activity and analysis is available at

<https://github.com/GradinaruLab/Jellyfish>

3.10 Supplemental Movies

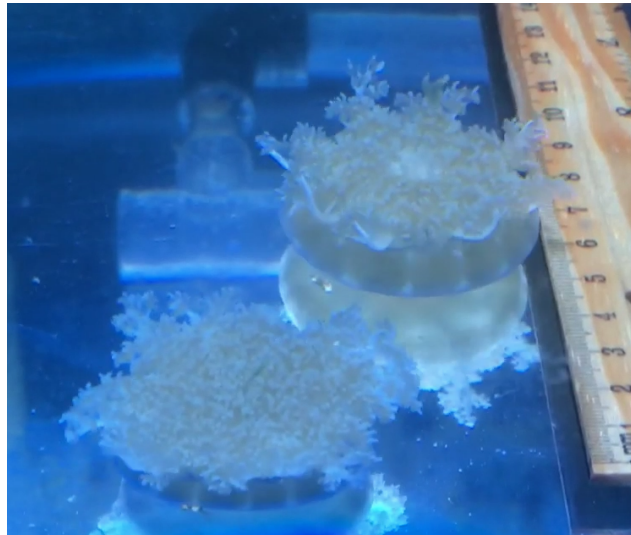


Figure Movie S1: *Cassiopea* Pulsing Behavior Two jellyfish pulsing during the day with ruler for scale.

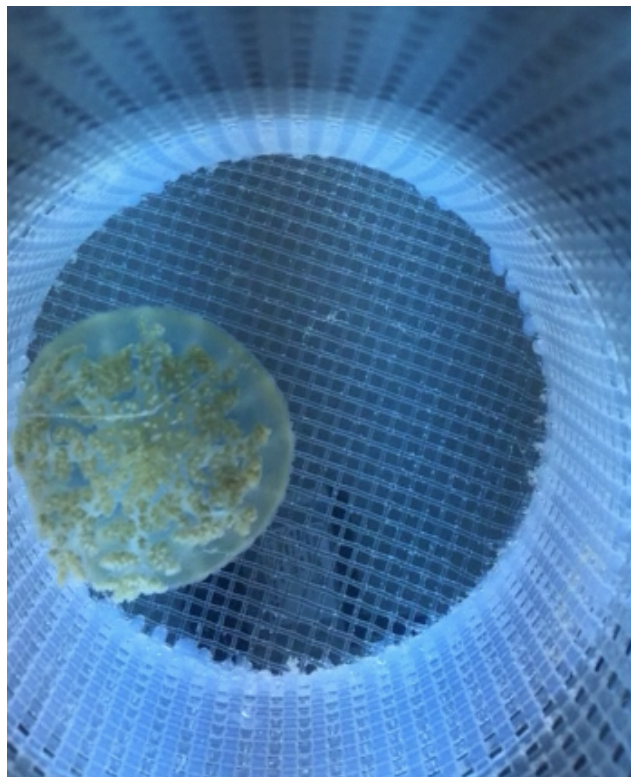


Figure Movie S2: *Cassiopea* Exposed to Brief Water Pulse Perturbation A mechanical stimulation perturbs a single jellyfish. .

References

- [1] Joan C Hendricks et al. “Rest in *Drosophila* is a sleep-like state”. In: *Neuron* 25.1 (2000), pp. 129–138.
- [2] Paul J Shaw et al. “Correlates of sleep and waking in *Drosophila melanogaster*”. In: *Science* 287.5459 (2000), pp. 1834–1837.
- [3] David M Raizen et al. “Lethargus is a *Caenorhabditis elegans* sleep-like state”. In: *Nature* 451.7178 (2008), p. 569.
- [4] Andrew J Hill et al. “Cellular stress induces a protective sleep-like state in *C. elegans*”. In: *Current Biology* 24.20 (2014), pp. 2399–2405.
- [5] Nicholas F Trojanowski and David M Raizen. “Call it worm sleep”. In: *Trends in neurosciences* 39.2 (2016), pp. 54–62.
- [6] Ravi Allada and Jerome M Siegel. “Unearthing the phylogenetic roots of sleep”. In: *Current biology* 18.15 (2008), R670–R679.
- [7] William J Joiner. “Unraveling the evolutionary determinants of sleep”. In: *Current Biology* 26.20 (2016), R1073–R1087.
- [8] Leonie Kirszenblat and Bruno van Swinderen. “The yin and yang of sleep and attention”. In: *Trends in neurosciences* 38.12 (2015), pp. 776–786.
- [9] Casey W Dunn et al. “Animal phylogeny and its evolutionary implications”. In: *Annual review of ecology, evolution, and systematics* 45 (2014), pp. 371–395.
- [10] Detlev Arendt, Maria Antonietta Tosches, and Heather Marlow. “From nerve net to nerve ring, nerve cord and brain—evolution of the nervous system”. In: *Nature Reviews Neuroscience* 17.1 (2016), p. 61.
- [11] Takeo Katsuki and Ralph J Greenspan. “Jellyfish nervous systems”. In: *Current Biology* 23.14 (2013), R592–R594.
- [12] Douglas H Erwin and Eric H Davidson. “The last common bilaterian ancestor”. In: *Development* 129.13 (2002), pp. 3021–3032.
- [13] Andreas Hejnol and Fabian Rentzsch. “Neural nets”. In: *Current Biology* 25.18 (2015), R782–R786.
- [14] Iva Kelava, Fabian Rentzsch, and Ulrich Technau. “Evolution of eumetazoan nervous systems: insights from cnidarians”. In: *Phil. Trans. R. Soc. B* 370.1684 (2015), p. 20150065.
- [15] Thomas CG Bosch et al. “Back to the basics: cnidarians start to fire”. In: *Trends in neurosciences* 40.2 (2017), pp. 92–105.

- [16] Cornelis JP Grimmelikhuijzen and JA Westfall. “The nervous systems of cnidarians”. In: *The nervous systems of invertebrates: an evolutionary and comparative approach*. Springer, 1995, pp. 7–24.
- [17] Richard A Satterlie. “Do jellyfish have central nervous systems?” In: *Journal of Experimental Biology* 214.8 (2011), pp. 1215–1223.
- [18] Hiroshi Watanabe, Toshitaka Fujisawa, and Thomas W Holstein. “Cnidarians and the evolutionary origin of the nervous system”. In: *Development, growth & differentiation* 51.3 (2009), pp. 167–183.
- [19] Christophe Dupre and Rafael Yuste. “Non-overlapping neural networks in *Hydra vulgaris*”. In: *Current Biology* 27.8 (2017), pp. 1085–1097.
- [20] Cornelis JP Grimmelikhuijzen, Michael Williamson, and Georg N Hansen. “Neuropeptides in cnidarians”. In: *Canadian Journal of Zoology* 80.10 (2002), pp. 1690–1702.
- [21] Maya Kremien et al. “Benefit of pulsation in soft corals”. In: *Proceedings of the National Academy of Sciences* 110.22 (2013), pp. 8978–8983.
- [22] A Garm et al. “Opposite patterns of diurnal activity in the box jellyfish *Tripedalia cystophora* and *Copula sivickisi*”. In: *The Biological Bulletin* 222.1 (2012), pp. 35–45.
- [23] Jamie E Seymour, Teresa J Carrette, and Paul A Sutherland. “Do box jellyfish sleep at night?” In: *Medical journal of Australia* 181.11/12 (2004), p. 706.
- [24] Ravi D Nath et al. “The jellyfish *Cassiopea* exhibits a sleep-like state”. In: *Current Biology* 27.19 (2017), pp. 2984–2990.
- [25] Richard Cresswell et al. “History of animals”. In: (1883), pp. 97–98.
- [26] J Lee Kavanau. “Is sleep’s ‘supreme mystery’ unraveling? An evolutionary analysis of sleep encounters no mystery; nor does life’s earliest sleep, recently discovered in jellyfish”. In: *Medical hypotheses* 66.1 (2006), pp. 3–9.
- [27] Irina V Zhdanova et al. “Melatonin promotes sleep-like state in zebrafish1”. In: *Brain research* 903.1-2 (2001), pp. 263–268.
- [28] Nathaniel Kleitman. “Sleep”. In: *Physiological Reviews* 9.4 (1929), pp. 624–665.
- [29] Jerome M Siegel. “Clues to the functions of mammalian sleep”. In: *Nature* 437.7063 (2005), p. 1264.
- [30] Scott S Campbell and Irene Tobler. “Animal sleep: a review of sleep duration across phylogeny”. In: *Neuroscience & Biobehavioral Reviews* 8.3 (1984), pp. 269–300.
- [31] Jerome M Siegel. “Do all animals sleep?” In: *Trends in neurosciences* 31.4 (2008), pp. 208–213.

- [32] Allan Rechtschaffen and JM Siegel. “Sleep and dreaming”. In: *Principles of neuroscience* 4 (2000).
- [33] Irene Tobler. “Is sleep fundamentally different between mammalian species?” In: *Behavioural brain research* 69.1-2 (1995), pp. 35–41.
- [34] Jerome M Siegel. “The REM sleep-memory consolidation hypothesis”. In: *Science* 294.5544 (2001), pp. 1058–1063.
- [35] Alexander A Borb and Peter Achermann. “Sleep homeostasis and models of sleep regulation”. In: *Journal of biological rhythms* 14.6 (1999), pp. 559–570.
- [36] William Dement. “The effect of dream deprivation”. In: *Science* 131.3415 (1960), pp. 1705–1707.
- [37] Mircea Steriade. “Brain electrical activity and sensory processing during waking and sleep states”. In: *Principles and Practice of Sleep Medicine (Fourth Edition)*. Elsevier, 2005, pp. 101–119.
- [38] Harold Zepelin, Jerome M Siegel, and Irene Tobler. “Mammalian sleep”. In: *Principles and practice of sleep medicine* 4 (2005), pp. 91–100.
- [39] Miroslaw Mackiewicz et al. “Macromolecule biosynthesis: a key function of sleep”. In: *Physiological genomics* 31.3 (2007), pp. 441–457.
- [40] Reto Huber et al. “Local sleep and learning”. In: *Nature* 430.6995 (2004), p. 78.
- [41] VV Vyazovskiy and Irene Tobler. “Handedness leads to interhemispheric EEG asymmetry during sleep in the rat”. In: *Journal of neurophysiology* 99.2 (2008), pp. 969–975.
- [42] Allan Rechtschaffen et al. “Physiological correlates of prolonged sleep deprivation in rats”. In: *Science* 221.4606 (1983), pp. 182–184.
- [43] Paul J Shaw et al. “Stress response genes protect against lethal effects of sleep deprivation in *Drosophila*”. In: *Nature* 417.6886 (2002), p. 287.
- [44] Adam M Reitzel, Lars Behrendt, and Ann M Tarrant. “Light entrained rhythmic gene expression in the sea anemone *Nematostella vectensis*: the evolution of the animal circadian clock”. In: *PLoS One* 5.9 (2010), e12805.
- [45] Eiichi Shoguchi et al. “A genome-wide survey of photoreceptor and circadian genes in the coral, *Acropora digitifera*”. In: *Gene* 515.2 (2013), pp. 426–431.
- [46] Aisling K Brady, Kevin A Snyder, and Peter D Vize. “Circadian cycles of gene expression in the coral, *Acropora millepora*”. In: *PLoS One* 6.9 (2011), e25072.
- [47] Carin Jantzen et al. “Enhanced pore-water nutrient fluxes by the upside-down jellyfish *Cassiopea* sp. in a Red Sea coral reef”. In: *Marine Ecology Progress Series* 411 (2010), pp. 117–125.

- [48] Brenden S Holland et al. “Global phylogeography of Cassiopea (Scyphozoa: Rhizostomeae): molecular evidence for cryptic species and multiple invasions of the Hawaiian Islands”. In: *Marine Biology* 145.6 (2004), pp. 1119–1128.
- [49] Arvind Santhanakrishnan et al. “Flow structure and transport characteristics of feeding and exchange currents generated by upside-down Cassiopea jellyfish”. In: *Journal of Experimental Biology* 215.14 (2012), pp. 2369–2381.
- [50] Irina V Zhdanova. “Sleep and its regulation in zebrafish”. In: *Reviews in the Neurosciences* 22.1 (2011), pp. 27–36.
- [51] John E Zimmerman et al. “Conservation of sleep: insights from non-mammalian model systems”. In: *Trends in neurosciences* 31.7 (2008), pp. 371–376.
- [52] Ravi D Nath et al. “C. elegans stress-induced sleep emerges from the collective action of multiple neuropeptides”. In: *Current Biology* 26.18 (2016), pp. 2446–2455.
- [53] Casey W Dunn, Sally P Leys, and Steven HD Haddock. “The hidden biology of sponges and ctenophores”. In: *Trends in ecology & evolution* 30.5 (2015), pp. 282–291.
- [54] Rafael Peres et al. “Developmental and light-entrained expression of melatonin and its relationship to the circadian clock in the sea anemone *Nematostella vectensis*”. In: *EvoDevo* 5.1 (2014), p. 26.
- [55] Amnon Brzezinski et al. “Effects of exogenous melatonin on sleep: a meta-analysis”. In: *Sleep medicine reviews* 9.1 (2005), pp. 41–50.
- [56] Maria Antonietta Tosches et al. “Melatonin signaling controls circadian swimming behavior in marine zooplankton”. In: *Cell* 159.1 (2014), pp. 46–57.
- [57] Avni V Gandhi et al. “Melatonin is required for the circadian regulation of sleep”. In: *Neuron* 85.6 (2015), pp. 1193–1199.
- [58] Pamela E Moriarty et al. “Vertical and horizontal movement patterns of scyphozoan jellyfish in a fjord-like estuary”. In: *Marine Ecology Progress Series* 455 (2012), pp. 1–12.
- [59] Michael Stat et al. “Specificity in communities of Symbiodinium in corals from Johnston Atoll”. In: *Marine Ecology Progress Series* 386 (2009), pp. 83–96.
- [60] R Vrijenhoek et al. “DNA primers for amplification of mitochondrial cytochrome c oxidase subunit I from diverse metazoan invertebrates”. In: *Molecular marine biology and biotechnology* 3.5 (1994), pp. 294–299.

- [61] Stéfan van der Walt, S Chris Colbert, and Gael Varoquaux. “The NumPy array: a structure for efficient numerical computation”. In: *Computing in Science & Engineering* 13.2 (2011), pp. 22–30.
- [62] John D Hunter. “Matplotlib: A 2D graphics environment”. In: *Computing in science & engineering* 9.3 (2007), pp. 90–95.
- [63] Michael J Abrams et al. “Self-repairing symmetry in jellyfish through mechanically driven reorganization”. In: *Proceedings of the National Academy of Sciences* 112.26 (2015), E3365–E3373.
- [64] Jennifer B Treweek et al. “Whole-body tissue stabilization and selective extractions via tissue-hydrogel hybrids for high-resolution intact circuit mapping and phenotyping”. In: *Nature protocols* 10.11 (2015), p. 1860.

Chapter 4

DISCUSSION

I described in this thesis two main discoveries within cnidarian scyphomedusae. First, in Chapter 2, a new strategy of self-repair in the moon jellyfish *Aurelia*, where in response to severe injuries, ephyrae reorganize their remaining parts to recover body symmetry. Second, in Chapter 3, a behavioral sleep-like state in the upside-down jellyfish *Cassiopea*, the first in an animal without a centralized nervous system. Here I discuss some of the implications and limitations of these findings and several possible future directions.

To study *Aurelia* and *Cassiopea* we designed new setups and assays to address our questions, often re-purposing tools and techniques developed for other models. Histology and pharmacology have proven useful in characterization and perturbation of our systems. In the future we could try more directed approaches, for example, neuronal recordings using electrophysiology [1] or non-invasive magnetometry [2], and *in vivo* morpholinos to perturb specific pathways [3, 4]. Genomes in both *Aurelia*, by the Jacobs Lab at the University of California Los Angeles, and *Cassiopea*, by the Medina Lab at Pennsylvania State University, are being annotated and will facilitate forward genetic approaches. This, in combination with transcriptomics, already published for certain developmental stages in *Aurelia* [5, 6] and soon to be completed in *Cassiopea*, also by the Medina Lab, support further comparative -omics and epigenetic analysis. Together, further investigations using jellyfish will continue to make these organisms more accessible to deeper analysis.

4.1 Self-repair strategies in *Aurelia*

Recovery processes tend to be inhibited if the restored structure cannot be used, known as the utilitarian imperative (described in the introduction of Chapter 2), and

this may be a lens through which to interpret symmetrization in *Aurelia*. The recovery of body symmetry is driven by mechanical forces generated by the propulsion system, which itself relies on radial symmetry to function [7, 8]. Ephyrae that fail to regain symmetry, either naturally or by preventing pulsation, have impaired swimming and do not develop properly, so the functional recovery of the propulsion system during symmetrization appears to both adaptive and utilitarian. Previous examples of the utilitarian imperative involve tissue remodeling to recover specific structures lost to injury in order to regain function [9], making our finding a novel expansion of the concept.

Reorganization is involved in many self-repair mechanisms; we know, for instance, that in response to spinal cord injury, corticospinal tract fibers reorganize to allow recovery of dexterous movements in primates [10]. A similar overarching strategy of reorganization is also employed by neurons in the brain after a stroke [11], and by muscle spindle fibers after spinal cord injury [12]. These strategies may be analogous to what we see in jellyfish, in the sense that they both reorganize existing parts to regain lost function. Moreover, the similarity may extend to the underlying mechanism, as mechanical forces have been implicated in the reorganizing of neurons [13], blood vessels [14], bones [15] and muscle [12]. Cells are influenced by mechanical forces in their environment, such as softness or rigidity of extracellular matrix (ECM), differentiated adhesion to substrate or the tension exerted by neighboring cells [16]. The differentiation of cells can also be affected by microenvironmental signals, for example, the loss of contact with the basement membrane and the transfer of cells to a higher layer can direct them to terminally differentiate [17]. Together, it is clear that internally generated mechanical forces can have substantial impact on an animal's self-repair capabilities.

Many methods that aid in wound closure (e.g., stitches, staples and tapes) involve the broad application of mechanical forces [18]. Recent advances in bio-inspired materials, including tough adhesives that stick to diverse wet surfaces [19], allow for the application of mechanical forces without some of the deleterious effects

of more invasive techniques. It is also known that cycles of mechanical force can increase bone mass at the healing site post-fracture [20]. It is possible to image how a combination of adhesives and electroactively-contractile materials could aid in self-repair, and progress towards this aim has already begun [21]. Our work in *Aurelia* supports a deep and central role for mechanical forces in self-repair and the recovery of function.

In addition to self-repair, our work may also connect mechanical forces to development in ephyrae. The naturally occurring non-octamers we observed are frequently radially symmetrical; how ephyrae develop additional arms while maintaining radial symmetry has not been studied. Ephyrae begin pulsing early in strobilation, and it would be interesting to test if blocking pulsation affects the formation of symmetry in both octamers and non-octamers. We have shown that symmetry can be achieved through force-balancing, though mechanical forces also play an important role in developmental patterning [22, 23]. Gene expression can be visualized in *Aurelia* using *in situ* hybridizations [5], and we may be able to determine if genes known to be involved in bilaterian patterning change their expression based on the level of pulsation. Through this analysis we would begin to understand how symmetry in ephyrae is generated during strobilation.

We also wonder why ephyrae tend to have eight arms, is this number somehow adaptive? While the medusae stage can have considerable variation in morphology, ephyrae across species are similar in size and proportion with eight radially placed arms. However, with the prevalence of non-octamers and their capacity to symmetrize, ephyrae may be an interesting model for studying how bodyplan impacts fitness. We know the spacing of their arms would affect the formation of a viscous boundary layer important for the functionality of the propulsion system [8, 24, 25]. By closely tracking ephyrae as they swim and eat, in conjunction with particle image velocimetry, we could determine how arm number impacts survival, and the formation of the paddling surface. Perhaps eight arms is optimal; however, it is also possible that this number of arms, in combination with symmetrization, creates

a buffer against having fewer arms, whether naturally or from injury. This would allow ephyrae the capacity to lose arms without severely impacting their swimming and feeding capacity.

Finally, it is interesting to consider a potential role for symmetrization in self-repairing robotics. Soft robots are useful for interacting with uncertain and dynamic task environments, and could be especially useful when working with humans [26]. However, because of their intrinsic softness, these robots are susceptible to cuts, shears, punctures and over-pressured pneumatics. Recent advances in materials science has allowed for self-healing polymers to be made into soft pneumatic actuators, including artificial muscle and grippers [27, 28]. Through the proper application of mechanical forces and functional geometries, it may be possible to drive self-repair in soft robots.

4.2 A sleep-like state in *Cassiopea*

Though future studies in other cnidarians are required before we can broadly claim the presence of sleep in this early branching metazoan lineage, some field studies have reported cycles in behavior that are often associated with sleep-like states, indicating sleep may not be specific to *Cassiopea* [29–32]. Our observations of significant behavioral, and possible mechanistic, conservation of sleep in *Cassiopea* acts as evidence that sleep may have been present before the cnidarian-bilaterian divergence over 700 million years ago. To gain insight into the role of sleep in *Cassiopea* it will be important to determine their level of conservation of bilaterian sleep mechanisms.

Sleep in other systems, detected through local field potential recordings and calcium imaging, involves neuronal down-regulation during sleep [33–35]. There is a central debate in the sleep field around how this global brain state arises. There are two major theories: specialized regions control the switch between wakefulness and sleep (a top-down mechanism) [36]; alternatively, neural networks may have an emergent bias towards certain global states that are affected by local regulatory

circuits (a bottom-up mechanism) [35, 37, 38]. Our finding of a sleep-like state in *Cassiopea* gives us a unique opportunity to determine how sleep functions in an early nerve network. Tracking neural activity throughout the *Cassiopea* as they transition between wake and sleep, react to stimuli in either state, or respond to sleep regulators such as melatonin, would give us insight into how the global sleep state emerges in *Cassiopea*. As described in Chapter 1, *Cassiopea* have important neural network subfunctionalizations (rhopalia), and it would be fascinating if sleep is controlled by these regions. We could also determine if each neural cluster falls asleep independently or if it is an organized global process. By characterizing their neural activity it may even be possible to see if *Cassiopea* have sleep stages.

Understanding how *Cassiopea* shifts between behavioral states will require analysis at the mechanistic level. Exogenous melatonin is known to have sleep-promoting effects in diurnal vertebrates from zebrafish to humans [39–42], and can entrain [43, 44] and phase shift [45] the circadian clock in some contexts. Melatonin has been proposed as an indirect promoter of sleep by phase advancing the circadian clock [46] or by inhibiting the circadian drive for wakefulness [47]; therefore, melatonin is generally considered a regulator of circadian rhythms [48]. The overall function of melatonin, however, is complicated by a recent study that found endogenous melatonin acts downstream of the circadian clock components in zebrafish [49]. Though we have evidence of circadian behavior in *Cassiopea*, we have not yet determined if sleep in these animals is regulated by clock genes. Similarly, we have evidence that melatonin induces quiescence in *Cassiopea*, yet we have not shown that it induces sleep. It will be important to determine if exogenous melatonin in *Cassiopea* can entrain the circadian rhythm, or if it can directly drive sleep behavior. Perhaps, as transgenic techniques are developed in *Cassiopea*, we can determine the endogenous role of melatonin in this ancestral lineage.

Another fundamental question in the sleep field involves understanding the complex interplay of circadian and metabolic inputs that regulate sleep homeostasis [50]. One issue is that circadian and metabolic circuits regulate each other, making it

difficult to decouple one from the other to determine their hierarchy [51]. *Cassiopea* utilizes the photosynthetic output of its algal-like (dinoflagellate) symbiote as a main source of metabolic inputs, in a way similar to coral. Therefore, we may be able to molecularly affect the circadian components of the jellyfish without directly affecting a major source of its energy. It is also possible to swap dinoflagellate strains for ones with different metabolic characteristics, thereby allowing us to modify the metabolism of *Cassiopea* without changing its genetic circuitry [52–54]. In this way we can gain insights into the ancient hierarchy between metabolism and circadian rhythms in regulating sleep homeostasis.

It has been hypothesized that sleep has multiple functions, including synaptic homeostasis, regulation of neurotransmitters, repair of cellular damage, removal of toxins, memory consolidation, and energy conservation [55]. Each of these potential roles for sleep involve certain assumptions about the capabilities of the animals in which sleep functions. It is an open question whether sponges, animals without neurons, or a metazoan sister group (*e.g.*, choanoflagellates), could have sleep-like states. Though quantifying behaviors in these organisms may be possible, it will be critical and challenging to detect the three core behavioral components to a sleep-like state in these organisms. However, even reversible quiescence would be an interesting finding, showing perhaps a step in the evolution of sleep. Our discovery of a sleep-like state in an ancient metazoan phylum suggests that the ancestral role of sleep is rooted in basic requirements that are conserved across the animal kingdom.

References

- [1] Robert W Meech. “The electrophysiology of swimming in the jellyfish *Aglantha digitale*”. In: *Evolution of the first nervous systems*. Springer, 1989, pp. 281–298.
- [2] John F Barry et al. “Optical magnetic detection of single-neuron action potentials using quantum defects in diamond”. In: *Proceedings of the National Academy of Sciences* 113.49 (2016), pp. 14133–14138.

- [3] Lasse Dahl Jensen et al. “Opposing effects of circadian clock genes *bmal1* and *period2* in regulation of VEGF-dependent angiogenesis in developing zebrafish”. In: *Cell reports* 2.2 (2012), pp. 231–241.
- [4] David P Ferguson, Lawrence J Dangott, and J Timothy Lightfoot. “Lessons learned from vivo-morpholinos: How to avoid vivo-morpholino toxicity”. In: *Biotechniques* 56.5 (2014), p. 251.
- [5] Björn Fuchs et al. “Regulation of polyp-to-jellyfish transition in *Aurelia aurita*”. In: *Current Biology* 24.3 (2014), pp. 263–273.
- [6] Vera Brekhman et al. “Transcriptome profiling of the dynamic life cycle of the scyphozoan jellyfish *Aurelia aurita*”. In: *BMC genomics* 16.1 (2015), p. 74.
- [7] Brad J Gemmell et al. “Suction-based propulsion as a basis for efficient animal swimming”. In: *Nature communications* 6 (2015), p. 8790.
- [8] KE Feitl et al. “Functional morphology and fluid interactions during early development of the scyphomedusa *Aurelia aurita*”. In: *The Biological Bulletin* 217.3 (2009), pp. 283–291.
- [9] Michael J Abrams and Lea Goentoro. “Symmetrization in jellyfish: reorganization to regain function, and not lost parts”. In: *Zoology* 119.1 (2016), pp. 1–3.
- [10] Hiroshi Nakagawa et al. “Reorganization of corticospinal tract fibers after spinal cord injury in adult macaques”. In: *Scientific reports* 5 (2015), p. 11986.
- [11] Michael A Dimyan and Leonardo G Cohen. “Neuroplasticity in the context of motor rehabilitation after stroke”. In: *Nature Reviews Neurology* 7.2 (2011), p. 76.
- [12] Aya Takeoka et al. “Muscle spindle feedback directs locomotor recovery and circuit reorganization after spinal cord injury”. In: *Cell* 159.7 (2014), pp. 1626–1639.
- [13] William J Tyler. “The mechanobiology of brain function”. In: *Nature Reviews Neuroscience* 13.12 (2012), p. 867.
- [14] Donald R Senger and George E Davis. “Angiogenesis”. In: *Cold Spring Harbor perspectives in biology* 3.8 (2011), a005090.
- [15] Julie C Crockett et al. “Bone remodelling at a glance”. In: *J Cell Sci* 124.7 (2011), pp. 991–998.
- [16] Joanna Rosińczuk et al. “Mechanoregulation of wound healing and skin homeostasis”. In: (2018).
- [17] Moe Tsutsumi et al. “Mechanical-stimulation-evoked calcium waves in proliferating and differentiated human keratinocytes”. In: *Cell and tissue research* 338.1 (2009), p. 99.

- [18] Kemal Levi et al. “Mechanics of Wound Closure: Emerging Tape-Based Wound Closure Technology vs. Traditional Methods”. In: *Cureus* 8.10 (2016).
- [19] J Li et al. “Tough adhesives for diverse wet surfaces”. In: *Science* 357.6349 (2017), pp. 378–381.
- [20] Blaž Mavčič and Vane Antolič. “Optimal mechanical environment of the healing bone fracture/osteotomy”. In: *International orthopaedics* 36.4 (2012), pp. 689–695.
- [21] Reza Gharibi et al. “Stimulation of wound healing by electroactive, antibacterial, and antioxidant polyurethane/siloxane dressing membranes: in vitro and in vivo evaluations”. In: *ACS applied materials & interfaces* 7.43 (2015), pp. 24296–24311.
- [22] Rita R Ferreira and Julien Vermot. “The balancing roles of mechanical forces during left-right patterning and asymmetric morphogenesis”. In: *Mechanisms of development* 144 (2017), pp. 71–80.
- [23] Carl-Philipp Heisenberg and Yohanns Bellaiche. “Forces in tissue morphogenesis and patterning”. In: *Cell* 153.5 (2013), pp. 948–962.
- [24] JC Nawroth et al. “Phenotypic plasticity in juvenile jellyfish medusae facilitates effective animal–fluid interaction”. In: *Biology letters* 6.3 (2010), pp. 389–393.
- [25] Brad J Gemmell et al. “Passive energy recapture in jellyfish contributes to propulsive advantage over other metazoans”. In: *Proceedings of the National Academy of Sciences* 110.44 (2013), pp. 17904–17909.
- [26] Randy H Ewoldt. “Extremely soft: design with rheologically complex fluids”. In: *Soft Robotics* 1.1 (2014), pp. 12–20.
- [27] Seppe Terryn et al. “Development of a self-healing soft pneumatic actuator: A first concept”. In: *Bioinspiration & biomimetics* 10.4 (2015), p. 046007.
- [28] Seppe Terryn et al. “Self-healing soft pneumatic robots”. In: *Sci. Robot.* 2 (2017), eaan4268.
- [29] Maya Kremien et al. “Benefit of pulsation in soft corals”. In: *Proceedings of the National Academy of Sciences* 110.22 (2013), pp. 8978–8983.
- [30] A Garm et al. “Opposite patterns of diurnal activity in the box jellyfish *Tripedalia cystophora* and *Copula sivickisi*”. In: *The Biological Bulletin* 222.1 (2012), pp. 35–45.
- [31] Jamie E Seymour, Teresa J Carrette, and Paul A Sutherland. “Do box jellyfish sleep at night?” In: *Medical journal of Australia* 181.11/12 (2004), p. 706.
- [32] Pamela E Moriarty et al. “Vertical and horizontal movement patterns of scyphozoan jellyfish in a fjord-like estuary”. In: *Marine Ecology Progress Series* 455 (2012), pp. 1–12.

- [33] Douglas A Nitz et al. “Electrophysiological correlates of rest and activity in *Drosophila melanogaster*”. In: *Current biology* 12.22 (2002), pp. 1934–1940.
- [34] Daniel Bushey, Giulio Tononi, and Chiara Cirelli. “Sleep-and wake-dependent changes in neuronal activity and reactivity demonstrated in fly neurons using in vivo calcium imaging”. In: *Proceedings of the National Academy of Sciences* 112.15 (2015), pp. 4785–4790.
- [35] Annika LA Nichols et al. “A global brain state underlies *C. elegans* sleep behavior”. In: *Science* 356.6344 (2017), eaam6851.
- [36] Clifford B Saper et al. “Sleep state switching”. In: *Neuron* 68.6 (2010), pp. 1023–1042.
- [37] JAMES M KRUEGER and FERENC OBÄL. “A neuronal group theory of sleep function”. In: *Journal of sleep research* 2.2 (1993), pp. 63–69.
- [38] Vladyslav V Vyazovskiy et al. “Local sleep in awake rats”. In: *Nature* 472.7344 (2011), p. 443.
- [39] Irina V Zhdanova et al. “Melatonin promotes sleep-like state in zebrafish1”. In: *Brain research* 903.1-2 (2001), pp. 263–268.
- [40] Amnon Brzezinski et al. “Effects of exogenous melatonin on sleep: a meta-analysis”. In: *Sleep medicine reviews* 9.1 (2005), pp. 41–50.
- [41] Irina V Zhdanova et al. “Melatonin promotes sleep in three species of diurnal nonhuman primates”. In: *Physiology & behavior* 75.4 (2002), pp. 523–529.
- [42] Irina V Zhdanova. “Melatonin as a hypnotic: pro”. In: *Sleep medicine reviews* 9.1 (2005), pp. 51–65.
- [43] SW Lockley et al. “Melatonin administration can entrain the free-running circadian system of blind subjects”. In: *Journal of Endocrinology* 164.1 (2000), R1–R6.
- [44] Robert L Sack et al. “Entrainment of free-running circadian rhythms by melatonin in blind people”. In: *New England Journal of Medicine* 343.15 (2000), pp. 1070–1077.
- [45] Alfred J Lewy et al. “Melatonin shifts human circadian rhythms according to a phase-response curve”. In: *Chronobiology international* 9.5 (1992), pp. 380–392.
- [46] J Arendt. “Importance and relevance of melatonin to human biological rhythms”. In: *Journal of neuroendocrinology* 15.4 (2003), pp. 427–431.
- [47] Frank AJL Scheer and Charles A Czeisler. “Melatonin, sleep, and circadian rhythms”. In: *Sleep medicine reviews* 9.1 (2005), pp. 5–9.
- [48] Idan Elbaz et al. “Circadian clocks, rhythmic synaptic plasticity and the sleep-wake cycle in zebrafish”. In: *Frontiers in neural circuits* 7 (2013), p. 9.

- [49] Avni V Gandhi et al. “Melatonin is required for the circadian regulation of sleep”. In: *Neuron* 85.6 (2015), pp. 1193–1199.
- [50] Ritchie E Brown et al. “Control of sleep and wakefulness”. In: *Physiological reviews* 92.3 (2012), pp. 1087–1187.
- [51] Deanna Marie Arble et al. “Circadian disruption and metabolic disease: findings from animal models”. In: *Best Practice & Research Clinical Endocrinology & Metabolism* 24.5 (2010), pp. 785–800.
- [52] Aki H Ohdera et al. “Upside-Down but Headed in the Right Direction: Review of the Highly Versatile *Cassiopea xamachana* System”. In: *Frontiers in Ecology and Evolution* 6 (2018), p. 35.
- [53] Daniel J Thornhill et al. “Natural infections of aposymbiotic *Cassiopea xamachana* scyphistomae from environmental pools of *Symbiodinium*”. In: *Journal of Experimental Marine Biology and Ecology* 338.1 (2006), pp. 50–56.
- [54] Kathrin P Lampert. “*Cassiopea* and Its Zooxanthellae”. In: *The Cnidaria, Past, Present and Future*. Springer, 2016, pp. 415–423.
- [55] William J Joiner. “Unraveling the evolutionary determinants of sleep”. In: *Current Biology* 26.20 (2016), R1073–R1087.